

ABSTRACT

Title of Document: AUTOIGNITION DELAY TIME
MEASUREMENTS FOR NATURAL GAS
FUEL COMPONENTS AND
THEIR MIXTURES

Maclain Marshall Holton, M.S., 2008

Directed By: Associate Professor, Dr. Gregory Jackson,
Mechanical Engineering

Recent studies have indicated that small changes in concentration of higher hydrocarbons in natural gas can severely reduce ignition delay times of methane-based fuels. To increase the database of autoignition delay times for methane-based fuel mixtures characteristic of natural gas, experiments to measure autoignition delay times have been performed for a variety of gaseous fuels in an atmospheric flow reactor. Autoignition delay times were measured for pure fuels in air including methane, ethylene, ethane, and propane. The effect of higher hydrocarbon addition on methane-based fuel ignition delay was then investigated for fuel mixtures composed of methane/ethylene, methane/ethane, and methane/propane where methane composition varied from 25-95% by volume. Autoignition delay times were also measured for multi-component methane-based fuels composed of methane/ethane/propane and air. Finally the effect of CO₂ addition on methane

autoignition was investigated. For all experiments, Φ ranged between 0.5 and 1.25 and temperatures ranged from 931 K to 1137 K. The measurements made in this study will benefit the combustion community by both providing valuable insight into the effects of additives on methane ignition as well as validation data for chemical kinetics mechanisms for predicting ignition of methane-based fuels.

AUTOIGNITION DELAY TIME MEASUREMENTS FOR NATURAL GAS FUEL
COMPONENTS AND THEIR MIXTURES

By

Maclain Marshall Holton

Thesis submitted to the Faculty of the Graduate School of the
University of Maryland, College Park, in partial fulfillment
of the requirements for the degree of
Master of Science
2008

Advisory Committee:
Associate Professor Gregory Jackson, Chair
Professor Michael Zachariah
Assistant Professor Peter Sunderland

© Copyright by
Maclain Marshall Holton
2008

Acknowledgements

The time, equipment and resources of Combustion Science & Engineering, Inc., who funded this study, are greatly appreciated. I would like to thank the following people for their technical guidance in completing this study: P. (Gokul) Gokulakrishnan, Gregory Jackson, Michael Klassen, and Richard Roby. I would further like to acknowledge the efforts of the following individuals who helped build and characterize the experimental setup and helped perform autoignition delay time experiments: Brent Turner, Casey Fuller, Nasir Hussain, and Christopher Nolan.

Table of Contents

ACKNOWLEDGEMENTS.....	II
TABLE OF CONTENTS.....	III
LIST OF TABLES.....	V
LIST OF FIGURES.....	VI
NOMENCLATURE.....	VIII
CHAPTER 1: INTRODUCTION.....	9
1.1 Problem Definition.....	9
1.1.1 Natural Gas Composition.....	10
1.1.2 Metric for Investigating Ignition Behavior.....	11
1.1.3 Impact of Composition of Natural Gas on Combustion Performance.....	12
1.2 Previous Experimental Autoignition Delay Time Studies.....	13
1.2.1 Summary of Methane Autoignition Delay Time Studies.....	14
1.2.2 Summary of Ethane Autoignition Delay Time Studies.....	17
1.2.3 Summary of Propane Autoignition Delay Time Studies.....	18
1.2.4 Summary of Ethylene Autoignition Delay Time Studies.....	19
1.2.5 Summary of Methane-Based Fuel Mixtures Autoignition Delay Time Studies.....	21
1.3 Overview of the Presentation of the Current Study.....	23
CHAPTER 2: EXPERIMENT.....	25
2.1 Experimental Setup.....	25
2.1.1 Fuel and Air Supply, Preheat, & Delivery.....	28
2.1.2 Flow Reactor.....	32
2.1.3 Photomultiplier Tube.....	33
2.1.4 Data Acquisition & Control.....	33
2.2 Experimental Procedure.....	34
2.3 Apparatus Characterization.....	36
2.3.1 Flow Reactor Axial Temperature Profiles.....	36
2.3.2 Fuel and Oxidizer Mixedness Investigation.....	39
2.4 Design of Experiment.....	41
2.4.1 Temperature, Pressure, & Equivalence Ratio Range Selection.....	42
2.4.2 Fuel Selection.....	44
CHAPTER 3: APPARATUS VALIDATION USING ETHYLENE.....	48
3.1 Ethylene Combustion Data.....	50
3.2 Chemical Kinetics Mechanism Validation.....	52
3.2.1 Available Kinetics Mechanisms for Ethylene Combustion.....	53
3.2.2 Chemical Kinetics Mechanism Predictions of Literature Data.....	55
3.3 Chemical Reactor Model Development.....	61
3.3.1 CRM Methodology.....	62
3.3.2 CRM Results.....	64
CHAPTER 4: AUTOIGNITION DELAY MEASUREMENTS.....	70
4.1 Pure Fuels.....	72
4.1.1 Methane.....	73

4.1.2	Ethane	76
4.1.3	Propane	79
4.2	Methane-Based Binary Mixtures	83
4.2.1	Methane-Ethane	84
4.2.2	Methane-Propane	89
4.2.3	Methane-Ethylene	95
4.3	Methane-Based Ternary Mixtures	99
4.4	CO ₂ Addition	102
CHAPTER 5: CONCLUSIONS		105
5.1	Summary of Results	105
5.1.1	Autoignition Delay Time Trends	105
5.1.2	Accuracy of Predictive Tools	106
5.1.3	Contribution to Combustion Community	107
5.2	Future Work	108
REFERENCES		110

List of Tables

1.1	Worldwide natural gas constituent composition ranges.	11
2.1	Grades and purities of gases.	28
2.2	Experimental conditions of temperature, pressure and equivalence ratio as well as a description of the pure fuels and fuel blends studied.	42
3.1	Available ethylene ignition delay time data from the literature.	51
3.2	Goodness of fit (χ^2) for each chemical mechanism in predicting each literature data set.	61
3.3	CRM predictions of total time compared to uncorrected ethylene ignition delay time measurements.	65
3.4	Transit time correction factors, values are in units of milliseconds.	69
4.1	Methane and methane/hydrocarbon autoignition delay time correlations from the literature.	71
4.2	Derived Arrhenius expressions for autoignition delay time for pure fuels methane, ethane, and propane, and binary methane/ethane, methane/propane, and methane/ethylene mixtures.	72

List of Figures

2.1	Experimental system schematic.	26
2.2	Experimental flow reactor apparatus.	27
2.3	Fuel and air mixing section of flow reactor apparatus.	27
2.4	Schematic of fuel & diluent mixing plenum.	30
2.5	Flow reactor axial temperature profiles.	39
2.6	Radial species profiles of CO ₂ and O ₂ at three axial locations within the test section.	41
3.1	Uncorrected ethylene/air autoignition measurements compared to UCSD ethylene mechanism predictions and literature data.	49
3.2	Chemical kinetics mechanism performance in predicting Thomas & Brown's experimental data.	56
3.3	Chemical kinetics mechanism performance in predicting Kumar's experimental data.	57
3.4	Chemical kinetics mechanism performance in predicting Lefebvre's experimental data.	57
3.5	Chemical kinetics mechanism performance in predicting Thorton's experimental data.	60
3.6	Flow reactor zones and associated temperature profile.	63
3.7	Analytical predictions of ethylene autoignition delay time inclusive of transit time and true autoignition delay time calculated in CRM, compared to uncorrected ethylene autoignition delay time measurements.	65
3.8	Corrected ethylene autoignition delay time measurements compared with UCSD ethylene mechanism predictions.	67
3.9	Corrected ethylene autoignition delay time measurements compared with literature data and UCSD mechanism predictions.	67
4.1	Methane autoignition delay time measurements plotted alongside literature data and chemical kinetics predictions using GRI mechanism.	74
4.2	Methane autoignition measurements plotted with Arrhenius correlation.	76
4.3	Ethane autoignition delay time measurements plotted alongside chemical kinetics predictions using GRI mechanism.	77
4.4	Ethane autoignition measurements plotted with Arrhenius correlation.	79
4.5	Propane autoignition delay time measurements plotted alongside literature data and chemical kinetics predictions using GRI mechanism.	80
4.6	Propane autoignition measurements plotted with Arrhenius correlation.	83

4.7	Binary methane/ethane mixture autoignition delay time measurements as a function of ethane mole fraction in the fuel mixture.	84
4.8	Binary methane/ethane mixture autoignition delay time measurements as a function of temperature.	85
4.9	Stoichiometric methane/ethane mixture autoignition delay time measurements plotted alongside literature data and chemical kinetics predictions using GRI mechanism.	88
4.10	Methane/ethane autoignition measurements plotted with Arrhenius correlation.	89
4.11	Binary methane/propane mixture autoignition delay time measurements as a function of propane mole fraction in the fuel mixture.	90
4.12	Binary methane/propane mixture autoignition delay time measurements as a function of temperature.	90
4.13	Stoichiometric methane/propane mixture autoignition delay time measurements plotted alongside literature data and chemical kinetics predictions using GRI mechanism.	93
4.14	Methane/propane autoignition measurements plotted with Arrhenius correlation.	94
4.15	Binary methane/ethylene mixture autoignition delay time measurements as a function of ethylene mole fraction in the fuel mixture.	95
4.16	Binary methane/propane mixture autoignition delay time measurements as a function of temperature.	95
4.17	Stoichiometric methane/ethylene mixture autoignition delay time measurements plotted alongside chemical kinetics predictions using GRI mechanism.	98
4.18	Methane/ethylene autoignition measurements plotted with Arrhenius correlation.	99
4.19	Ternary methane/ethane/propane mixture autoignition delay time measurements.	100
4.20	Ternary methane/ethane/propane mixture autoignition delay time measurements plotted alongside literature data and chemical kinetics predictions using GRI mechanism.	102
4.21	75% Methane/25% ethane/CO ₂ mixture autoignition delay time measurements as a function of reactor temperature.	104

Nomenclature

Φ	Equivalence Ratio
τ_{ig}	Autoignition Delay Time
A	Rate Constant
a	Fuel Concentration Order
b	Oxidizer Concentration Order
E_{act}	Global Activation Energy (units of kcal·mol ⁻¹)
R	Universal Gas Constant (1.987 x 10 ⁻³ kcal·mol ⁻¹ ·K ⁻¹)
T	Temperature

Chapter 1: Introduction

1.1 Problem Definition

Natural gas is a very common fuel used in a variety of combustion systems due to its relatively low cost, low emissions, and prevalent availability [1]. Composition of natural gas can vary widely based on geographic region [2]. As gas-fueled combustion devices are being tasked with burning more varied fuel blends, a better understanding of the effect of variations in gas composition on combustion device performance is needed. Recent studies have indicated that even small changes in the concentrations of higher-order hydrocarbons can severely reduce the ignition delay time (τ_{ig}) of methane-based fuels. This effect can have a significant impact on premixed combustion systems where premature fuel autoignition can result in reduced combustor performance and possible hardware damage [3]. There is a need to increase the pool of autoignition data of methane-based fuels to gain a better understanding of the effect of fuel composition on ignition phenomena. Additionally, this data is needed for the development and validation of chemical kinetics models to predict ignition behavior of natural gas fuels.

The current study reports τ_{ig} measurements for natural gas components in an atmospheric pressure flow reactor and investigates the effect of higher-order hydrocarbon addition on methane τ_{ig} . Along with measurements of τ_{ig} of pure fuels methane, ethane, propane, and ethylene, this study investigates the effects of higher-

order hydrocarbon composition in methane-based fuel mixtures on the mixture's τ_{ig} . In order to explore this problem, the fuel components of interest and the ranges of possible natural gas compositions must be identified. Also, a comparative metric must be identified to evaluate the difference in ignition behavior of the various fuels and blends. Finally, comments can be made about the potential impact of these differences on ignition behavior.

1.1.1 Natural Gas Composition

Typical natural gas in the United States is composed of on average 93.9% methane, 3.2% ethane, 0.7% propane, 0.1% higher-order hydrocarbons. The balance of the composition is made up of carbon dioxide, oxygen, nitrogen, and hydrogen sulfide [4]. Further, U.S. natural gas composition can contain methane concentrations as low as 74.5% (by volume) and ethane and propane concentrations as high as 13.3%, and 23.7% (by volume), respectively [5]. Further compositional variation exists in natural gas from international sources; the ranges of worldwide natural gas constituent composition are given in Table 1.1 [6]. Because of the very broad range of compositions available, even just domestically, the potential for significant variation in fuel properties exists.

Table 1.1. Worldwide natural gas constituent composition ranges.

Constituent		Concentration
Methane	CH ₄	70-90%
Ethane	C ₂ H ₆	0-20%
Propane	C ₃ H ₈	
Butane	C ₄ H ₁₀	
Carbon Dioxide	CO ₂	0-8%
Oxygen	O ₂	0-0.2%
Nitrogen	N ₂	0-5%
Hydrogen sulphide	H ₂ S	0-5%
Rare gases	A, He, Ne, Xe	trace

1.1.2 Metric for Investigating Ignition Behavior

It was the goal of this study to investigate the ignition behavior of natural gas fuel components and mixtures. Autoignition delay time is a key characteristic of fuel chemistry that can serve as a key validation parameter in the development of chemical kinetics mechanisms [7].

Recent studies have shown that hydrocarbon chemistry characteristic of most natural gas compositions can be suitably represented by methane/ethane/propane mixtures [8, 9]. It was the goal of this study to provide reliable τ_{ig} measurements of methane/ethane/propane/ethylene pure fuels and their appropriate mixtures at low to intermediate temperatures and atmospheric pressure. In addition to providing insight into relative reactivities of the fuels studied, this data will extend the current database of available ignition data for natural gas fuels, providing much needed validation for the development of kinetics models in this parameter space. The experimental results expand the available oxidation database for natural gas-type fuels from previous

studies. Most τ_{ig} data exists for much higher pressures and temperatures than those studied herein and exist mostly for pure methane and methane blends containing very small concentrations of higher-order hydrocarbons.

1.1.3 Impact of Composition of Natural Gas on Combustion Performance

Variations in supply gas composition of even a few percent of higher-order hydrocarbon have been shown to significantly promote the ignition of methane-based fuels [2]. This is of serious concern in premixed systems such as industrial dry-low-emissions (DLE) gas turbines, which use aerodynamic methods to stabilize a premixed flame in a combustor. Variations in autoignition phenomena based on fuel composition could result in flashback and/or flame stabilization in unintended locations, causing performance problems and hardware damage [10]. Researchers have recognized the need to quantify the promotional effects of higher-order hydrocarbons on natural gas ignition and combustion processes [11].

Many researchers have addressed the need for a comparative index for use in evaluating the suitability of fuels of varying composition in fuel-flexible combustion systems. Richards et al. [12] provide an excellent analysis of the issues which need attention in premixed combustion with fuels of varying composition: flashback and flame holding, autoignition, static and dynamic stability, and emissions. Regarding autoignition, the authors present an Arrhenius correlation derived by Spadaccini and Colket [3] which relates τ_{ig} of a natural gas mixture to the concentrations of methane and other hydrocarbons. This correlation lumps all higher-order hydrocarbons in a single term. Elliot et al. [1] developed an approach to determine fuel compatibility

for combustion systems including an analysis of the Wobbe Index, Joule-Thompson cooling, and an enthalpy-temperature-pressure-dew point relationship. Lieuwen et al. [13, 14] found that flame speed and τ_{ig} of methane-based fuel blends behave highly non-linear with fuel composition, concluding that comparative indices such as the Wobbe index are not sufficient in capturing the impact of varying fuel composition on combustion device performance. They also conclude that the effects of fuel variability on combustor performance are very significant and require further investigation.

1.2 Previous Experimental Autoignition Delay Time Studies

Limited data exist for practical, non-dilute mixtures at the atmospheric pressure conditions and intermediate temperatures studied herein. Further, only very limited experimental τ_{ig} data exists for methane-based blends composed of more than 15% additives. The current study investigates the ignition of non-dilute pure fuels methane, ethane, propane, and ethylene; methane based fuel blends containing 0 to 100% additive (ethane and propane); as well as ternary combinations of methane, ethane, and propane. Further, the data collected spans the equivalence ratio, Φ , range from 0.5 to 1.25, providing a comprehensive matrix of pure fuels and fuel blends at conditions not previously covered in the literature.

The fuels of interest in this study have been the focus of many autoignition studies reported in the literature. The vast majority of autoignition studies have used shock tubes which are capable of creating high temperature and high pressure conditions. Lower temperature τ_{ig} measurements are typically not capable of being made in

shock tubes as the longer residence times required are not achievable in such a rig. The long residence times required call for low shock velocities and long tubes, which can lead to boundary layer build-up and bifurcated shocks which make controlling the experimental conditions very difficult [15].

Methane ignition has been most widely studied because of its prominence in natural gas. Ethane and propane autoignition has been studied less extensively, yet much ignition data exists for these fuels at higher temperatures and pressures than those of interest in this study. Ethylene autoignition has been widely studied for decades as it is an important fuel in high-speed propulsion engines [16]. Further, ethylene is an important intermediate in the combustion of higher-order hydrocarbons and as such, much ethylene τ_{ig} data has been collected for the purpose of validating chemical kinetics mechanisms designed to model the oxidation of higher-order hydrocarbons [10]. There have been many studies within the past three years which have collected experimental τ_{ig} measurements of methane-based fuel blends containing ethane and propane. As the issue of changes in ignition chemistry with variations in fuel composition has become apparent, researchers have begun to address the need for quantitative understanding of the effects of fuel composition on τ_{ig} and the need for further combustion mechanism validation.

1.2.1 Summary of Methane Autoignition Delay Time Studies

The availability, relative low-cost, and low-emissions qualities of methane-based fuels have made it the primary fuel for several industrial combustion technologies. As such, there has historically been an interest in studying various aspects of

methane-based fuel combustion. Hence, pure methane oxidation has been extensively studied experimentally for a number of years. A summary of the ignition delay time measurements made through 1969, mostly focusing on temperatures above 1400 K and pressures near atmospheric, is provided by Spadaccini and Colket [3]. In recent years, the parameter space for methane autoignition has been well investigated for pressures up to 300 atm and temperatures ranging from 849 K to 1600 K.

Petersen et al. [17] studied methane oxidation using shock tubes at Φ ranging from 0.5 to 4.0, pressures ranging from 9 atm to 480 atm and temperatures ranging from 1410 K to 2040 K for the purpose of providing validation data for chemical kinetics mechanisms. The authors found the most deviation in the available kinetics mechanism and their data in the high-pressure, fuel rich regime. Petersen et al [18] again studied methane autoignition in a shock tube this time at Φ ranging from 0.4 to 6.0, pressures ranging from 35 atm to 260 atm, and temperatures from 1040 atm to 1600 atm. The purpose of this study was to investigate the changes in activation energy (E_{act}) of the oxidation reaction for the different temperature regimes studied. The authors found a very significant decrease in effective E_{act} for the lower temperatures studied. Goy et al. [15] studied methane oxidation in shock tubes for pressures ranging from 5 atm to 20 atm and temperatures ranging from 852 K to 1428 K. The authors report ignition delay times for the purpose of comparison to, and improvement of, chemical kinetics predictive tools. They found very poor agreement between their results and predictions made by the GRI 3.0 mechanism [19], particularly at temperatures below about 1100 K. Huang et al. [20] also used a shock tube to study methane oxidation. τ_{ig} are reported for mixtures having Φ ranging from

0.7 to 1.3, pressures ranging from 16 atm to 40 atm, and temperatures ranging from 1000 K to 1350 K for the purpose of developing a chemical kinetics mechanism. Petersen et al. [2] again collected methane τ_{ig} for lean ($\Phi=0.5$) mixtures at pressures ranging from 0.54 atm to 25.3 atm and temperatures 1451 K to 2001 K for the purpose of making modifications to the GRI 3.0 mechanism to reflect the data collected. Finally, de Vries and Peteresen [21] measured autoignition of lean ($\Phi = 0.5$) methane mixtures at temperatures near 800 K and average pressures of 20 atm. The authors report that very weak ignition occurred at the low temperatures studied and suggest that further study is needed in this regime to validate the current kinetics models.

Most data available in the literature exists for higher temperatures and pressures than what is of interest in the current study. The data collected has been used to develop and validate chemical mechanisms; therefore these mechanisms are typically only thoroughly validated for higher temperatures and pressures. While many combustion systems, such as industrial gas turbine engines, operate at elevated pressures and thus benefit from experimentation in higher pressure regimes, other combustion devices such as some augmenters and boilers operate at pressures near atmospheric. The experiments conducted in the current study will fill in holes in the methane oxidation database, thus providing validation data for mechanism development in the atmospheric pressure regime, benefiting atmospheric pressure combustion systems.

1.2.2 Summary of Ethane Autoignition Delay Time Studies

Pure ethane oxidation has been less extensively studied than methane. However, because the combustion of higher-order hydrocarbons leads to the generation of C2 and C3 intermediates, a thorough understanding of the oxidation and ignition chemistry of ethane is essential. An excellent summary of available experimental ethane τ_{ig} measurements and their application to kinetics models is provided by de Vries et al. [22].

Only a handful of studies exist which report ethane τ_{ig} for temperatures near those of interest in the current study. Petersen et al. [10] report τ_{ig} of highly dilute stoichiometric ethane mixtures for temperatures ranging from 1230 K to 1840 K and near atmospheric pressure. The authors found that the available kinetics mechanisms predicted the experimental results well for less-dilute mixtures and suggest that more research is needed in the higher-concentration mixtures to improve the accuracy of the predictive mechanisms. deVries et al. [22] collected τ_{ig} for ethane mixtures ranging in Φ from 0.5 to 2.0, temperatures between 1218 K to 1860 K, and pressures between 0.57 atm and 3.0 atm. The authors developed a master correlation relating ignition delay time to temperature, E_{act} , and mixture concentration and report that the current kinetics mechanisms predict the ethane τ_{ig} remarkably well within the parameter space of their study. The authors do suggest that further study is required for higher pressures and fuel-rich mixtures. Because of the dearth of ethane τ_{ig} data within the temperature and pressure ranges of interest in the current study, the measurements reported herein will provide key validation points for chemical kinetics

mechanisms as well as provide a broader practical understanding of the ignition behavior of ethane.

1.2.3 Summary of Propane Autoignition Delay Time Studies

As with ethane, less propane τ_{ig} data is available than exists for methane. And again, because the combustion of higher-order hydrocarbons promotes the generation of C2 and C3 intermediates, it is of interest to characterize propane combustion chemistry.

Lefebvre et al. [23] studied lean propane and air mixtures at temperatures ranging from 833 K to 1000 K and pressures between 1 atm and 10 atm. This study measured τ_{ig} using a flow reactor where fuel and air flow rates were adjusted to initiate ignition at a specific axial location in the flow reactor. τ_{ig} was then calculated based on the fuel and oxidizer flow rates and this predetermined distance. This experiment provides data extracted at comparable temperature and pressure conditions to those of the current study. However, mixing time was not accounted for in Lefebvre's study, and as shown in the present study, mixing time contributes to the difference seen in the experimental results of the two studies. Brown and Thomas [24] collected propane τ_{ig} measurements for highly dilute stoichiometric mixtures at temperatures ranging from 1228 K to 1756 K and pressures ranging from 2.6 atm to 5.0 atm. The authors intended to provide some validation data for future researchers to incorporate into a chemical kinetics model. Cadman et al. [25] studied lean ($\Phi = 0.5$) propane autoignition in the temperature regime of interest (845 K to 1280 K) at pressures

ranging from 5 atm to 40 atm. This study was conducted in order to determine the effective E_{act} of propane oxidation within the parameter space and improve kinetics models within the temperature regime studied. Herzler et al. [26] studied lean ($\Phi = 0.5$) propane ignition for temperatures ranging from 900 K to 1300 K and pressures from 10 atm to 30 atm. The motivation for this study was to investigate current kinetics model predictions and provide validation data for kinetics model development. The authors found that the existing mechanisms do not predict autoignition of propane well at temperatures below 1050 K and suggest that further research be conducted in this parameter space.

1.2.4 Summary of Ethylene Autoignition Delay Time Studies

Ethylene oxidation has been widely studied as it is an important stand-alone fuel as well as a combustion intermediate. A comprehensive summary of the research that has been conducted to date on the ignition chemistry of ethylene is provided by Varatharajan and Williams [27]. τ_{ig} of ethylene are very quick compared to many higher order fuels for which ethylene is a decomposition intermediate. Thus, ethylene facilitates the propagation of higher-order hydrocarbon combustion and it is widely studied by many researchers to develop kinetics mechanisms.

Many ethylene autoignition studies have been conducted at conditions relevant to the temperature range studied herein. Baker and Skinner [28] collected shock tube τ_{ig} measurements for ethylene for Φ between 0.125 and 2, pressures between 3 atm and 12 atm, and temperatures between 1058 K and 1628 K. The authors developed an Arrhenius correlation for ethylene oxidation and determined

effective E_{act} of 34.2 kcal/mol. Lefebvre et al. [23] collected ethylene τ_{ig} using the same reactor and technique described for the propane measurements. Measurements were made between 1 atm and 10 atm and 813 K and 944 K. Brown and Thomas [24] collected shock-tube ignition delay time experimental data for dilute stoichiometric ethylene mixtures at pressures averaging 2 atm, and temperatures ranging from 1073 K to 2211 K. The authors mainly focused on the effects of dilution on τ_{ig} and conclude that the available kinetics mechanisms overpredict the trends seen in their experiments. Colket and Spadaccini [29] collected shock tube τ_{ig} measurements of dilute ethylene mixtures for pressures ranging from 4.8 atm to 7.5 atm and temperatures ranging from 1127 K to 1414 K. The authors concluded that the available empirical correlations for τ_{ig} did not agree with their measurements, thus new correlations were developed. Cadman et al. [30] studied stoichiometric and lean ($\Phi = 0.5$) ethylene mixture ignition in a shock tube at temperatures ranging from 800 K to 1620 K and pressures ranging from 2 atm to 6 atm. This study used Schlieren photography to identify the different regimes of ethylene combustion, and in the process determined τ_{ig} which have been used in ethylene mechanism validation. Petersen et al. [10] have studied dilute ethylene mixtures of $\Phi = 0.5$ and 1 at atmospheric pressure and temperatures ranging from 1115 K to 1900 K and have collected τ_{ig} measurements. The authors determined an E_{act} of 26.6 kcal/mol for ethylene oxidation in this temperature regime. Further, a detailed submechanism for hydroxyl radical quenching was added to the existing chemical kinetics mechanisms to improve the accuracy of the models in predicting the data reported in this study.

Sims et al. [31] measured ethylene τ_{ig} at 16 atm and 850 K at Φ ranging from 2.6 to 3.3 in a flow reactor. The authors found good agreement with model predictions of their data at the conditions investigated. Finally, Kumar et al. [32] measured τ_{ig} of dilute ethylene mixtures in a rapid compression machine. The experimental conditions studied were pressures from 15 atm to 50 atm, and temperatures ranging from 850 K to 1050 K. The authors identified several reactions within the chemical kinetics mechanisms that required adjustments of rate parameters to better predict their measurements.

Many detailed kinetics mechanisms have been developed to model ethylene oxidation. These mechanisms rely on experimental measurements of combustion phenomena such as ignition delay times, blow out temperatures, and flame speeds. Several ethylene combustion mechanisms are discussed in detail in Chapter 3 where an evaluation of the experimental apparatus using ethylene τ_{ig} measurements is discussed.

1.2.5 Summary of Methane-Based Fuel Mixtures Autoignition Delay Time Studies

In recent years, there has been increased interest in studying the promotional effects of concentrations of higher-order hydrocarbons on methane ignition. The conclusions drawn from researchers in this area indicate that the effects are significant, current kinetics models do not reflect these effects well, and further study is recommended to explore the effects at broader conditions. As was the case for the

pure fuels, the conditions studied for the methane-based fuel mixtures were mostly at higher pressures and temperatures.

de Vries and Petersen [21] provide an thorough summary of experimental studies to date which have investigated the effects of higher-order hydrocarbons on methane ignition behavior. Goy et al. [15] studied the effect of significant (15% by volume) additions of ethane and propane on methane autoignition delay for temperatures ranging from 952 K to 1428 K and pressures up to 20 atm using a shock tube.

Significant changes in E_{act} for the fuel blends was observed, which were not captured by available kinetics models. Petersen et al [5] conducted shock tube τ_{ig} experiments for methane/ethane (90/10% and 70/30%) and methane/propane (80/20%) fuel blends for pressures up to 25 atm and temperatures ranging from 1091 K to 1655 K.

Significant reductions in τ_{ig} were observed for the mixtures compared to pure methane measurements. The experiments resulted in the modification of some reaction parameters in the GRI 3.0 mechanism. Huang and Bushe [33] studied the effect of ethane and propane on methane autoignition for temperatures ranging from 900 K to 1400 K and high pressures (16 atm to 40 atm) using a shock tube. The methane/ethane mixtures studied were composed of 96.4/3.6%, 93/7%, and 90/10%. The methane/propane mixtures studied were composed of 98.7/1.3%, 97/3%, and 95/5%. The authors also studied a ternary methane-based mixture composed of methane/ethane/propane in the following ratio: 95/3.7/1.3%. Significant promotional effects of ethane and propane on methane autoignition were observed and an analytical study of the important reaction pathways of the various fuel systems was performed. Antonovski et al. [9] collected τ_{ig} measurements for several ternary fuel

mixtures composed of methane, ethane, and propane for pressure conditions up to 58 atm and temperatures ranging from 1032 K to 1577 K using a shock tube. The fuels studied were composed of the following ratios of methane/ethane/propane: 90/7/3%, 70/15/15%, and 70/20/10%. Antonovski et al. found increasing concentrations of higher order hydrocarbons to significantly decreased fuel mixture τ_{ig} . The most recent study by de Vries and Petersen [21] presented experimental τ_{ig} data for methane blends containing up to 50% ethane and 25% propane for temperatures ranging from 811 K to 1107 K and pressures around 20 atm. Promotional effects of higher-order hydrocarbons on methane mixture autoignition were again observed. The authors indicate that within the temperature and pressure ranges studied, little difference was observed between C2 to C5 component addition of 25-50% mixture composition. Further exploration of the promotional effect of concentrations of higher-order hydrocarbons on methane fuel mixtures was recommended at broader temperature and pressure regimes.

1.3 Overview of the Presentation of the Current Study

The following is an overview of the organization of the current presentation. A description of the experimental apparatus is presented which includes a discussion addressing the experimental procedure, a discussion of the required characterization of the experimental system, and a discussion of the parameters investigated. An explanation of the determination of the measured values of τ_{ig} follows. This includes a very detailed analysis of the validation of the experimental apparatus which

involved comparing ethylene τ_{ig} measurements to the results of a chemical reactor model specifically developed to represent the flow reactor. The experimental results and a discussion of the findings are then presented. τ_{ig} measurements are reported graphically and in table form for the pure fuels, binary, and ternary methane-based fuels. The results are displayed along with Arrhenius correlation fits and compared with chemical kinetics mechanism predictions as well. Conclusions summarizing the findings are then presented.

Chapter 2: Experiment

The goal of this study was to gain a better understanding of the effects of natural gas composition on fuel ignition behavior. Autoignition delay time is a key characteristic of a fuel which indicates its relative reactivity at given conditions. Further, τ_{ig} measurements are extremely useful as validation data in the development of chemical kinetics predictive tools. Measurements of autoignition delay times for a variety of single and multiple-component fuels were made in an atmospheric flow reactor. A description of the experimental apparatus as well as a discussion of the execution of the experiments follows. Also, the experiment methodology and the selection of fuels and conditions are discussed.

2.1 *Experimental Setup*

The autoignition delay measurement apparatus is a modified version of a rig previously used to measure autoignition delay times of kerosene-type fuels [34, 35]. A schematic of the experimental system is provided in Figure 2.1, a diagram of the flow reactor apparatus is provided in Figure 2.2, and a closer view of the fuel and air mixing zone is provided in Figure 2.3. In Gokulakrishnan's work [34, 35], a vaporizer was required to pre-vaporize the liquid fuel before it entered the flow reactor. In this study, the vaporizer was not required as all the fuels studied were gaseous. The flow reactor apparatus consisted of a fuel preheating system, an air preheating system, fuel and air delivery systems, a premixing section, and a test

section. Preheated fuel was injected into a preheated air stream and ignited at some distance down the reactor. The time difference between when the fuel was injected into the air stream and when the fuel and air mixture ignited was defined as the total ignition delay time inclusive of the transit time required for the fuel to reach the steady temperature zone of the reactor. An explanation of how this transit time was accounted for is included in the apparatus validation section in Chapter 3. The actual ignition delay time, then, was determined as measured delay time minus the transit time. Injection time was identified through the use of an electronically controlled injection valve and ignition events were identified using a photomultiplier tube equipped with a CH radical filter.

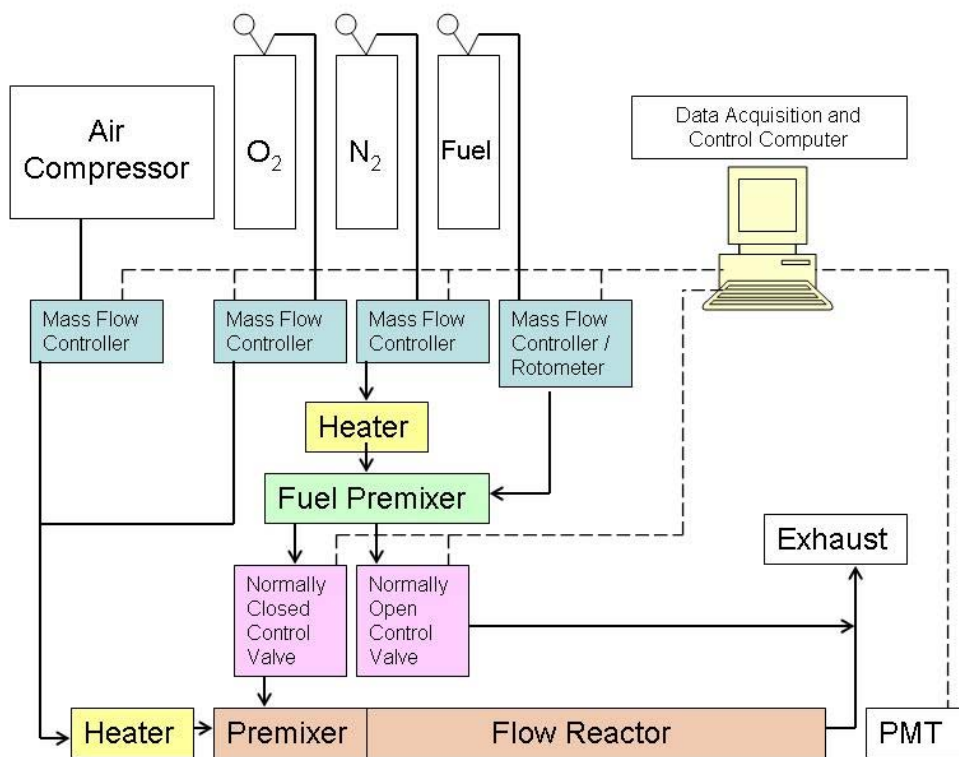


Figure 2.1. Experimental system schematic.

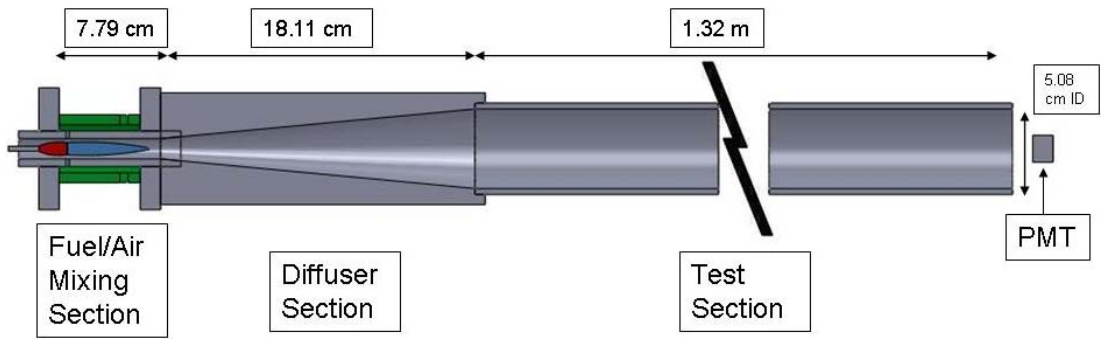


Figure 2.2. Experimental flow reactor apparatus.

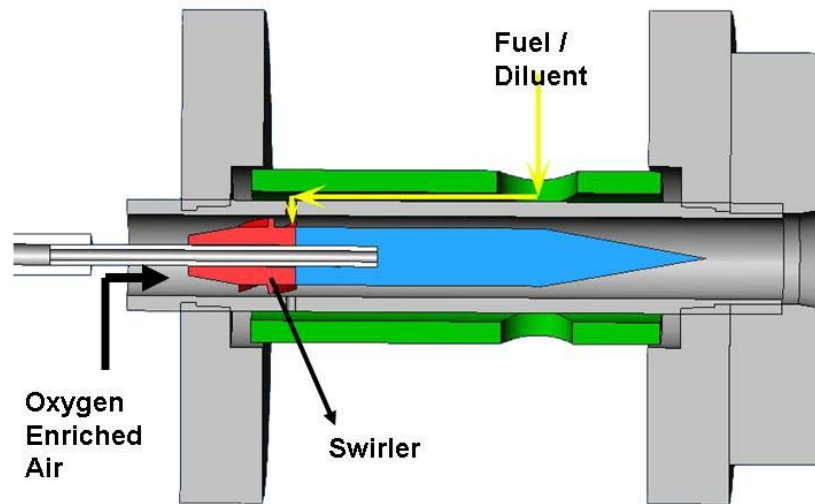


Figure 2.3. Fuel and air mixing section of flow reactor apparatus.

2.1.1 Fuel and Air Supply, Preheat, & Delivery

Fuel, air, nitrogen, and oxygen were metered with a series of mass flow controllers and rotometers. Air was supplied by an Ingersol Rand 7.5 HP air compressor capable of delivering 680 LPM at 175 psig. The oxygen content of the compressed air was measured using a Seimens Oxymat 5E oxygen analyzer and found to be 21.0%. This gas analyzer has an accuracy of +/- 1% of full scale where the full scale range of this instrument is 25% oxygen. All other gases were supplied with compressed gas cylinders. Table 2.1 lists the compressed gases used in the experiments along with their grades and purities.

Table 2.1. Grades and purities of gases.

Compressed Gas	Grade	Minimum Purity (%)
Nitrogen	Zero	99.998
Oxygen	Zero	99.8
Methane	Research	99.999
Ethylene	Ultra High Purity	99.9
Ethane	Instrument	99.5
Propane	Instrument	99.5
Carbon Dioxide	Instrument	99.99

Air, nitrogen, and oxygen were metered using Porter 200 Series mass flow controllers. Fuel for the single-component autoignition delay experiments was metered using an MKS 1179 mass flow controller. For the multi-component fuel autoignition experiments, methane was metered using the MKS 1179 mass flow controller while the other fuel components were metered using rotometers.

All mass flow controllers and rotometers were calibrated at the test flow rates using a displacement gas meter to ensure accurate gas delivery. Each mass flow controller was found to meter within 1% of the set-point flow rates of air, oxygen, and nitrogen, and fuel.

Once metered, the fuels were mixed in a heat-traced section of 6.35 mm ID tubing having a length of 30 cm as well as several bends. The high L/D ratio and tubing bends were included in the design to promote fuel mixing. The fuel then entered a heating chamber where it was mixed with a hot nitrogen stream. This nitrogen was heated to 758 K using a triple-pass Convectorics 2 kW flow heater. Because the flow rate of the fuel was changed to collect data at various Φ , the nitrogen preheat temperature was controlled using a thermocouple placed inside the plenum where the fuel and nitrogen were mixed. Figure 2.4 is a schematic of the fuel and diluent mixing chamber. Fuel entered the chamber through a nozzle located in the center of the plenum. The preheated nitrogen entered the plenum through the top of the chamber and the diluent and fuel mixture exited the plenum through the bottom of the chamber. The outer shell of the plenum was maintained at 758 K using heating tapes; fiberglass insulation was used to minimize the heat losses from the plenum. Further, beads were used in the bottom of the plenum to provide thermal mass to the plenum to retain heat in the chamber and promote heat transfer to the fuel/nitrogen mixture. Fuel preheat temperature was chosen both to minimize the temperature differential between the reactor, fuel, and oxidizer and to minimize premature fuel decomposition before the fuel enters the flow reactor. Natural gas fuels can begin to decompose at temperatures above about 850 K [36].

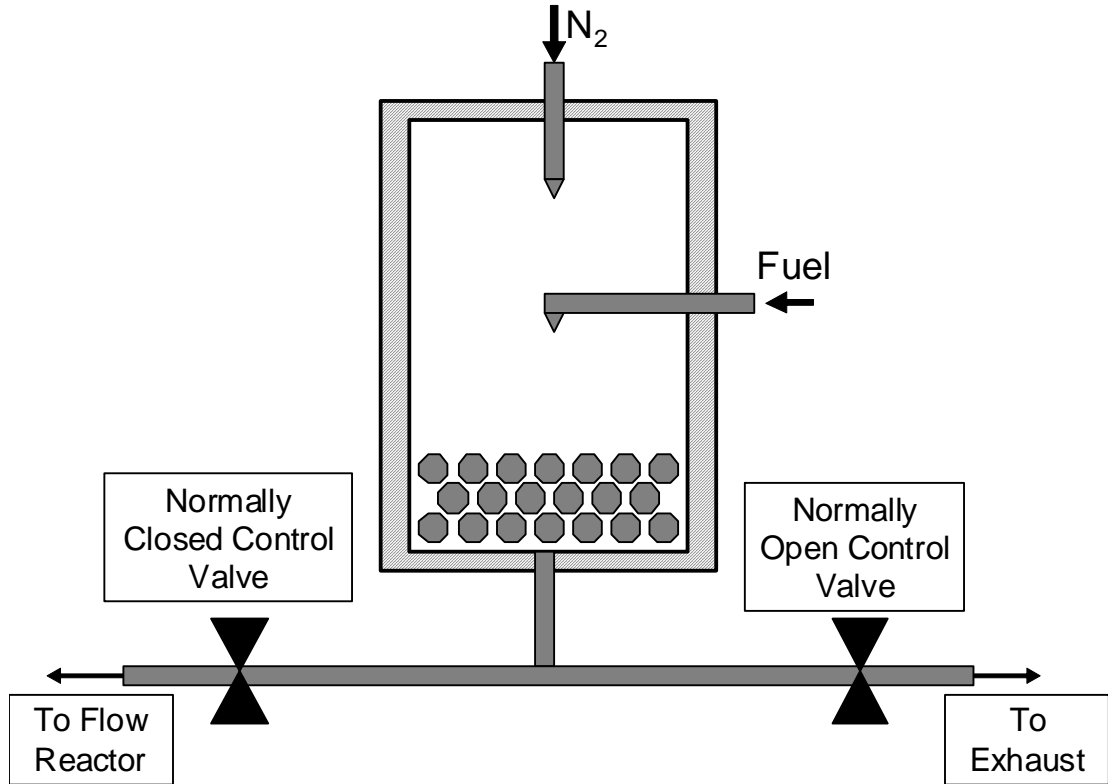


Figure 2.4. Schematic of fuel & diluent mixing plenum.

Once the preheated fuel and nitrogen were combined in the plenum, the mixture flowed through an elbow mixer to ensure adequate mixing of the nitrogen and fuel. Figure 2.4 shows that there were two flow paths controlled by electronic solenoid valves downstream of the elbow mixer. One solenoid valve was normally open when no power is supplied and allowed the fuel and diluent to flow to the exhaust. The other solenoid valve was located between the elbow mixer and the fuel injection site in the flow path and was normally closed when no power is supplied. To begin an ignition test, power was supplied simultaneously to both solenoid valves, closing the path to the exhaust and opening the path to the fuel injectors. The diluent and fuel

mixing section and tubing to the injection site was insulated to reduce heat losses to the environment.

The oxidizer stream was preheated separately from the diluent/fuel stream. At the initiation of a test, the fuel mixture was injected into the oxidizer stream. Because the fuel was preheated using hot nitrogen, oxygen was added to air of the oxidizer stream so that when the fuel mixture was injected into the oxidizer, the fuel burned in air composed of 20.95% oxygen and 79.05% nitrogen.

Downstream of their respective mass flow controllers, the oxygen and air were mixed and heated to 873 K using an Osram Sylvania 1.6 kW flow heater. The enriched air then entered an annulus equipped with a swirler before entering the air and fuel pre-mixing section of the reactor. Because the air and oxygen travel through a flow heater having a dimensionless L/D ratio of greater than 10 as well as a swirler, they were assumed to be well-mixed.

A schematic of the fuel and diluent injection system is shown in Figure 2.3. The fuel and diluent were introduced through two injectors located 180° from one another and perpendicular to the swirling, annular, oxygen-enriched air flow. The swirling oxygen-enriched air enhanced the mixing of fuel and air by creating turbulent eddies. The flow path is then expanded as the fuel and air mixture enters a diffuser which increases the diameter of the flow path to match the entrance of the flow reactor. The expanding section also serves to generate eddies which further enhance mixing. An investigation into the mixedness of the fuel and air was conducted and is discussed in the apparatus investigation section. The fuel and air

mixing section, including the injection section and the diffuser, were heavily insulated with fiberglass to reduce heat loss from the fluid.

2.1.2 Flow Reactor

The flow reactor used was a 1.32 m long alumina (Al_2O_3) tube of 5.08 cm inside diameter heated by a three zone electric heater. The manufacturer of the reactor including the tube, heater, and control system was Mellon and the model numbers are PS205-230 and SV13 for the temperature controllers and heater, respectively. The temperature zones of the heater were individually set such that the axial temperature through the reactor remained as consistent as possible as to create a uniform test section in the reactor. Further, the heaters were in a well-insulated ceramic enclosure, and the test section is assumed to be an adiabatic reactor. The tube functions as a plug flow reactor; the swirling fuel and air mixture travels down the tube as a radially well-mixed plug until the mixture ignites at some distance along the reactor. Because the flow reactor is at a constant temperature, the time between fuel and air mixing and ignition is defined as the τ_{ig} of the mixture at that specific temperature. The measurement of τ_{ig} using the experimental apparatus is inclusive of the mixing time and the chemical reaction time. Because the mixing time can not be experimentally measured, the time between fuel injection and adequate mixing was analytically determined using a chemical reactor model. The resulting calculated mixing time was then subtracted from the experimental measurement, resulting in a corrected τ_{ig} which is representative of only the time associated with the initiation of a chemical reaction. A detailed explanation of the methodology used in determining the mixing

time is included in the apparatus validation section in Chapter 3. The average Reynolds number of the fuel and air fluid flow in the flow reactor was 408, indicating smooth, constant, laminar flow.

2.1.3 Photomultiplier Tube

CH radical emission, associated with ignition of the fuel, was identified with a Hamamatsu R928 side-mount photomultiplier tube (PMT) equipped with a 430 nm narrow band filter. This filter allows only chemiluminescence emitted by CH* radical excitation at 430 nm to pass. The PMT was mounted at the exit of the tube such that the photo detector had a direct line of sight axially down the tube. During an ignition event, CH* radicals emitted light at the 430 nm. The photo detector recorded the chemiluminescence emission of the ignition event. The exhaust from the exit of the flow reactor was directed upwards using a tee into an exhaust hood. The PMT was mounted at the exit of the tube on the straight section of the tee and was protected by a quartz window within the tee.

2.1.4 Data Acquisition & Control

A data acquisition and control computer collected the relevant signals from the system and controlled the mass flow controllers. National Instrument's Labview 7.1 was used to develop software to log the signals from the control valves and the PMT, as well as control the mass flow controllers. The signals necessary to determine the autoignition delay time measurement were the opening of the fuel injection control

valve and the photomultiplier tube response. These signals were logged at a rate of 10 kHz, giving the ignition delay time measurement a resolution of 0.1 milliseconds.

2.2 Experimental Procedure

The experimental procedure involved setting the flow reactor to the appropriate test conditions including temperature and flow rate, executing a test, and determining the ignition delay time. The testing procedure began with allowing the flow heaters, heat trace, and flow reactor heaters to equilibrate to the appropriate test temperatures while flowing the appropriate flow rates of fluids through the flow paths. A test was begun by introducing fuel into the oxidizer stream using the injection control valve. Finally, the resulting ignition delay time result was determined by extracting the difference between the fuel injection time and the identification of ignition time by the PMT.

The procedure for running an experiment began with allowing the oxidizer and fuel/diluent heater, heat trace, and test section heaters to reach an equilibrium test temperature. The three flow reactor heaters were set to the test temperature set points; the heater temperatures required for constant axial reactor temperatures are discussed in the apparatus investigation section. Air and oxygen flow rates were set to 85.0 slpm and 4.5 slpm respectively and the oxidizer flow heater was set to 873 K. Nitrogen diluent flow rate was set to 17.0 slpm and the diluent flow heater was set to 758 K. The heating traces on the fuel delivery tube, plenum, and diluent/fuel transfer tube were controlled to 758 K as well. Fuel flow rate varied to control Φ . As the fuel flow rate was changed, the controllers responsible for maintaining the temperatures of

the fuel delivery tube, plenum, diluent/fuel tube, and diluent preheat compensated by adjusting heater power to maintain temperatures at the set points. All flows and temperatures were maintained for several minutes between tests to ensure the conditions had equilibrated and steady state had been reached.

To begin an experiment, power was simultaneously supplied to both of the solenoid valves controlling the fuel flow path. This event changed the flow path of the fuel and diluent from the exhaust to the injectors, introducing fuel into the oxidizer stream. The time at which power was supplied to the control valves was recorded by the data acquisition system and referenced as the fuel injection time. The time at which chemiluminescence emissions were identified by the PMT was recorded as the ignition time. The difference between the injection time and the ignition time was defined as the ignition delay time inclusive of the fuel transit time at that test temperature. The fuel transit time is the time it takes for the fuel to reach the constant temperature section of the flow reactor from the fuel injectors. Again, an explanation of how this time was determined is found in the apparatus validation section in Chapter 3.

Because each ignition event resulted in an exothermic reaction which heated the reactor, the test section was allowed several minutes to equilibrate to the next test condition before another experiment was performed. Repeats of each experimental condition were completed and the conditions were randomized as to minimize systematic errors in the data collection process.

2.3 Apparatus Characterization

The difficulties of making τ_{ig} measurements in flow reactor apparatus include attaining a zero temperature gradient at the entrance to the reactor and achieving instantaneous mixing [35]. In order to promote confidence in the resulting τ_{ig} measurements, several characteristics of the flow reactor required investigation. Firstly, axial temperature profiles of the flow reactor were measured in order to gain an understanding of what the set points of the reactor temperature controllers need to be for each test temperature. The temperature profiles of the flow reactor at each test temperature also allowed insight into where the constant temperature section of the flow reactor began. Secondly, an investigation into the quality of the mixing of diluent/fuel in the enriched air stream was conducted. This study addressed the assumption that the fuel and oxidizer were well mixed in the test section, which is a key assumption in ignition delay studies.

2.3.1 Flow Reactor Axial Temperature Profiles

The effect of temperature on autoignition delay time for components of natural gas was a key objective of this study. Six test temperatures ranging between 931 K and 1137 K were chosen as the test conditions for these experiments. In order to perform autoignition delay time measurements at these test temperatures, a constant axial temperature profile was required in the flow reactor. The temperature of the flow reactor was controlled by three independent heaters, and the axial profile was influenced by the heat input of each of these heaters as well as the velocity and temperature of the fluid passing through the reactor.

Because the bulk flow rate and reactor inlet temperature of the gases flowing through the reactor varied very little between tests, the flow reactor temperature was thus only a function of the heat input of the reactor heaters. Six test temperatures were chosen for autoignition measurements. For each test temperature, the heater controller set points were adjusted to maintain a constant axial temperature.

The procedure for achieving this constant temperature began with setting the flow rate of the fluid passing through the reactor. Air was used as the sole fluid for determining the reactor heater set points. The fuel of course was not added to the air as this would result in ignition in the reactor. The air flow rate was set to 112.4 slpm. This flow rate accounts for the flow rates of air (85 slpm), nitrogen (17 slpm), and oxygen (4.5 slpm) used in the each test condition. Additionally, a value of 5.9 slpm of air was used as an approximate flow rate for the fuel, making the total fluid flow through the reactor 112.4 slpm. This approximation of the fuel flow rate 5.9 slpm was chosen as an average fuel flow rate for all the test cases performed. The fuel flow rates ranged from 2.2 to 13.9 slpm. Because the fuel flow rate only made up between 2 and 12% of the total flow through the reactor, it was assumed that the variation in fuel flow rate did not affect the reactor temperature significantly.

The preheat temperatures for the flow heaters and transfer lines were set to the test conditions. The oxidizer preheater was set to deliver the air at 873 K and all heat tracing along the fuel injectors and expansion diffuser was powered as well. A thermocouple was inserted along the centerline of the reactor at the reactor exit and temperature measurements were made every 15 cm along the reactor axis. Measurements were made from the reactor exit to the beginning of the diffuser.

Adjustments were made to each of the reactor heaters to maintain as close to a constant temperature along the reactor axis as possible for each test temperature. Figure 2.5 shows the reactor temperature profiles for each test temperature as well as the set points for the reactor heater controllers. The heater controllers are numbered 1 through 3 such that heater controller 3 controls the temperature of the reactor closest to the reactor entrance and heater controller 1 controls the temperature of the reactor closest to the reactor exit.

There is a significant temperature gradient at both the inlet and outlet of the reactor. This is primarily due to the lack of heat input to the sections of reactor tube which extend approximately 20 cm from the entrance and exit of the reactor heater. The gradient at the outlet is of little significance as during a test, ignition occurs in the hotter, upstream portion of the test section. The temperature gradient at the entrance to the reactor is of much greater significance as it has a direct impact on the measurement of the autoignition delay time. The diffuser and the unheated portion of the test section were heated with heating tapes and insulated to minimize the heat loss from this section of the apparatus. There is a significant delay associated with the time required for the fuel and oxidizer to reach the steady, constant-temperature test section of the reactor from the fuel injection site. An explanation of the accounting of this time delay is provided in the apparatus validation section in Chapter 3.

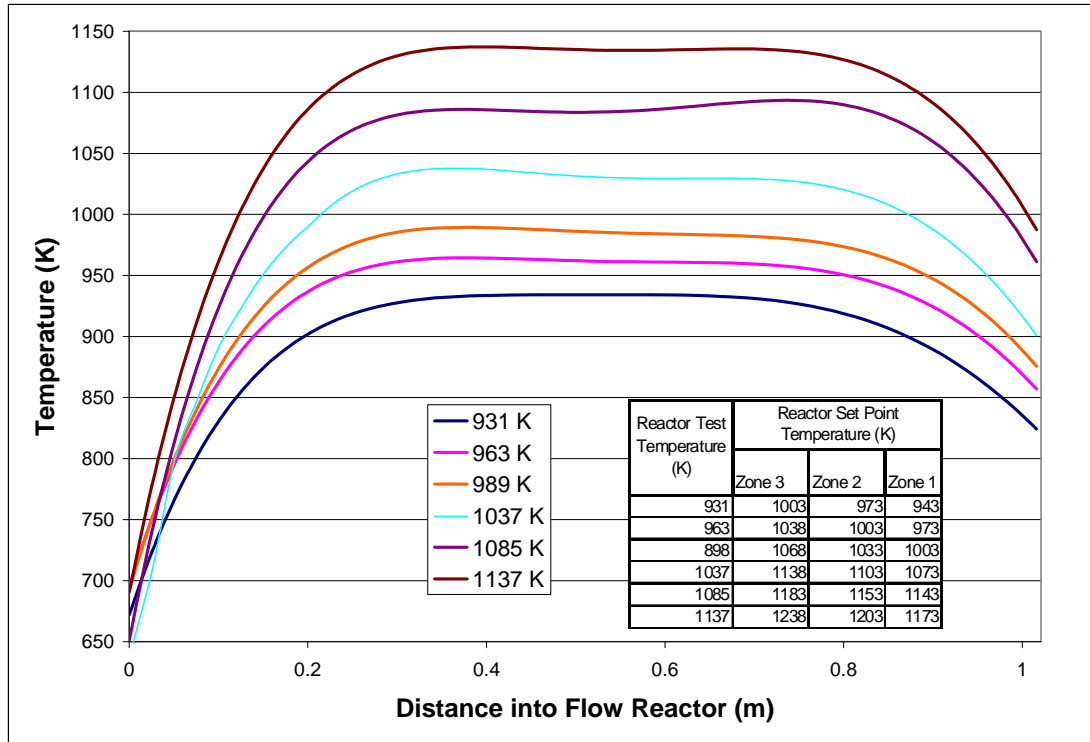


Figure 2.5. Flow reactor axial temperature profiles.

2.3.2 Fuel and Oxidizer Mixedness Investigation

The autoignition delay time measured in these experiments is defined as the time required for a well-mixed fuel and oxidizer mixture to ignite at certain steady temperature and pressure conditions. An important assumption in reporting autoignition delay measurements is that the fuel and oxidizer are, in fact, well-mixed. One serious challenge in flow reactor experimentation is quick and adequate mixing of fuel and oxidizer at the entrance to the reactor [34, 35]. In the current study, fuel was injected into turbulent, swirling air to promote adequate mixing as described in Figure 2.3. In order to validate the assumption that this injection and mixing technique adequately mixed the

fuel and air, a method was developed to measure the quality of the mixing of a fuel surrogate in air.

The degree of mixing of the fuel and oxidizer at the test conditions was investigated using a quantifiable fuel surrogate, CO₂. This investigation was performed prior to this autoignition study on the same flow reactor rig [35]. While maintaining all other test conditions, CO₂ was substituted for the fuel stream and a gas analysis probe was inserted through the exit of the flow reactor. The probe drew the gases from the locations in the flow reactor and delivered them to a gas analysis system capable of measuring CO₂ and O₂ concentration. The probe was mounted to a translation stage that could move the probe radially in increments of 1 mm. Measurements of CO₂ and O₂ concentration were taken in horizontal and vertical radial directions at 1 mm increments at 1", 2", and 3" axial positions from the exit of the diffuser. Figure 2.6 shows typical concentrations of CO₂ and O₂ both as a function of radial distance across the reactor as well as axial distance down the reactor.

The flow rates used in this mixedness study were 7.20 slpm CO₂ and 115.29 slpm Air. This translates to a mixture concentration of 5.88% CO₂ and 19.67% O₂ (mole percentages). As indicated by Figure 2.6, the mixture in the flow reactor was fairly well mixed radially; the concentration profiles at each axial distance have little variation in concentration. Also, the figures indicate that by the time the mixture had reached 2 to 3 inches into the flow reactor test section, the injected fluid and the air were well mixed. This is indicated by the fact that the CO₂ and O₂ concentrations have reached their mixture concentrations defined above at 2 to 3 inches into the reactor.

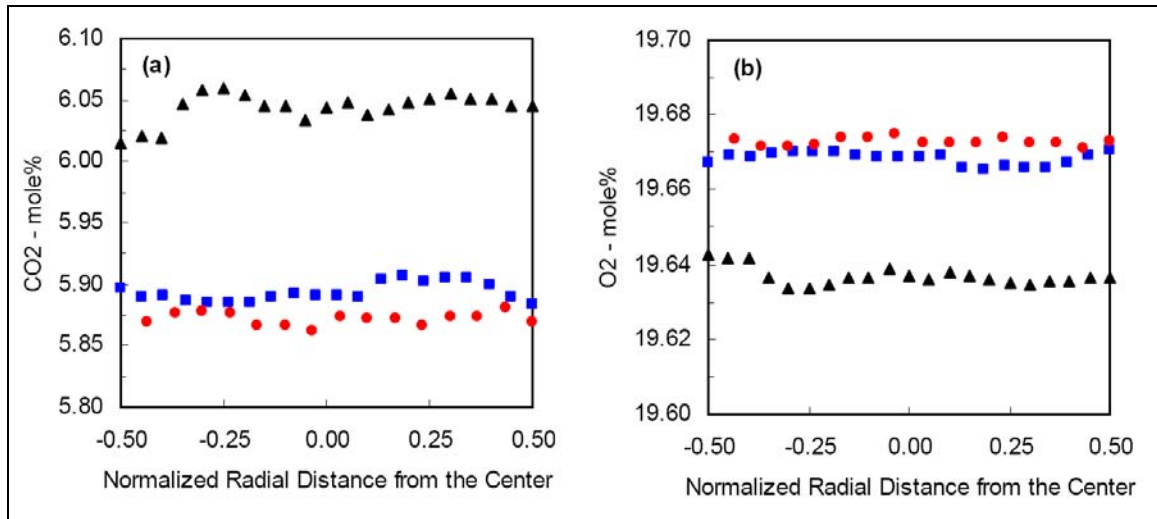


Figure 2.6. Radial species profiles of CO₂ (a) and O₂ (b) at three axial locations within the test section.

Key: axial distance from the exit of the diffuser: ▲ - 1"; ● - 2"; ■ - 3"

2.4 Design of Experiment

The objectives of this study were to measure ignition delay times for methane, ethane, and propane, as well as investigate the effect of ethane and propane addition to methane on ignition delay time. Further, it was of interest to examine the effect of temperature and fuel concentration on the ignition delay time of natural gas fuel components and mixtures. One of the desired outcomes of this research was to provide useful data for developing kinetics models for combustion device applications. Improvements made to predictive tools will benefit the combustion community including industries involving gas turbine, spark ignition, diesel, and homogenous charge, compression ignition internal combustion engines as well as industrial burners [7]. In order to accomplish the desired objectives, a scope was determined for the experiment defining fuel compositions,

temperature, pressure, and Φ conditions which have not been previously studied. Table 2.2 provides the fuels and conditions studied in this experiment.

Table 2.2. Experimental conditions of temperature, pressure and equivalence ratio as well as a description of the pure fuels and fuel blends studied.

Fuels	Pure	Methane, Ethane, Propane
	Binary	Methane with Ethane, Propane, or Ethylene (5, 10, 25, 50, 75% by volume addition)
	Ternary	85% Methane, 10% Ethane, 5% Propane by volume 50% Methane, 25% Ethane, 25% Propane by volume
	CO ₂ Addition	75% Methane, 25% Ethane, diluted with 5 and 10% CO ₂ by volume
Temperature	931, 963, 989, 1037, 1085, 1137 K	
Pressure	Atmospheric	
Equivalence Ratio	0.5, 0.75, 1.0, 1.25	

2.4.1 Temperature, Pressure, & Equivalence Ratio Range Selection

In order to investigate the effect of fuel composition on ignition delay time as well as provide data which would be useful in improving kinetics predictive tools for use in combustion applications, it was important to attempt to fill in some of the gaps within the pool of available ignition delay time data for the fuels of interest. Much data has been produced in the literature for ignition delay time measurements for natural gas fuels at pressures above atmospheric and at temperatures above 1200 K. However, few data exist for the atmospheric conditions and temperatures studied herein. Further, only very limited experimental τ_{ig} data exists for methane-based blends composed of more than 15% additives. The current study investigates the ignition of methane-based fuel blends containing 0 to 100% additive (ethane, propane, and ethylene) as well as ternary

combinations of methane, ethane, and propane. Further, the data collected spans the Φ range from 0.5 to 1.25, providing a comprehensive matrix of fuel blends and conditions.

Ignition delay data in this temperature regime is of interest for natural gas fuels as many combustion systems, including gas turbines, operate at inlet temperatures below 1200 K [31]. Further, researchers have recently found that ethane and propane have had significant promotional effects on ignition delay time of methane for temperatures lower than 1100 K [33]. The temperature range studied herein was therefore constrained to less than 1200 K; the lower limit of the temperature range studied was defined by the apparatus limitations. Given the geometry and flow parameters of the experimental apparatus and test conditions, the flow reactor had a maximum residence time of about 2 seconds. Therefore, a lower limit on temperature was chosen as to capture fuel ignition delay times up to 2 seconds. Six reactor temperatures were chosen as test temperatures: 931 K, 963 K, 989 K, 1037 K, 1085 K, and 1137 K. While not all fuels and fuel mixtures would auto-ignite at atmospheric conditions at the lower test temperatures, they would ignite for some of the test temperatures, indicating that the lowest temperature ignition delay time data achievable for that fuel using the test apparatus was measured.

The configuration of the flow reactor was such that test pressures other than atmospheric would be unfeasible. In order for ignition delay time measurements to be made at pressures above or below atmospheric pressure using the flow reactor, the entire reactor would have to be placed in a pressure vessel, which would be very cumbersome. It is recognized that many combustion devices operate at high pressure (above 15 atm) and ignition delay time data at these pressures is valuable for optimizing kinetics models [2,8-9, 12, 15, 17-18, 20-21, 23, 25-26, 31-32, 37-45]. For the purposes of this study,

however, atmospheric pressure measurements were adequate. The promotional effect of increased pressure on ignition delay times of natural gas fuels has been well documented [23] and has been addressed in chemical kinetics mechanism development [7, 27, 40, 44-46].

Equivalence ratio is a key characteristic of a combustion system [12] and it is very common for premixed combustion devices to operate in a lean environment to reduce emissions [4, 34]. Controlling the Φ of a combustion system effectively controls the flame temperature, which has a very significant effect on NO_x production [47]. The Φ investigated in the study were selected in order to examine the effect of fuel concentration on ignition delay time for the fuels studied. Further, the selected Φ were chosen such that lean, stoichiometric, and rich mixtures were analyzed: $\Phi = 0.5, 0.75, 1.0,$ and 1.25 . This range of Φ was designed both to provide an understanding of the effect of fuel concentration on ignition delay time and to generate validation data for kinetics modeling tools.

2.4.2 Fuel Selection

The fuels studied in this research were selected to make a valuable contribution to the combustion community with respect to natural gas ignition behavior. Natural gas composition varies widely globally and to a lesser extent, within the United States. In the United States, a typical natural gas may consist of 93.9% methane, 3.2% ethane, and 0.7% propane with the remaining composition made up of higher-order hydrocarbons, carbon dioxide, oxygen, nitrogen, and hydrogen sulfide [4, 6]. U.S. natural gas composition can vary widely and can contain methane concentrations as low as 74.5%

(by volume) and ethane and propane concentrations as high as 13.3%, and 23.7% (by volume) [5]. While methane is the dominant species in natural gas, other hydrocarbons present in the composition can greatly affect the fuel's combustion [48]. Based on the research of Turbiez, et al., natural gas combustion can be appropriately represented by methane/ethane/propane mixtures [33, 48]. Therefore, the ignition delay characteristics of methane, ethane, and propane were studied.

Methane, ethane, and propane were studied individually as pure fuels. τ_{ig} were measured for these fuels at the reactor test temperatures, pressure and Φ given above. Also, the effect of propane and ethane addition on methane autoignition delay time was investigated. Further, the effect of ethylene addition on methane τ_{ig} was studied as well. Ethylene typically does not make up a significant portion of natural gas. Therefore, these measurements may not have direct relevance in natural gas combustion applications. However, because ethylene is a relatively reactive gaseous fuel, applications could exist where it would be advantageous to dope methane or natural gas with ethylene in order to significantly affect the ignition properties of the gas mixture. The following binary mixtures of additive (ethane, propane, and ethylene) and methane were studied: 5%, 10%, 25%, 50%, and 75% (by mole). More binary mixtures made up of smaller amounts of additive rather than larger were tested because natural gas typically is composed of small amounts of ethane and propane with larger amounts of methane. By testing such a broad range of binary mixtures, a sizable amount of data was generated which will be useful in both understanding the effect of adding various amounts of ethane, propane, and ethylene to methane on τ_{ig} , as well as providing validation points for kinetics mechanism development.

τ_{ig} measurements were also made for ternary mixtures of methane, ethane, and propane. Two mixtures were studied: mixture 1: 85% methane / 10% ethane / 5% propane, and mixture 2: 50% methane / 25% ethane / 25% propane (by mole). Mixture 1 was chosen as an approximation of a typical U.S. natural gas composition [4, 12]. Mixture 2 was chosen to investigate the effect of greater amounts of ethane and propane, and possibly additive effects of multiple components, on the τ_{ig} of methane.

The effect of CO_2 concentration on the τ_{ig} of natural gas fuels was also investigated. CO_2 is a component found in natural gas, usually in quantities lower than 3% [49]. It was hypothesized that CO_2 would have a lengthening effect on the ignition delay time of the fuel to which it is added because it not only dilutes the fuel, but it is a product of combustion. Being a combustion product, its presence in the fuel may affect the fuel and air equilibrium such that the combustion reaction will favor the products less than if CO_2 were not present. It was hypothesized that this effect may result in longer ignition delay times. One binary mixture was chosen to study this effect: 75% methane / 25% ethane. The fuel of this mixture was altered such that the composition would contain 5% and 10% CO_2 . Such large quantities of CO_2 were added to the fuel to exaggerate the effect of CO_2 addition on fuel τ_{ig} ; detection of any deviation from the τ_{ig} measured for the mixture without CO_2 addition would be more apparent. τ_{ig} measurements were made for these mixtures containing CO_2 and then compared to the measurements made for the original binary mixture containing no CO_2 .

A description of the experimental apparatus as well as a discussion of the experimental conditions and testing procedure has been presented. The important issues

regarding the difficulties involved in making τ_{ig} measurements in a flow reactor have also been addressed. Using a flow reactor to make τ_{ig} measurements requires that the time associated with the fuel and oxidizer mixing and reaching the test temperature be quantified. The following chapter addresses the methodology and execution of quantifying this mixing time.

Chapter 3: Apparatus Validation Using Ethylene

Ethylene combustion has been widely studied in the literature because it is an important fuel in high speed propulsion systems and an important intermediate in the oxidation of higher-order hydrocarbons. Therefore, the ignition characteristics and kinetics details of ethylene combustion are fairly well known. In order to validate the experimental apparatus, experiments were performed using the atmospheric flow reactor to measure the ignition delay time of ethylene-air mixtures. These measurements were then compared to the experimental ethylene ignition delay time data found in the literature for temperatures near the range of the experiments herein (930 K to 1140 K) [23-24, 29, 32]. Figure 3.1 indicates a significant offset between the experimental data and the data found in the literature as well as the predictions by available ethylene chemical mechanisms. It was hypothesized that this offset was due to the delay in transporting the fuel and air mixture from the injection site to the test section.

Measurements of τ_{ig} shown in Figure 3.1 were experimentally determined as the difference between the time the fuel was injected and the time ignition was detected; the time that the fuel actually reached the steady temperature zone of the reactor was unknown. An analytical approach was taken to determine the time at which the fuel reached this steady temperature zone to determine a more accurate measure of the actual ignition delay time from the experiments.

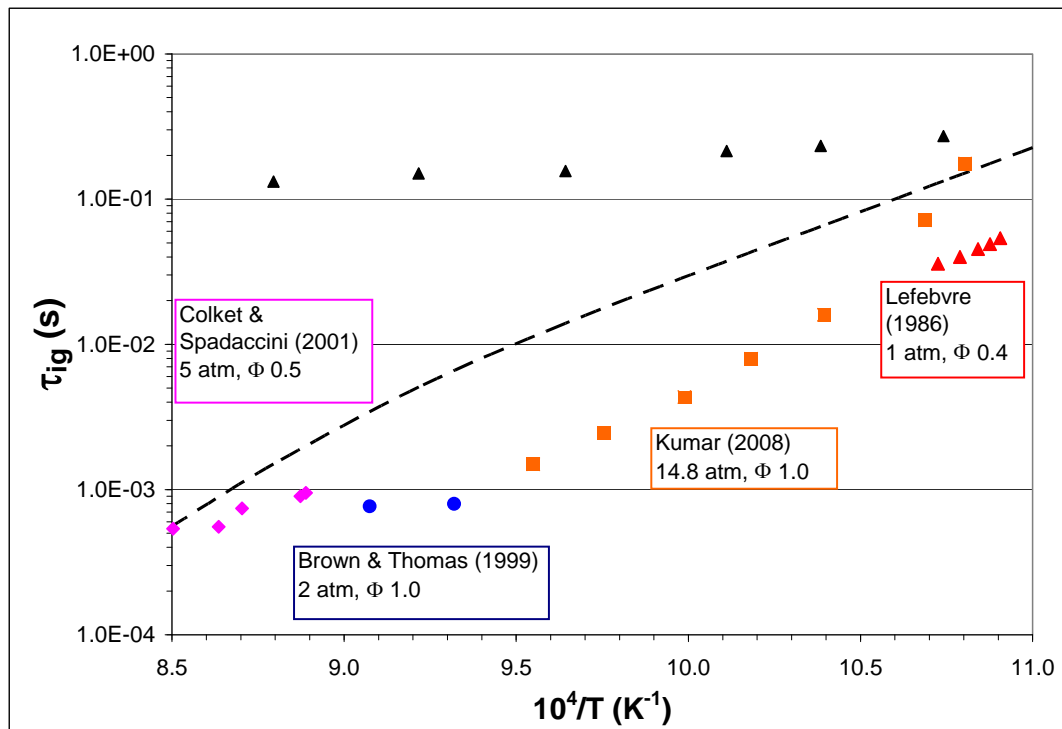


Figure 3.1. Uncorrected ethylene/air autoignition measurements (\blacktriangle) compared to UCSD ethylene mechanism predictions (--) and literature data.

A chemical reactor model (CRM) was developed to model the flow reactor geometry, flow parameters, and kinetics of the experiment. This model employed a chemical kinetics mechanism to predict the transit time of the fuel from the point where it is injected to the point where it reaches the desired test temperature of the test section. In order to have confidence in these predictions, several ethylene kinetics mechanisms were evaluated to find the most appropriate mechanism for modeling the conditions of the flow reactor experiment. A comprehensive search for ethylene combustion data was conducted. This data was modeled using available chemical reaction modeling tools which make use of chemical reaction mechanisms specifically designed to predict ethylene combustion. Based on the accuracy of the

mechanisms in predicting the data from the literature, a mechanism was chosen which was most appropriate for modeling the flow reactor experiments herein.

The model was executed using the preferred ethylene combustion mechanism at the test conditions to calculate transit times, which were then used to correct the ethylene experimental data. This corrected data was then compared to the data found in the literature as well as predictions from current kinetics models with very good agreement. The computed transit times were used to correct all the experimental data collected for all fuels and mixtures in this study.

3.1 Ethylene Combustion Data

Ethylene combustion has been widely studied using a variety of techniques over a broad range of conditions [10, 32, 41]. Ignition delay time is commonly studied to validate chemical kinetics mechanisms. Because of the availability of ignition delay time data for ethylene and the availability of multiple kinetics mechanisms specifically validated for ethylene combustion, ethylene was chosen as the calibration fuel for this study. Additional kinetics data for ethylene includes fuel decomposition data which can be modeled as well using chemical kinetics mechanisms.

Ethylene is very reactive, having a relatively short ignition delay. Most ignition delay experiments for ethylene have been conducted in shock tubes where high-pressure (up to ~50 atm) and very short residence time measurements are possible. Lower temperature (below 1200 K) measurements are not feasible in typical shock tube arrangements because the long residence times required for these measurements can cause low shock velocities and boundary layer build-up which can cause

bifurcated shocks within the test section, making data interpretation difficult [15].

Lower temperature measurements are reported in the literature for experiments using rapid compression machines (RCM) and flow reactors. Tables 3.1 summarize the available ignition delay time data for ethylene within the temperature range of interest using shock tubes, RCM, and flow reactors.

Table 3.1. Available ethylene ignition delay time data from the literature.

Reference		Experiment	Φ	Temperature	Pressure	Detection
				(K)	(atm)	
Kalitan et al. (2004)	[16]	Shock Tube	1.00	1220-1730	1	OH* Signal
Kalitan et al. (2004)	[16]	Shock Tube	1.00	1230-1750	2.91	OH* Signal
Colket & Spadaccini (2001)	[29]	Shock Tube	0.50	1175-1210	6	OH* Signal
Colket & Spadaccini (2001)	[29]	Shock Tube	0.75	1191-1350	7	OH* Signal
Colket & Spadaccini (2001)	[29]	Shock Tube	1.00	1380-1414	7	OH* Signal
Thomas & Brown (1999)	[24]	Shock Tube	1.00	1073-1565	2.3-4.8	CH* Signal
Thomas & Brown (1999)	[24]	Shock Tube	1.00	1102-1771	1.4-3.4	CH* Signal
Kumar et al. (2008)	[32]	RCM	1.00	850-1050	14.8	Pressure
Kumar et al. (2008)	[32]	RCM	1.00	850-1050	29.6	Pressure
Kumar et al. (2008)	[32]	RCM	1.00	850-1050	49.3	Pressure
Sims et al. (2005)	[31]	Flow Reactor	2.40 - 3.50	846 - 850	15.59	Light Emission
Lefebvre (1986)	[23]	Flow Reactor	0.40	900-932	1	Light Emission

Ethylene decomposition data is also available in the literature [50, 51]. In a Ph. D. dissertation from the University of Washington, Thorton measured ethylene exit concentration from a well-stirred reactor containing an initially known concentration of ethylene [51]. The reactor had a known residence time; measurements of exit ethylene concentration were made as a function of reactor temperature. Tests were performed at atmospheric pressure, temperatures between 1003 K and 1253 K, and Φ between 0.086 and 0.103.

3.2 Chemical Kinetics Mechanism Validation

Chemical kinetics modeling utilizes mechanisms which supply species thermodynamic and transport information as well as chemical reactions and their reaction rate parameters. These mechanisms exist in a format to be accessed by kinetics software codes such as Chemkin and Cantera. Mechanisms are typically specialized and therefore limited to certain species and reactions in an effort to reduce the computational load while maintaining the predictive performance. Many researchers have developed specialized mechanisms to best predict the kinetics of certain species and reactions. Available data from the literature is used to modify and validate the mechanism performance. Ignition delay time measurements are commonly used as a key metric in validating combustion mechanism performance. Several kinetics mechanisms have been developed to describe the reactions involved in ethylene combustion. These mechanisms were used to predict the results of the experiments listed in Table 3.1 as well as ethylene decomposition data reported in the literature.

3.2.1 Available Kinetics Mechanisms for Ethylene Combustion

3.2.1.1 GRI 3.0

The development of the GRI mechanism [19] was sponsored by the Gas Research Institute (GRI) and is the most widely known chemical kinetics mechanism used for natural gas combustion. The current version, GRI 3.0, incorporates 325 chemical reactions and 53 species. It was optimized to perform reliably for the following conditions: 1000 K to 2500 K, 10 Torr to 10 atm, and Φ between 0.1 to 5 for premixed systems. GRI 3.0 has been optimized for natural gas and methane as fuels. The authors warn that because the mechanism was not optimized for other pure hydrocarbon fuels, such as ethylene, the mechanism should not be used to model combustion of such pure fuels, even though the fuels are included as compounds in the mechanism species list. While not specifically validated for ethylene combustion, predictions were made using GRI 3.0 and its performance was evaluated for comparison.

3.2.1.2 UCSD Ethylene

Researchers at the University of California, San Diego developed a detailed chemical kinetics mechanism for the combustion of ethylene validated for the following conditions: 1000 K to 2500 K, 0.5 atm to 100 atm, and Φ between 0.5 and 2 [27]. The mechanism contains 148 reactions and 34 species and was validated with experimental shock tube ignition delay data of ethylene-oxygen-diluent systems.

3.2.1.3 USC C1-C4

The USC mechanism was developed for the combustion of H₂/CO/C1-C4 hydrocarbon systems [52]. The mechanism consists of 784 reactions and 111 species and was validated over the temperature range of 950 K to 2200 K and the pressure range of 0.7 atm to 3 atm. Shock tube ignition delay time, species profile, and laminar flame speed data sets were used to validate the mechanism.

3.2.1.4 LLNL Natural Gas

Lawrence Livermore National Laboratory developed a mechanism to predict the chemical kinetics of natural gas fuels (methane, ethylene, ethane, propene, and propane) [50]. The goal of the mechanism was to accurately describe the promotional effect of hydrocarbons on NO to NO₂ conversion. The mechanism consists of 639 reactions and 126 species and was validated over a temperature range of 600 K to 1100 K.

3.2.1.5 Konnov

The Konnov mechanism was specifically designed to predict the kinetics of lower-order hydrocarbon combustion. [53]. Ignition delay time, species profile, and laminar flame speed data from both flow reactor and shock tube experiments was used to validate the mechanism between 630 K and 1040 K. The mechanism consists of 1207 reactions and 127 species.

3.2.2 Chemical Kinetics Mechanism Predictions of Literature Data

3.2.2.1 Ethylene Ignition Delay Time Mechanism Performance

To evaluate the accuracy of a chemical mechanism in predicting ignition delay time data reported in the literature, calculations were performed using the chemical reaction modeling tool Cantera. A plug flow reactor (PFR) model was created and specified with the species concentration, temperature and pressure matching those of each of the τ_{ig} experiments from the literature shown in Table 3.1. The residence time of the PFR was iteratively increased until ignition was detected. Ignition detection was based on the method used in the experiment: temperature rise, pressure rise, OH or CH radical emission. The PFR model was executed using each of the chemical mechanisms available for ethylene combustion and ignition delay time data was extracted. Figures 3.2-3.4 show the typical performance of the available ethylene kinetics mechanisms in predicting ethylene τ_{ig} measurements reported in the literature made using shock tube, rapid compression machine and flow reactor apparatus, respectively. Figure 3.2 shows the accuracy of the ethylene kinetics mechanisms in predicting the τ_{ig} reported by Thomas & Brown [24] for stoichiometric ethylene mixtures at temperatures ranging from 1102 K to 1771 K and pressures between 1.4 atm and 3.4 atm made using a shock tube. Figure 3.3 shows the accuracy of the ethylene kinetics mechanisms in predicting the τ_{ig} reported by Kumar et al. [32] for stoichiometric ethylene mixtures at temperatures ranging from 850 K to 1050 K and 14.8 atm made using a rapid compression machine. And Figure 3.4 shows the accuracy of the ethylene kinetics mechanisms in predicting the τ_{ig}

reported by Lefebvre et al. [23] for ethylene mixtures at temperatures ranging from 900 K to 932 K and a Φ of 0.4 made using an atmospheric pressure flow reactor.

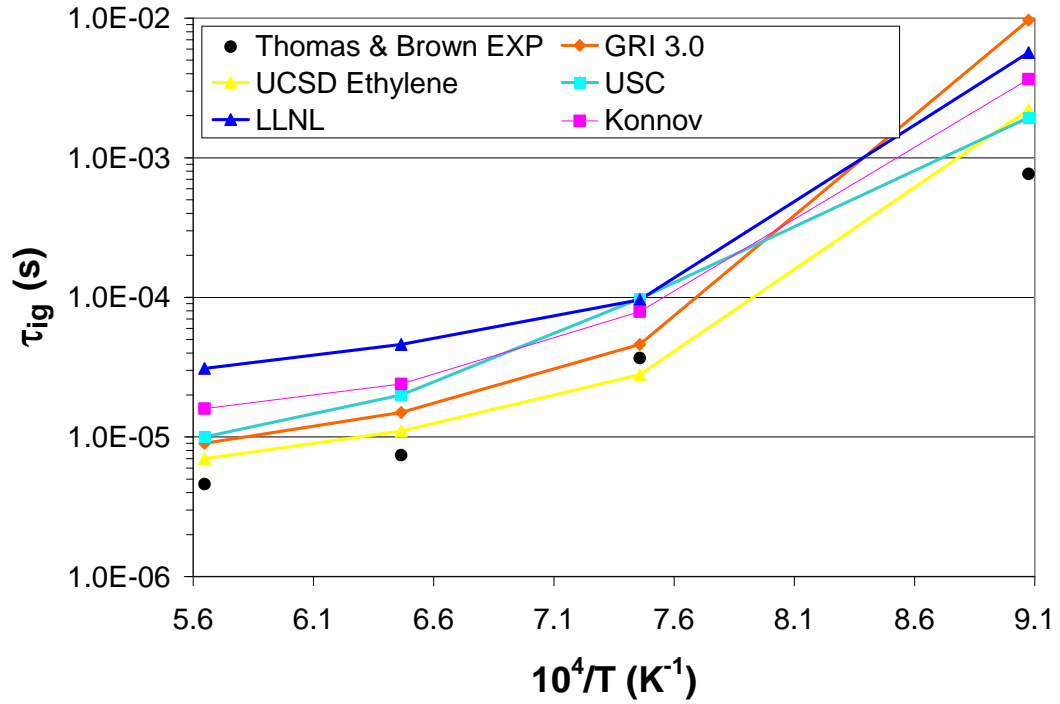


Figure 3.2. Chemical kinetics mechanism performance in predicting Thomas & Brown's experimental data [24].

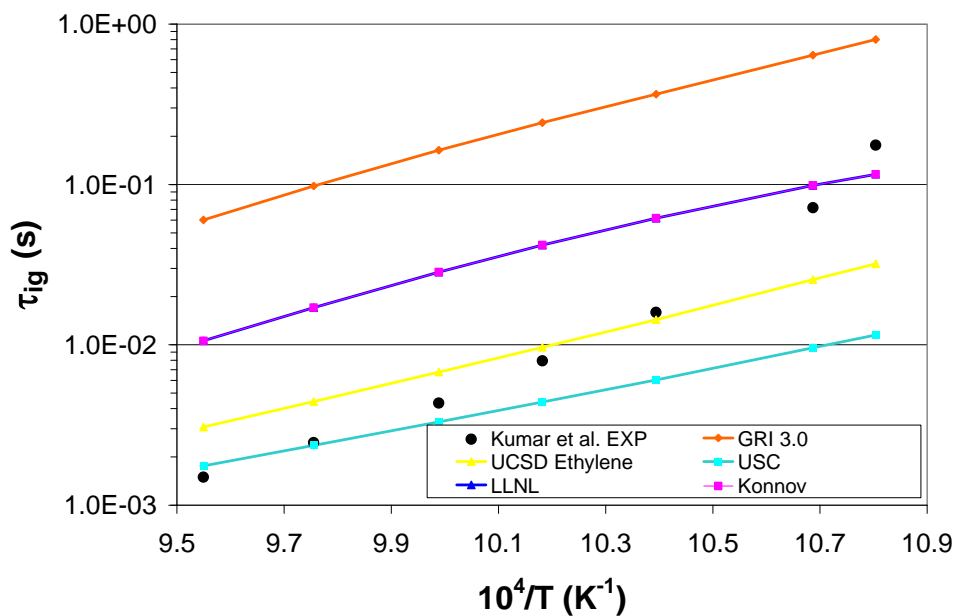


Figure 3.3. Chemical kinetics mechanism performance in predicting Kumar's experimental data [32].

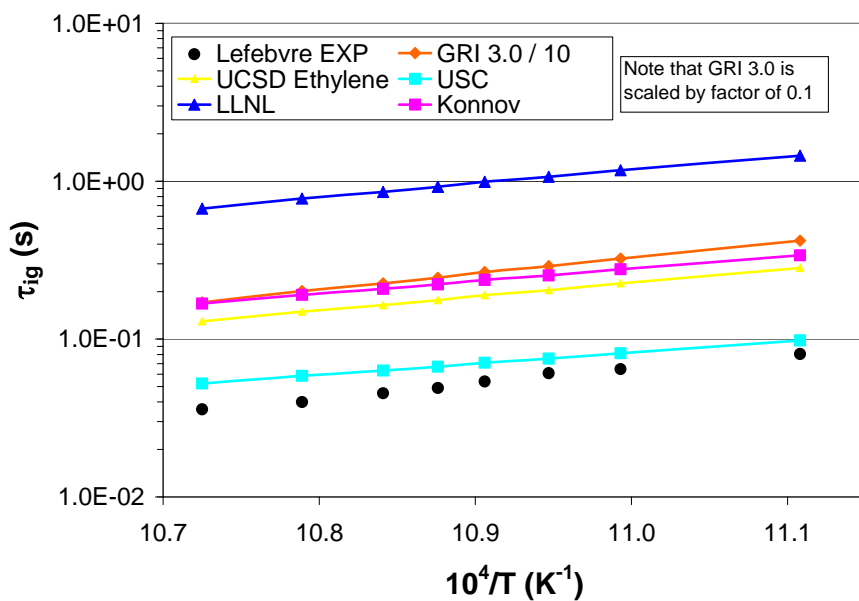


Figure 3.4. Chemical kinetics mechanism performance in predicting Lefebvre's experimental data [23].

In order to effectively develop a CRM to predict fuel transport in the flow reactor rig, a chemical mechanism must be chosen which can reliably and accurately predict ethylene kinetics in the temperature and pressure regimes seen in the flow reactor experiments herein. The performance of the mechanisms in predicting ignition behavior of ethylene was analyzed both qualitatively and quantitatively to determine which mechanism is the most appropriate choice for use in the flow reactor CRM.

This exercise in mechanism validation showed that qualitatively, all mechanisms capture the temperature, Φ , and pressure trends for ignition delay time experiments made in shock tubes and RCM. In the shock tube experiments, the UCSD ethylene mechanism seems to match the data most closely. The Konnov mechanism, while over-predicting ignition delay time, seems to match the temperature trend seen in the shock tube experiments, especially at lower temperatures. In the RCM experiments, which report ignition delay data at lower temperatures than shock tube studies, it can be seen that all but the GRI 3.0 mechanism begin to under-predict ignition delay times as temperature decreases. It should be noted that the GRI 3.0 mechanism severely over-predicts the ignition delay times in the RCM experiments. No mechanism adequately captures the temperature trend seen in these experiments; at higher temperatures, the UCSD ethylene mechanism seems to match the data the best, and at lower temperatures, the Konnov mechanism seems to match the data the best.

Figure 3.4 shows that while all mechanisms match the ignition delay time trends for temperature seen in the flow reactor experiments, the USC mechanism predicts the data reported by Lefebvre the best. It is unclear in the literature, however, how the transit and mixing times were accounted for in the measurements reported by

Lefebvre. Therefore, the accuracy of the mechanisms in predicting this particular data set is not as important as for the other data sets.

3.2.2.2 Ethylene Decomposition Mechanism Performance

To evaluate the accuracy of a chemical mechanism in predicting ethylene decomposition data, a perfectly stirred reactor (PSR) was created using Cantera to model the well-stirred reactor of Thorton's experiments. The inlet composition, temperature, pressure, and residence time of the PSR were set to match the conditions reported in Thorton's work. The PSR model was executed using each of the chemical mechanisms available for ethylene combustion. The exit concentration of ethylene was extracted from the model and compared to the experimental data. Figure 3.5 shows the accuracy of each mechanism in predicting the decomposition of ethylene reported in Thorton's work. All mechanisms except for the GRI 3.0 mechanism predicted the trends seen in Thorton's decomposition experiments. The Konnov and USC mechanisms seem to predict the data most accurately.

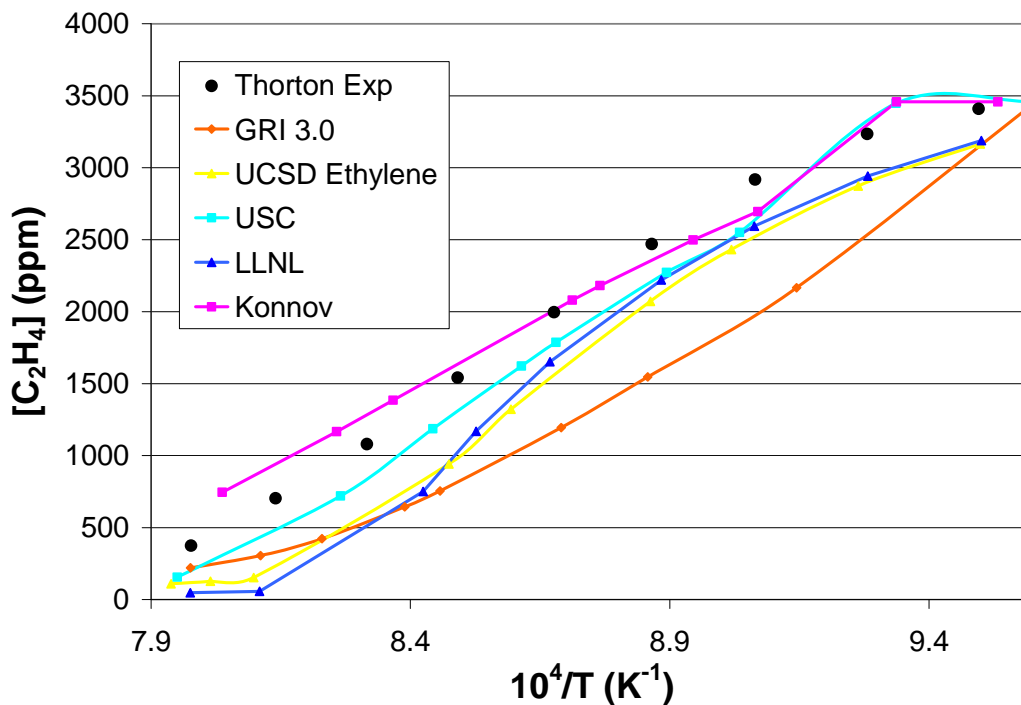


Figure 3.5. Chemical kinetics mechanism performance in predicting Thorton's experimental data [51].

3.2.2.3 Ethylene Mechanism Performance Evaluation

An attempt was made to analytically choose the mechanism which best predicts the literature data analyzed. A goodness of fit χ^2 analysis of the accuracy of each mechanism in predicting the results of ethylene combustion and decomposition experiments in the literature was performed. Table 3.2 shows the goodness of fit for each of the data sets modeled using each of the available chemical kinetics mechanisms. The values printed in bold indicate which mechanisms predicted the experimental data the most accurately.

The UCSD mechanism most consistently predicted the data reported from the experiments most accurately. This mechanism was therefore chosen to describe the

transport phenomena and kinetics pathways of ethylene and air in the chemical reactor model built to represent the flow reactor rig used to generate data in this experiment.

Table 3.2. Goodness of fit (χ^2) for each chemical mechanism in predicting each literature data set.

Reference	Experiment	Φ	Temperature (K)	Pressure (atm)	Best Fit χ^2				
					GRI 3.0	Konnov	LLNL	UCSD Ethylene	USC
Kalitan et al. (2004)	[16] Shock Tube	1.00	1220-1730	1	5.18E-03	2.92E-02	1.40E-02	3.04E-03	5.46E-03
Kalitan et al. (2004)	[16] Shock Tube	1.00	1230-1750	2.91	7.94E-04	3.77E-03	3.35E-03	4.36E-04	7.87E-04
Colket & Spadaccini (2001)	[29] Shock Tube	0.50	1175-1210	6	1.11E-01	2.03E-02	1.58E-02	7.36E-03	1.29E-02
Colket & Spadaccini (2001)	[29] Shock Tube	0.75	1191-1350	7	4.47E-03	3.16E-03	1.21E-03	2.80E-04	3.98E-04
Colket & Spadaccini (2001)	[29] Shock Tube	1.00	1380-1414	7	1.11E-05	1.75E-04	1.27E-04	1.66E-06	5.05E-06
Thomas & Brown (1999)	[24] Shock Tube	1.00	1073-1565	2.3-4.8	7.23E-01	2.73E-02	1.19E-01	7.87E-03	4.29E-03
Thomas & Brown (1999)	[24] Shock Tube	1.00	1102-1771	1.4-3.4	1.04E-01	1.10E-02	3.20E-02	2.73E-03	1.92E-03
Kumar et al. (2008)	[32] RCM	1.00	850-1050	14.8	3.32E+01	1.41E-01	5.82E-01	1.52E-01	2.15E-01
Kumar et al. (2008)	[32] RCM	1.00	850-1050	29.6	1.72E+01	7.46E-02	1.96E-01	1.01E-01	1.85E-01
Kumar et al. (2008)	[32] RCM	1.00	850-1050	49.3	1.23E+02	1.06E-01	2.36E-01	1.42E-01	3.61E-01
Sims et al. (2005)	[31] Flow Reactor	2.40 - 3.50	846 - 850	15.59	6.94E+02	1.94E-02	2.30E-01	2.75E-01	6.18E-01
Lefebvre (1986)	[23] Flow Reactor	0.40	900-932	1	1.03E+03	5.02E+00	1.30E+02	2.77E+00	4.68E-02
Thorton (1989)	[51] PSR Decomposition	0.086-0.103	1053-1253	1	3.64E+03	9.98E+02	1.23E+03	2.12E+03	2.41E+02

3.3 Chemical Reactor Model Development

A CRM was built using Cantera in a Python environment to represent the geometry of the atmospheric flow reactor downstream of the fuel injectors, including the diffuser and the test section having a steady temperature profile. The purpose of the model was to compute the residence times of different sections of the flow path and then the ignition delay time of the ethylene-air mixture after the mixture has

reached the steady temperature section of the reactor. It was hypothesized that the sum of the residence times of the sections of the flow reactor leading up to the steady temperature zone and the ignition delay time computed would be comparable to the ignition delay times measured experimentally in the flow reactor. The total residence time computed could then be subtracted from the experimental results, yielding the corrected ignition delay time. The flow conditions, temperature and pressure of the system were inputs to the model and the total residence time up to the steady temperature zone was the output extracted.

3.3.1 CRM Methodology

The CRM of the experimental flow reactor was composed of three sections: the diffuser, the temperature rise section, and the steady temperature section. The model was created in such a way to capture the reactor volume change seen in the diffuser and the reactor temperature change seen in the temperature rise section. Figure 3.6 shows how the temperature of the fuel and air remain at the inlet temperature (673 K) through the diffuser, then begins to ramp up through the test section until the steady test temperature is reached.

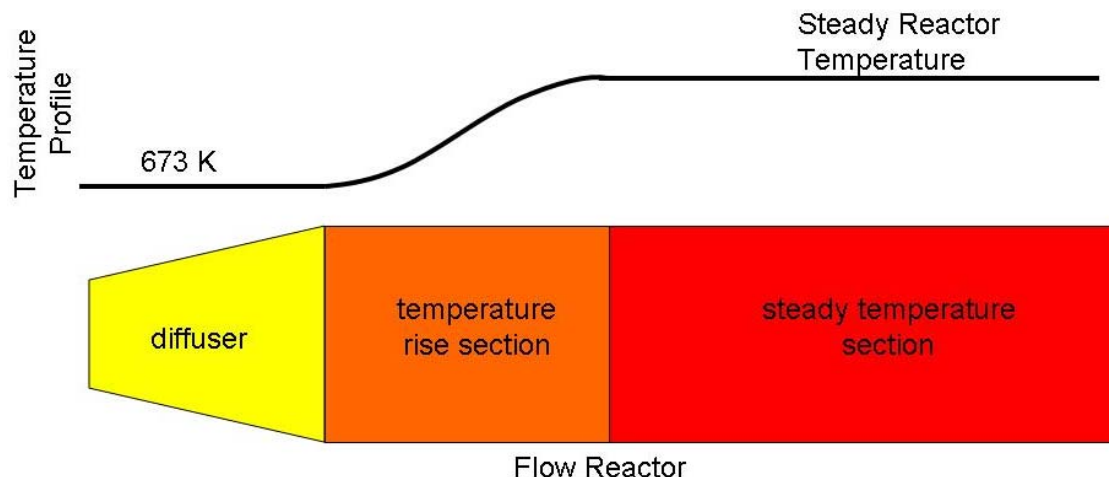


Figure 3.6. Flow reactor zones and associated temperature profile.

The diffuser was modeled as a PFR, which was represented as a series of PSRs, each increasing in volume from the previous one according to the geometry of the diffuser. The temperature of each of the PSRs was specified as 673 K and was experimentally verified. The temperature ramp section was also modeled as a PFR and again represented as a series of PSRs, each having an identical volume. Each temperature ramp PSR had a higher temperature from the one preceding it following the temperature profile measured for each reactor test temperature. These temperature profiles are provided in Figure 2.5. The steady temperature section of the reactor is where ignition delay time was calculated. This section was modeled as a PFR with the same methodology used previously in calculating ignition delay times when validating the ethylene mechanisms.

The model was executed using the flow conditions, temperatures, and pressures used in the ethylene flow reactor experiments herein. The UCSD ethylene chemical kinetics mechanism was used in the model to describe the kinetics and

thermodynamics processes. The model calculated the residence times for the strings of PSRs comprising the diffuser section and temperature ramp section. The model also calculated the ignition delay time of the decomposed ethylene-air mixture once it had reached the steady temperature zone.

3.3.2 CRM Results

3.3.2.1 CRM Predictions of Ethylene Autoignition Measurements

The results of the CRM were compared to the experimental data collected for ethylene-air ignition delay. The total time computed using the CRM is inclusive of the transit time (the residence time of the PSR series representing the diffuser and the residence time of the PSR series representing the temperature ramp section) as well as the ignition delay time (calculated in the PFR). This total time is comparable to the uncorrected ignition delay time data collected for ethylene-air mixtures. Figure 3.7 shows the predictions of the CRM in comparison to the data collected for the different flow conditions specified for tests ranging in Φ from 0.5 to 1.25. The model predicts the experimental data fairly well for all test conditions. With the exception of three data points, the model predicted the experimental measurements within 17%. Table 3.3 shows the experimental data and CRM predictions.

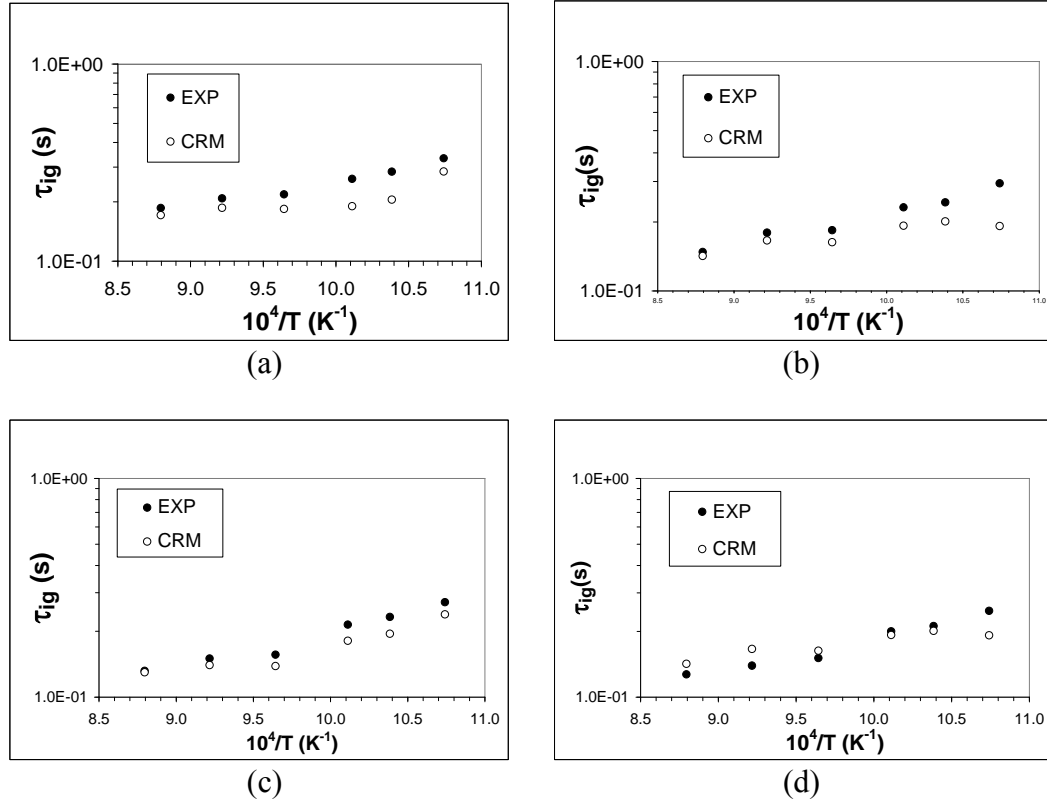


Figure 3.7. Analytical predictions of ethylene autoignition delay time inclusive of transit time and true autoignition delay time calculated in CRM (CRM), compared to uncorrected ethylene autoignition delay time measurements (EXP). (a) $\Phi = 0.5$, (b) $\Phi = 0.75$, (c) $\Phi = 1.0$, (d) $\Phi = 1.25$.

Table 3.3. CRM predictions of total time compared to uncorrected ethylene ignition delay time measurements.

Equiv. Ratio		Temperature (K)					
		931	963	989	1037	1085	1137
0.5	Uncorrected Measurement (s)	0.28509	0.20527	0.19003	0.18398	0.18639	0.17114
	CRM Total Time (s)	0.3327	0.28435	0.2614	0.21825	0.20825	0.186033
	% Error	14.3	27.8	27.3	15.7	10.5	8.0
0.75	Uncorrected Measurement (s)	0.19198	0.20113	0.1926	0.16319	0.16619	0.14219
	CRM Total Time (s)	0.294633	0.24355	0.23135	0.184	0.1795	0.14785
	% Error	34.8	17.4	16.7	11.3	7.4	3.8
1	Uncorrected Measurement (s)	0.23889	0.19491	0.18117	0.13873	0.14013	0.12988
	CRM Total Time (s)	0.271867	0.2327	0.21455	0.156399	0.15025	0.13185
	% Error	12.1	16.2	15.6	11.3	6.7	1.5
1.25	Uncorrected Measurement (s)	0.23013	0.18451	0.17479	0.14217	0.13397	0.12497
	CRM Total Time (s)	0.2485	0.2115	0.20015	0.15095	0.13945	0.1272
	% Error	7.4	12.8	12.7	5.8	3.9	1.8

3.3.2.2 Application of CRM Results to Ethylene Autoignition Measurements

The goal of using a CRM to model the flow reactor was to analytically account for the fuel transport time in the experimental rig. This time corresponds to the sum of the residence time of the diffuser PSR string and the residence time of the temperature ramp PSR string from the CRM. Subtracting the computed transit time from the experimental data provides corrected, true ignition delay time measurements. Figure 3.8 shows the corrected measurements of ignition delay time for ethylene-air mixtures at Φ from 0.5 to 1.25. The figure also includes the predicted ignition delay time using the UCSD ethylene kinetics mechanism. While relatively close agreement can be seen between the predicted values and the experimental values for all Φ , the fit appears to lose integrity for lower Φ at higher temperatures. At these conditions, the predicted ignition delay times are much faster than what was found experimentally.

Figure 3.9 shows the corrected experimental ethylene-air ignition delay measurements along with data available from the literature. The discrepancy between the experimental data and the data from other researchers can be attributed to the difference in test conditions, namely pressure. Increasing pressure has a very significant effect on reducing ignition delay times [23]. Included in Figure 3.9 is a prediction of ignition delay time using the UCSD ethylene kinetics mechanism at atmospheric pressure and Φ of 1.0.

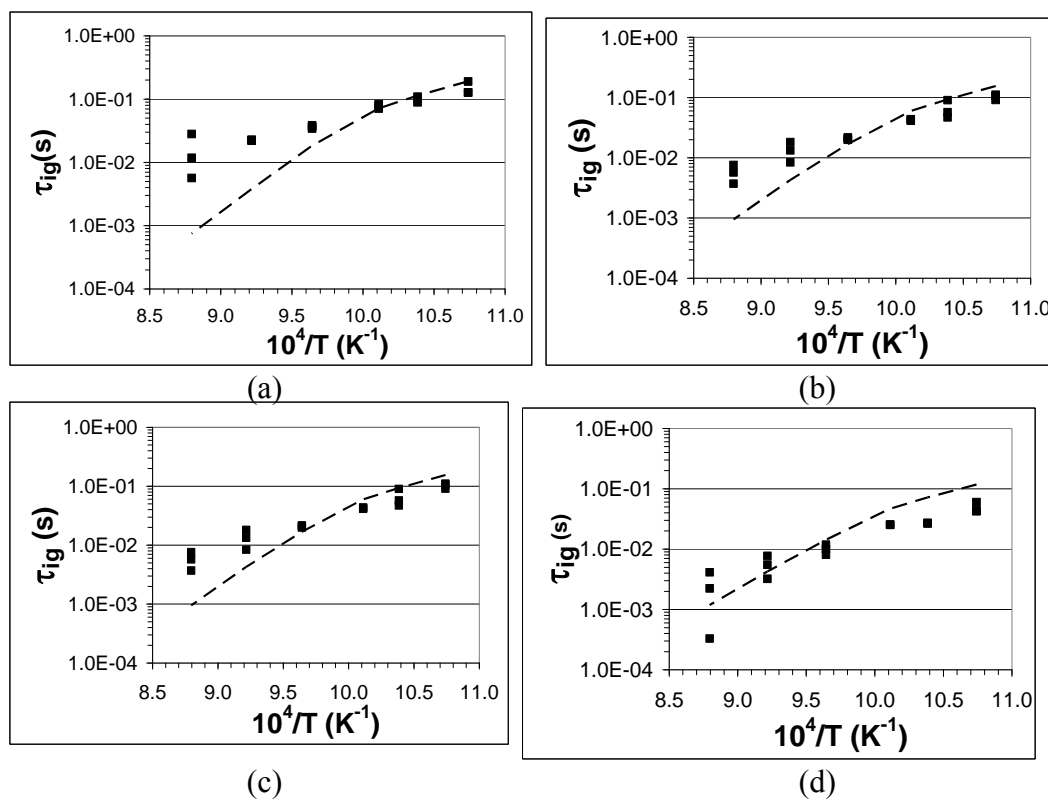


Figure 3.8. Corrected ethylene autoignition delay time measurements (■) compared with UCSD ethylene mechanism predictions (--). (a) $\Phi = 0.5$, (b) $\Phi = 0.75$, (c) $\Phi = 1.0$, (d) $\Phi = 1.25$.

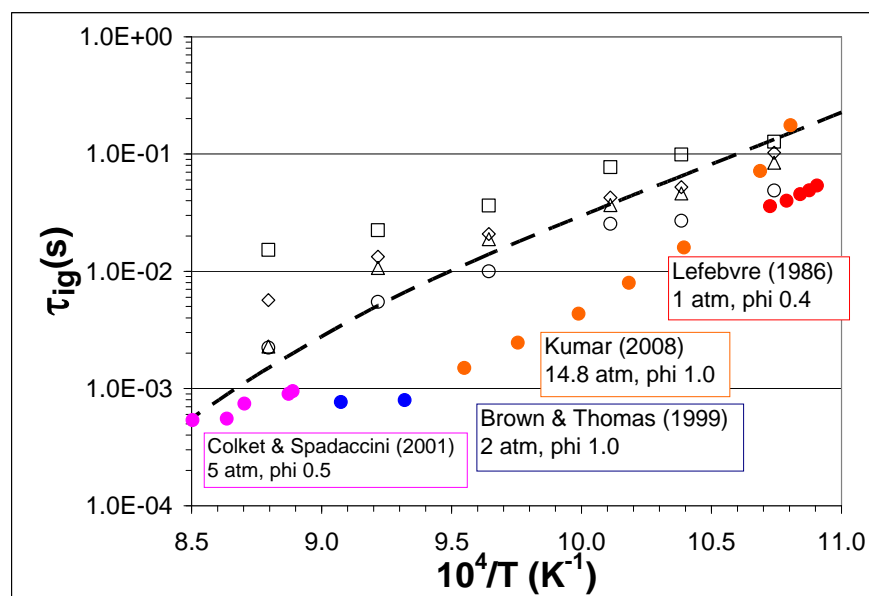


Figure 3.9. Corrected ethylene autoignition delay time measurements (\square $\phi = 0.5$, \diamond $\phi = 0.75$, Δ $\phi = 1.0$, \circ $\phi = 1.25$) compared with literature data and UCSD mechanism predictions (--).

Figure 3.8 shows that the CRM developed to model the flow reactor geometry and flow conditions effectively accounts for the fuel transit time required for the fuel to reach the steady temperature zone of the reactor. This can be seen by the relatively close agreement of the corrected experimental τ_{ig} measurements to the predictions of τ_{ig} made using the UCSD kinetics mechanism. Again, much better agreement is seen for the measurements made at lower temperature and richer conditions, than for the high temperature and lean conditions. Figure 3.9 shows that the corrected τ_{ig} measurements follow the trends reported in the literature. Unfortunately, little data for direct comparison is available at the conditions investigated in the current study.

3.3.2.3 Application of CRM Results to All Experimental Autoignition

Measurements

The result of using a CRM to analytically determine the transit time for the fuel to reach the steady temperature zone of the flow reactor from the injection site is a correction factor which can be applied to all the ignition delay time experiments performed in this study. Ethylene was chosen as the calibration fuel to determine the appropriate correction factors because ethylene transport and kinetics are well known in the temperature regime studied. Further, several kinetics mechanisms have been developed to predict ethylene combustion and were validated using ethylene combustion data. The satisfactory performance of the CRM is seen in Figures 3.8 and 3.9 comparing the corrected ignition delay times with data found in the literature and predictions made using the UCSD ethylene kinetics mechanism.

The experiments performed in this study measured the ignition delay times of methane, propane, and ethane, as well as various mixtures of these fuels. The correction factors determined for ethylene ignition delay time measurements were used to correct the measurements made for all experiments in this study. It is understood that the resulting corrected measurements rely on the quality of reported ethylene τ_{ig} measurements and predictions of the UCSD kinetics mechanism. Some error, therefore, inherently exists in using this method to correct for transit time. It is further recognized that some error will be introduced in assuming the transit times are identical between fuels, the main factors contributing to the calculation of transit time are bulk flow rates, temperature, and flow path geometry. Reactor geometry and temperature do not change depending on the fuel, but fuel flow rate will vary slightly. However, the fuel makes up a very small portion (less than 10% by volume) of the overall fluid flow through the reactor. The transit time correction factors were determined for Φ ranging from 0.5 to 1.25 to account for the variability in transit time based on fuel flow. The correction factors, found in Table 3.4, were then applied to the experimental data collected for ignition delay times of methane, ethane and propane pure fuels and mixtures.

Table 3.4. Transit time correction factors, values are in units of milliseconds.

Equiv. Ratio	Temperature (K)					
	931	953	973	1032	1092	1149
0.5	205.06	185.32	184.1	181.83	185.83	170.83
0.75	191.98	191.36	188.9	163.19	166.19	142.19
1	187.42	186.64	177.85	137.57	139.57	129.57
1.25	199.73	184.51	174.79	140.97	133.97	124.97

Chapter 4: Autoignition Delay Measurements

The results of the autoignition experiments are presented and the observed trends are discussed. The results are compared to relevant data found in the literature and to τ_{ig} predictions using the GRI chemical kinetics mechanism. The GRI mechanism is the most well-known natural gas mechanism has provided the basis for the development of many detailed mechanisms in order to improve predictions in certain regimes. The results of this experiment were compared to the GRI mechanism in order to analyze the performance of this mechanism in predicting ignition of natural gas fuels at the experimental conditions. The purpose of this was to identify areas of the parameter space where this mechanism performs well and where it needs additional optimization. The autoignition delay time data was to fit an Arrhenius expression of the following form:

$$\tau_{ig} = A \exp(E_{act}/RT) [C_x H_y]^a [O_2]^b \quad (4.1)$$

where E_{act} is equivalent to the global activation energy and A is an empirically determined constant. $[C_x H_y]$ and $[O_2]$ are molar concentrations of the fuel and oxygen, respectively. The empirical exponents, a and b , represent the power dependency of τ_{ig} on the molar concentrations of fuel and oxidizer, respectively. R is the universal gas constant and T is the mixture temperature. Fitting data to an expression of this form is common practice by τ_{ig} researchers [29]. This Arrhenius form was used to correlate τ_{ig} for the pure fuels studied.

Many similar empirical correlations have been developed by researchers to reflect the results of their hydrocarbon fuel ignition delay time studies [47]. Several

of these correlations, listed in Table 4.1, focus on methane autoignition at various conditions. The conditions at which the correlations were determined to be valid are included in the table. The E_{act} reported in Table 4.1 are in units of kcal/mol.

Table 4.1. Methane and methane/hydrocarbon autoignition delay time correlations from the literature.

Reference	Correlation	Conditions
Lefebvre (1986) [23]	$\tau_{ig} \propto \frac{1}{A} \exp\left(\frac{25.0}{R_U T}\right) [O_2]^{-0.80} [CH_4]^{-0.19} P^{-0.99} T^{-0.5}$	923K < T < 1000K 7 atm < P < 10 atm
Spadaccini & Colket (1994) [3]	$\tau_{ig} = 1.77 \times 10^{-14} \exp(18.693/T) [O_2]^{-1.05} [CH_4]^{0.66} [HC]^{-0.39}$	1300K < T < 2000K 3 atm < P < 5 atm 0.45 < Φ < 1.25
Petersen et al (1996) [17]	$\tau_{ig} = 4.05 \times 10^{-15} [CH_4]^{0.33} [O_2]^{-1.05} \exp\left(\frac{51.8}{RT}\right)$	High Pressures up to 480 atm
Petersen et al (1999) [18]	$\tau_{ig} = 1.26 \times 10^{-14} [CH_4]^{-0.02} [O_2]^{-1.20} \exp\left(\frac{32.7}{RT}\right)$	T > 1300 K, Lower Pressure, Fuel Lean & Rich
	$\tau_{ig} = 4.99 \times 10^{-14} [CH_4]^{-0.38} [O_2]^{-1.31} \exp\left(\frac{19.0}{RT}\right)$	T < 1300 K, Higher Pressure, Fuel Rich
Li & Williams (2000) [54]	$\tau_{ig} = \frac{2.60 \times 10^{-15} [O_2]^{-4/3} [CH_4]^{1/3}}{T^{-0.92} \exp(-13.18/T)}$	T < 1300 K
	$\tau_{ig} = 6.25 \times 10^{-16} [CH_4]^{1/3} [O_2]^{-4/3} \exp\left(\frac{23.0}{RT}\right)$	T > 1300 K

Only one study, by Spadaccini and Colkett [3], attempts to account for non-methane components in natural-gas type mixtures. In this correlation, all non-methane hydrocarbons are lumped together in a collective term. In the current study, an attempt is made to account for the effects of higher-order hydrocarbon addition to methane on methane τ_{ig} . Arrhenius expressions were developed to empirically

correlate τ_{ig} with conditions and compositions of methane and higher hydrocarbon fuels using the following form for binary mixtures with methane:

$$\tau_{ig} = A \exp(E_{act}/RT) [\text{CH}_4]^{a_1} [\text{C}_x\text{H}_y]^{a_2} [\text{O}_2]^b \quad (4.2)$$

The parameters in equation 4.2 are the same as in 4.1 except for the new fuel concentration exponents a_1 and a_2 . The Arrhenius expressions developed empirically with the data collected in the current study are presented in Table 4.2. Correlations were derived to model τ_{ig} for each of the pure fuels as well as each of the binary methane mixtures. An analysis of the quality of the fit of the correlation to the data collected for each pure fuel and fuel blend studied are discussed.

Table 4.2. Derived Arrhenius expressions for autoignition delay time for pure fuels methane, ethane, and propane, and binary methane/ethane, methane/propane, and methane/ethylene mixtures. E_{act} is in units of kcal/mol.

Fuel Constituent(s)	Arrhenius Autoignition Delay Time Correlation
Methane	$\tau_{ig} \text{ (s)} = 2.23 \cdot 10^{-15} [\text{CH}_4]^{-0.335} [\text{O}_2]^{-1.35} \exp(46.6 / RT)$
Ethane	$\tau_{ig} \text{ (s)} = 6.9 \cdot 10^{-14} [\text{C}_2\text{H}_6]^{0.11} [\text{O}_2]^{-1.39} \exp(40.0 / RT)$
Propane	$\tau_{ig} \text{ (s)} = 4.8 \cdot 10^{-14} [\text{C}_3\text{H}_8]^{0.36} [\text{O}_2]^{-1.16} \exp(38.5 / RT)$
Methane/Ethane	$\tau_{ig} \text{ (s)} = 1.9 \cdot 10^{-15} [\text{CH}_4]^{-0.41} [\text{C}_2\text{H}_6]^{-0.15} [\text{O}_2]^{-1.8} \exp(35.2 / RT)$
Methane/Propane	$\tau_{ig} \text{ (s)} = 6.1 \cdot 10^{-17} [\text{CH}_4]^{-0.55} [\text{C}_3\text{H}_8]^{-0.35} [\text{O}_2]^{-1.3} \exp(41.8 / RT)$
Methane/Ethylene	$\tau_{ig} \text{ (s)} = 8.1 \cdot 10^{-18} [\text{CH}_4]^{-0.30} [\text{C}_2\text{H}_4]^{-0.85} [\text{O}_2]^{-1.95} \exp(32.7 / RT)$

4.1 Pure Fuels

The τ_{ig} data collected for pure fuels methane, ethane, and propane in air at atmospheric pressure conditions is presented. The measurements are presented for each of the following Φ : 0.5, 0.75, 1.0, and 1.25.

4.1.1 Methane

Atmospheric pressure τ_{ig} were measured for methane and air mixtures.

Unfortunately, successful autoignition events were achieved at only the two highest of the six test temperatures (1085 K and 1137 K); autoignition did not occur within the test section at the lower temperatures. Figure 4.1 presents the methane/air τ_{ig} measurements at Φ of 0.5, 0.75, 1.0, and 1.25, along with relevant data found in the literature and predictions made using the GRI kinetics mechanism.

With successful ignition events occurring at only two test temperatures, it is difficult to discuss a trend of τ_{ig} with temperature. A significant decrease in τ_{ig} is evident with increased temperature. The measured τ_{ig} in Figure 4.1 show very little variation with the various Φ at 1085 K. For the measurements made at 1137 K, however, τ_{ig} decreased with increased Φ as expected. The predictions made using the GRI mechanism matched the experimental data very well. The GRI mechanism has been thoroughly validated for methane combustion over very broad conditions [19], therefore, its performance in accurately predicting the τ_{ig} measurements speaks to the reliability of the test apparatus in producing accurate measurements.

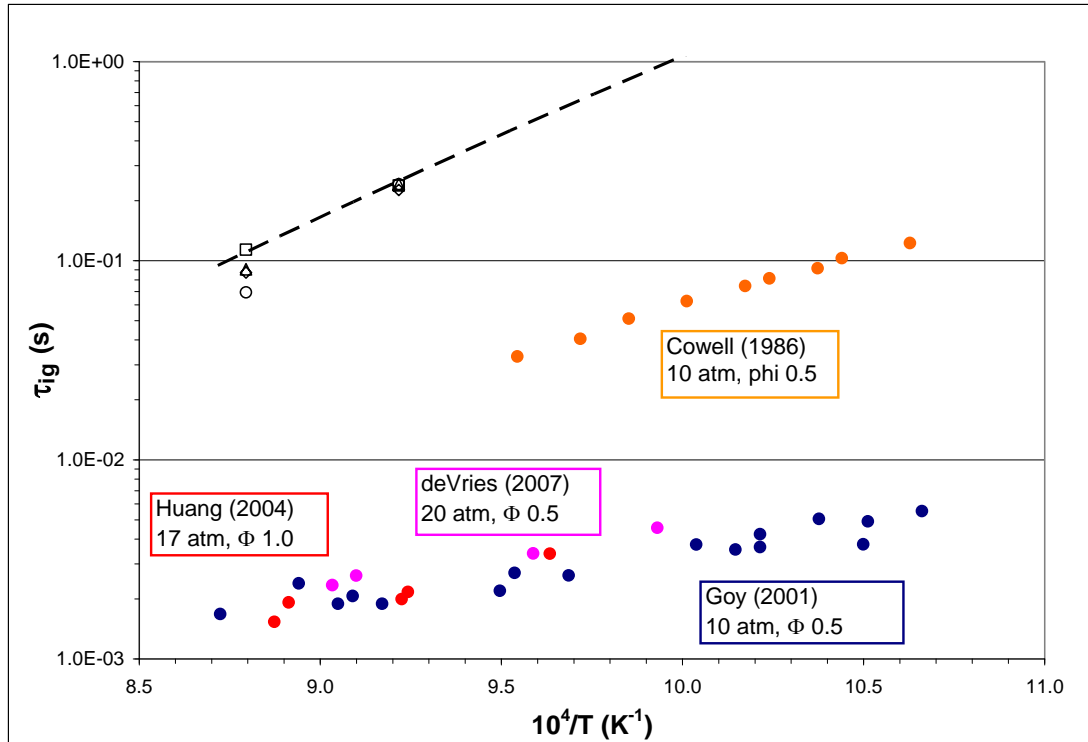


Figure 4.1. Methane autoignition delay time measurements (\square $\phi = 0.5$, \diamond $\phi = 0.75$, Δ $\phi = 1.0$, \circ $\phi = 1.25$) plotted alongside literature data and chemical kinetics predictions using GRI mechanism (--).

The available methane autoignition data in the literature was collected at high pressures. Huang et al. [20] measured τ_{ig} for methane/air mixtures in a shock tube at similar temperatures to the current experiment (1000 K to 1350 K). These measurements were made at elevated pressures (16 atm to 40 atm) in an effort to improve methane oxidation predictive model performance at high pressures. deVries et al.[21] performed methane/air autoignition experiments near 800 K and 20 atm using a shock tube as well. The goal of this study was to investigate the reduction in E_{act} of hydrocarbon oxidation in the low-temperature, high-pressure regime. This study focused on methane fuel blends, but pure methane oxidation was investigated as well. Goy et al. [15] conducted similar shock tube experiments using methane and

methane fuel blends at temperatures ranging from 900 K to 1700 K and pressures ranging from 5 atm to 20 atm. Cowell et al. [55] investigated the effect of pressure on pure hydrocarbon autoignition. Temperatures ranged from 670 K to 1020 K and pressures ranged from 1 atm to 10 atm in this study. Higher order hydrocarbons as well as methane were studied.

Figure 4.1 shows that increasing pressure significantly reduces autoignition times, and this explains the differences between the current atmospheric study and the higher pressure data found in the literature. The predictions made by the GRI mechanism, however, use the temperature and pressure conditions of the current experiment and match the results quite well.

A regression analysis was performed to fit the methane τ_{ig} measurements made to an Arrhenius correlation. Table 4.2 provides the empirically derived reaction parameters for the oxidation of methane. Figure 4.2 shows the quality of the fit of the correlation to the experimental data. Again, because only two test temperatures resulted in successful autoignition events, it is difficult to draw any meaningful conclusions about the resulting rate parameters. The E_{act} required for methane oxidation in the temperature regime was found to be 46.6 kcal/mol. Studies are available in the literature which have focused on determining the E_{act} required for methane oxidation in various temperature and pressure regimes [2, 20, 23, 17-18, 54]. Many of the correlations from these studies are listed in Table 4.1 along with the resulting E_{act} . Again, because of the minimal amount of data collected in the present study for methane autoignition, it is difficult to make any comparisons to E_{act} determined by other researchers.

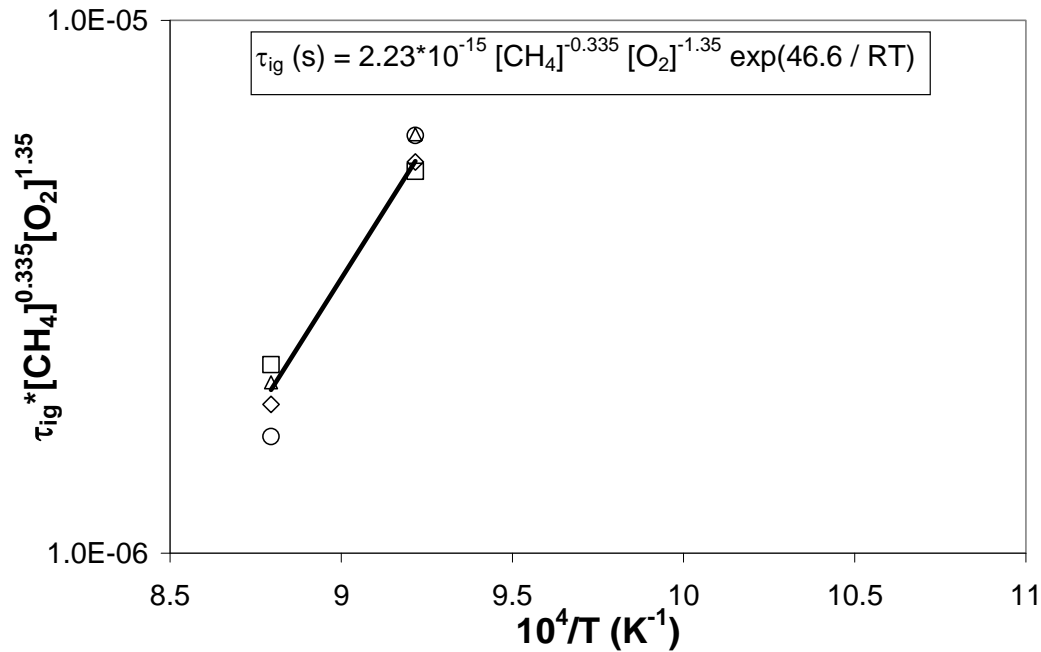


Figure 4.2. Methane autoignition measurements (\square $\phi = 0.5$, \diamond $\phi = 0.75$, Δ $\phi = 1.0$, \circ $\phi = 1.25$) plotted with Arrhenius correlation (-).

4.1.2 Ethane

Atmospheric pressure τ_{ig} were measured for ethane and air mixtures. Unfortunately, autoignition did not occur for any ethane/air mixture at the lowest test temperature (931 K). However, autoignition occurred at each of the other test temperatures for all of the Φ studied except for 0.5, where autoignition only occurred at test temperatures above 989 K. Figure 4.3 presents all of the τ_{ig} measurements for ethane/air mixtures at Φ of 0.5, 0.75, 1.0, and 1.25. Figure 4.3 also shows the predictions of τ_{ig} made by the GRI mechanism. Unfortunately, no ethane τ_{ig} data from the literature for comparison was available within the temperature range studied here.

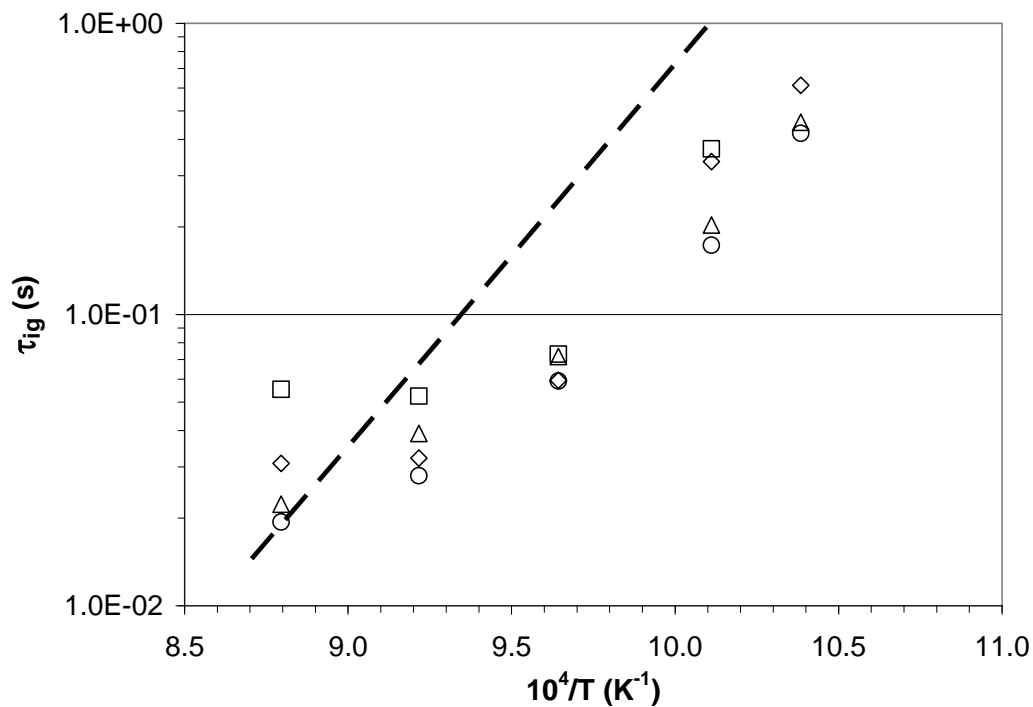


Figure 4.3. Ethane autoignition delay time measurements (\square $\phi = 0.5$, \diamond $\phi = 0.75$, Δ $\phi = 1.0$, \circ $\phi = 1.25$) plotted alongside chemical kinetics predictions using GRI mechanism (--).

Autoignition of ethane was possible at all the test temperatures except for 931 K, and therefore much more τ_{ig} data was collected for ethane than for methane. The data for each Φ follows a near exponential decrease with increasing temperature. However, at leaner Φ , τ_{ig} does not decrease as sharply with increasing temperatures as it does for richer Φ . At each test temperature, decreasing τ_{ig} are again evident with increasing Φ . The GRI mechanism predictions of ethane τ_{ig} do not match the experimental data very well. As temperature decreases, the mechanism tends to overpredict τ_{ig} . Further, the mechanism does not capture the asymptotic trend seen in τ_{ig} with higher temperature.

Unfortunately, no experimental data exists in the literature at conditions relevant to the measurements made in the current study. deVries et al. [22] studied ethane oxidation in a shock tube autoignition experiment at higher test temperatures between 1218 K and 1860 K for kinetics model validation, and his group found the current kinetics models to be accurate within most of the parameter space investigated. Petersen et al. [10] also collected ethane τ_{ig} data using a shock tube at a similar high temperature range in order to test and improve the accuracy of kinetics models. Hunter, et al. [40] studied ethane oxidation within the same temperature regime as the current study (915 K to 966 K) at pressures ranging from 3 atm to 10 atm. The data collected in this experiment, however, was limited to species concentration profiles, which proved useful in developing a detailed chemical kinetics model.

A regression analysis was performed to fit the ethane τ_{ig} measurements made to an Arrhenius correlation. Table 4.2 contains the empirically derived reaction parameters for the oxidation of ethane. Figure 4.4 shows the quality of the fit of the Arrhenius correlation to the experimental data. With much more data to compare to the Arrhenius correlation than the methane study, a more detailed analysis can be made of the ethane correlation. The correlation is structured such that $\ln(\tau_{ig})$ is proportional to the inverse of temperature. This fit, while approximating the experimental values of the τ_{ig} of ethane, does not capture the asymptotic trend of τ_{ig} with higher temperatures seen in the experimental data, especially at the leaner Φ .

The effective E_{act} for ethane ignition in the temperature range studied was found to be 40.0 kcal/mol. Again, since no ethane autoignition data was available in the

literature in this temperature regime, no directly comparable E_{act} exist for the conditions studied. However, the E_{act} reported by deVries et al. [22] of 39.6 kcal/mol agrees well with this value even though their data was for much different conditions: 1218 K to 1860 K, 0.57 atm to 3 atm, and Φ from 0.5 to 2.

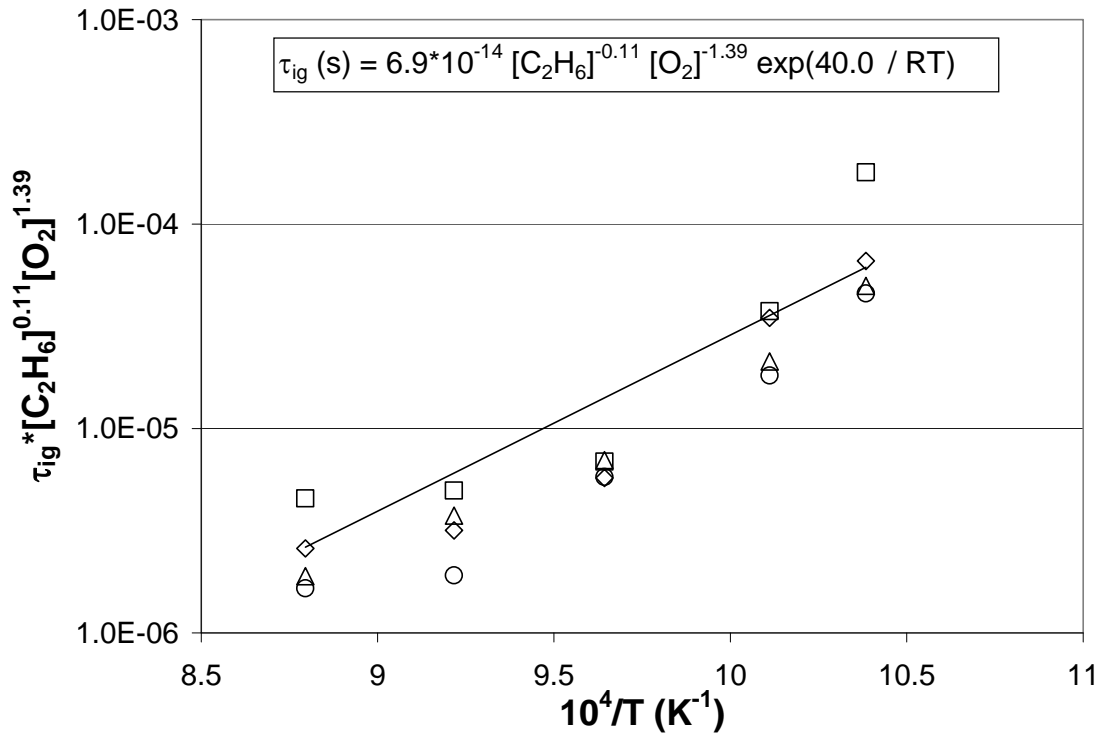


Figure 4.4. Ethane autoignition measurements (\square $\phi = 0.5$, \diamond $\phi = 0.75$, Δ $\phi = 1.0$, \circ $\phi = 1.25$) plotted with Arrhenius correlation (-).

4.1.3 Propane

Atmospheric pressure τ_{ig} were measured for propane and air mixtures.

Unfortunately, autoignition did not occur for any propane/air mixture at the lowest test temperature (931 K). However, autoignition occurred at all of the other test temperatures for all of the Φ studied except for 0.5, where autoignition only occurred

at test temperatures above 989 K. Figure 4.5 presents the τ_{ig} measurements for propane/air mixtures at Φ of 0.5, 0.75, 1.0, and 1.25, along with relevant data found in the literature and predictions made using the GRI kinetics mechanism.

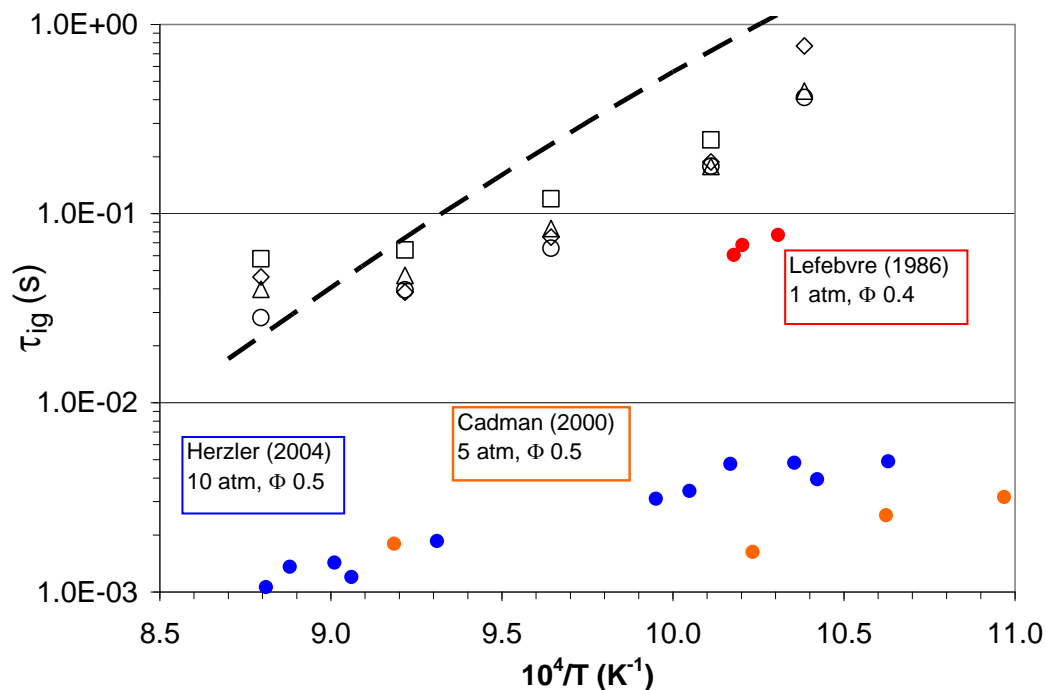


Figure 4.5. Propane autoignition delay time measurements (\square $\phi = 0.5$, \diamond $\phi = 0.75$, Δ $\phi = 1.0$, \circ $\phi = 1.25$) plotted alongside literature data and chemical kinetics predictions using GRI mechanism (--).

The τ_{ig} measurements for propane were similar (mostly within about 10%) to those for ethane at the same conditions. The same trends of decreasing τ_{ig} with increased temperature and Φ were observed. Further the asymptotic trend of τ_{ig} reduction with increased temperature, especially at leaner Φ , was again similarly observed for propane. Interestingly, the GRI mechanism overpredicts the τ_{ig} for

propane at low temperatures but underpredicts τ_{ig} at higher temperatures. Further, the mechanism fails to capture the asymptotic trend observed in the decreasing of τ_{ig} with increasing temperature.

Propane ignition within the temperature range of interest for this study has been investigated by other researchers as well; their data is also presented in Figure 4.5. Lefebvre et al. [23] studied lean propane and air mixtures at temperatures between 833 K and 1000 K and pressures between 1 atm and 10 atm. This study measured τ_{ig} using a flow reactor where flow rates were adjusted to achieve ignition within a certain predetermined distance down the flow reactor. τ_{ig} was then derived as a function of the fuel and oxidizer flow rates and this predetermined distance. This experiment provides data extracted at comparable temperature and pressure conditions to those of the current study. However, the resulting τ_{ig} determined herein were approximately an order of magnitude greater than those found by Lefebvre's group. These errors can be attributed to the difference in accounting for the mixing and chemical components of τ_{ig} .

Cadman et al. [25] studied propane autoignition in the temperature regime of interest at pressures ranging from 5 atm to 40 atm. This study was conducted in order to determine the E_{act} of propane oxidation within the parameter space and improve kinetics models within the temperature regime studied. Herzler et al. [26] studied propane ignition in the temperature range of interest as well between 10 atm and 30 atm. The motivation for this study was to provide validation data for kinetics models.

A regression analysis was performed to fit the propane τ_{ig} measurements made to an Arrhenius correlation. Table 4.2 provides the empirically derived reaction parameters for the oxidation of propane. Figure 4.6 shows the fit of the Arrhenius correlation to the experimental data. As was seen with the fit of the Arrhenius expression to the ethane data, the propane correlation, while approximating the values of τ_{ig} of propane, does not capture the asymptotic trend with higher temperatures seen in the experimental data, especially at the leaner Φ .

The E_{act} required for propane oxidation in the temperature range studied was found to be 38.5 kcal/mol. Limited reported E_{act} for propane oxidation is available in the literature. Cadman et al. [25] reports an E_{act} of 9.08 kcal/mol at 5 atm, $\Phi=1$, and temperatures ranging from 850 K to 1280 K ; and an E_{act} of 25.8 kcal/mol at 5 atm, $\Phi=0.5$, and temperatures ranging from 998 to 1357 K. The researchers conclude that significant changes in E_{act} of propane oxidation occur in the temperature range of 850 K to 1100 K and that current chemical mechanisms do not reflect these changes well.

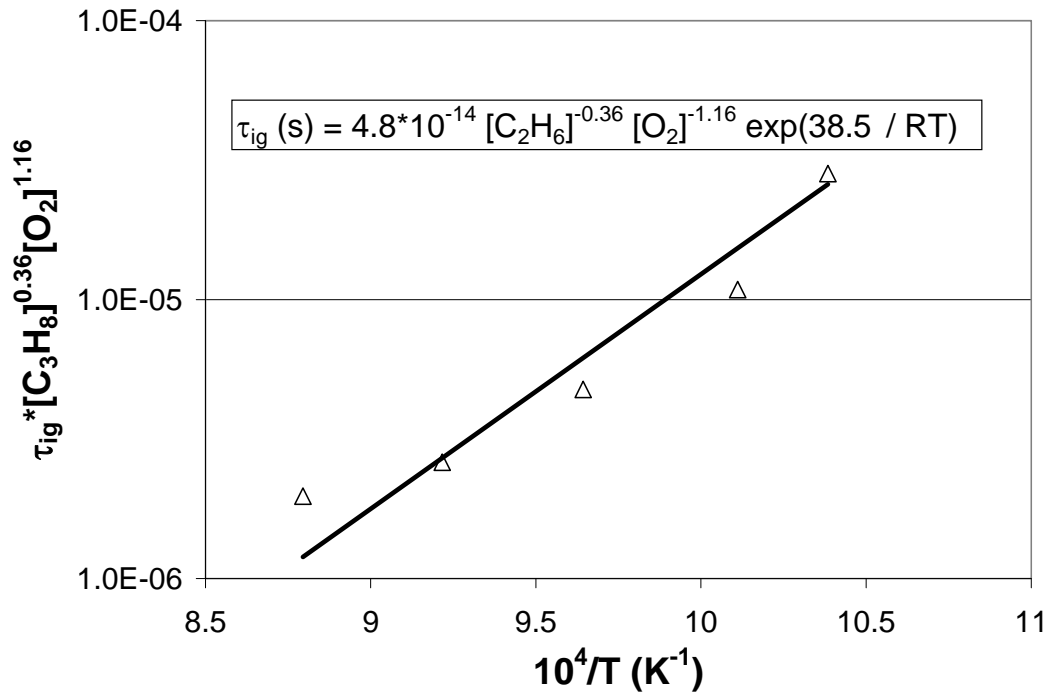


Figure 4.6. Propane autoignition measurements (\square $\phi = 0.5$, \diamond $\phi = 0.75$, Δ $\phi = 1.0$, \circ $\phi = 1.25$) plotted with Arrhenius correlation (-).

4.2 Methane-Based Binary Mixtures

The effect of additives ethane, propane, and ethylene on methane τ_{ig} was investigated for binary mixtures of methane and the higher-order additives and air. The following compositions of methane-based binary fuel mixtures were investigated with the first value representing the volume fraction of methane and the second representing the volume fraction of additive: 95/5, 90/10, 75/25, 50/50, and 25/75. τ_{ig} measurements were made at Φ of 0.5 and 1.0 and are presented both as a function of fuel composition (in terms of additive mole fraction), and as a function of temperature.

4.2.1 Methane-Ethane

Atmospheric pressure τ_{ig} were measured for methane/ethane binary fuel and air mixtures. Unfortunately, autoignition did not occur for any mixture at the lowest test temperature (931 K). However, autoignition occurred at each of the other test temperatures for the tests at stoichiometric Φ . Autoignition only occurred at test temperatures above 989 K for $\Phi = 0.5$. Figure 4.7 present the τ_{ig} measurements for methane/ethane/air mixtures at Φ of 0.5 and 1.0 as a function of ethane mole fraction in the fuel. Figure 4.8 present the same data as a function of reactor temperature.

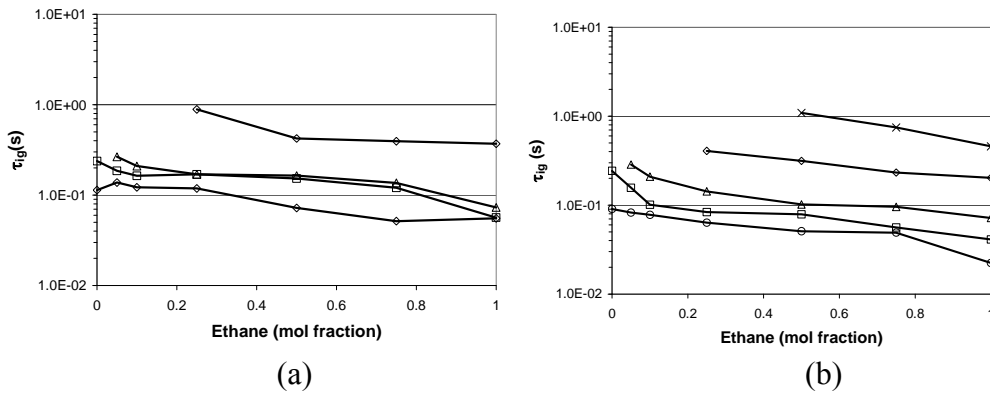


Figure 4.7. Binary methane/ethane mixture autoignition delay time measurements as a function of ethane mole fraction in the fuel mixture ($x=963$ K, $\diamond=989$ K, $\Delta=1037$ K, $\square=1085$ K, $\circ=1137$ K. (a) $\Phi = 0.5$, (b) $\Phi = 1.0$).

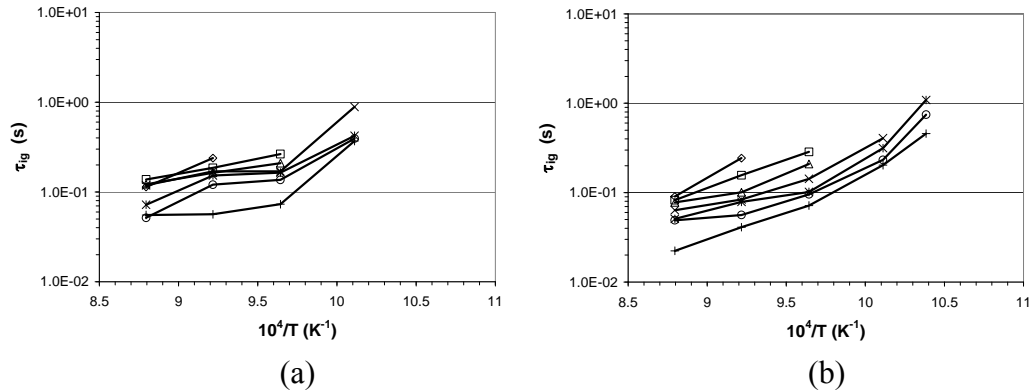


Figure 4.8. Binary methane/ethane mixture autoignition delay time measurements as a function of temperature (ethane mole %: $\diamond=0\%$, $\square=5\%$, $\Delta=10\%$, $\times=25\%$, $\ast=50\%$, $\circ=75\%$, $\ +=100\%$). (a) $\Phi = 0.5$, (b) $\Phi = 1.0$.

Figure 4.7 shows that with the addition of small amounts (5-10 mole %) of ethane to methane, τ_{ig} can be reduced significantly. This trend can be seen most evidently at the 1085 K test temperature. Unfortunately, because autoignition of pure methane and mixtures containing little additive were not achievable in the experimental reactor at the lower test temperatures, conclusions cannot be made regarding the effect of adding small amounts of ethane to methane on methane τ_{ig} at lower temperatures. Further, because autoignition occurred at more fuel rich test conditions than at fuel lean test conditions, the effect of ethane addition is more evident in Figure 4.8 which shows the τ_{ig} collected at stoichiometric Φ . Reductions in methane τ_{ig} of up to 50% were observed in the mixtures composed of up to 10% ethane by volume. It was also observed that the promotional effect of ethane addition on methane autoignition greatly diminished above fuel concentrations of about 25% by volume ethane. Above this concentration, additional ethane reduced the methane τ_{ig} only slightly.

A strong increase in ignition delay time between binary mixtures containing 25% methane and 75% ethane and pure ethane at many of the test conditions indicates that small additions of methane to ethane can significantly increase the τ_{ig} of ethane.

Increases in ethane τ_{ig} of up to 50% were seen with the addition of 25% methane.

Figure 4.8 displays the τ_{ig} measurements as a function of temperature, so the trends of decreasing τ_{ig} with increasing temperature for each binary mixture are more evident. It can be seen for both stoichiometric mixtures and mixtures of $\Phi = 0.5$, at a given temperature, continued addition of ethane will decrease the τ_{ig} of the binary fuel mixture. Also, as with the pure fuels, τ_{ig} of the binary methane/ethane mixtures decreased nearly exponentially with increased temperature. However, at the test temperatures above about 1000 K, τ_{ig} tended to decrease at a rate less than exponential with further temperature increase; this trend, again, was more evident in the leaner mixtures.

Figure 4.9 presents the τ_{ig} data of stoichiometric binary methane/ethane fuel mixtures along with predictions made using the GRI mechanism as well as relevant data from the literature. Limited data exists in the literature with which to compare the experimental results of this study. Goy et al. [15] conducted a series of shock tube experiments to determine τ_{ig} of simulated natural gas fuel blends composed of combinations of methane, ethane, and propane. The goal was to improve existing kinetics models. Measurements were made for a fuel blend of 15% ethane/85% methane in the temperature range of interest, at 10 atm, and Φ of 0.5. Huang et al.

[33] also conducted shock tube experiments to determine τ_{ig} of stoichiometric methane/ethane and methane/propane fuel mixtures for the purpose of improving chemical kinetics models. Measurements were made for binary methane/ethane fuel mixtures containing between 4 and 10% ethane within the temperature range of interest at pressures ranging from 15 atm to 40 atm. Because the measurements made in these two studies were made at pressures much greater than atmospheric, the resulting ignition delay times are much faster than those determined in the current study.

Predictions of τ_{ig} of methane/ethane mixtures were made using the GRI mechanism. The mixture used in the GRI mechanism predictions was a 90% methane/10% ethane stoichiometric mixture at atmospheric conditions. The GRI mechanism underpredicted the measurements significantly. This is interesting because the GRI mechanism overpredicted the measured τ_{ig} for both the methane and ethane pure fuels.

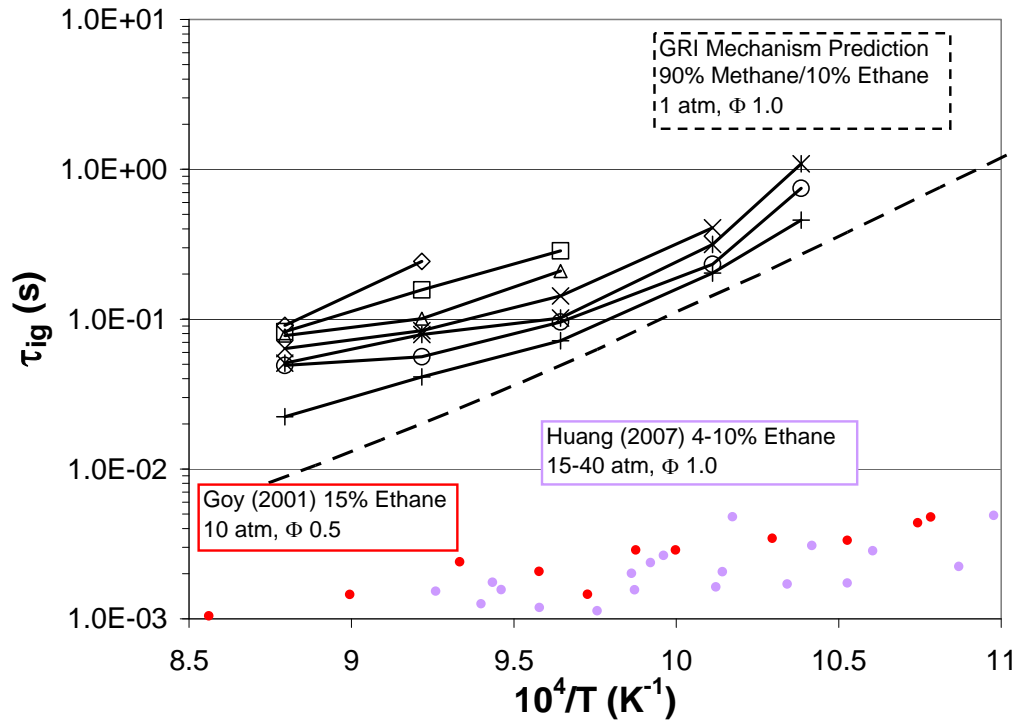


Figure 4.9. Stoichiometric methane/ethane mixture autoignition delay time measurements (ethane mole %: $\diamond=0\%$, $\square=5\%$, $\Delta=10\%$, $\times=25\%$, $\ast=50\%$, $\circ=75\%$, $\pm=100\%$) plotted alongside literature data and chemical kinetics predictions using GRI mechanism (--).

A regression analysis was performed to fit the methane/ethane binary fuel mixture τ_{ig} measurements made to an Arrhenius correlation. Table 4.2 provides the empirically derived reaction parameters for the oxidation of binary methane/ethane mixtures. Figure 4.10 shows the Arrhenius fit to the experimental data for the τ_{ig} for the methane/ethane mixtures for the temperature range of 963 K to 1137 K. The correlation cannot capture the asymptotic trend with higher temperatures seen in the experimental data, especially at the leaner Φ . Unfortunately, other researchers who have studied ignition of similar mixture concentrations do not report E_{act} derived from

their experimental data. Goy et al. [15] provides rate constants for specific reactions studied, but no global E_{act} for methane/ethane fuel blend oxidation is provided.

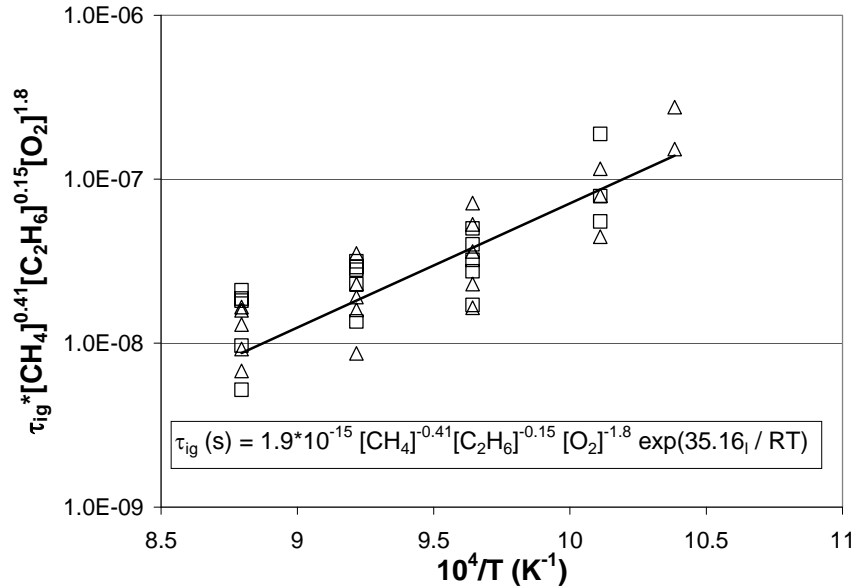


Figure 4.10. Methane/ethane autoignition measurements ($\square \Phi = 0.5$, $\Delta \Phi = 1.0$) plotted with Arrhenius correlation (-).

4.2.2 Methane-Propane

Atmospheric pressure τ_{ig} were measured for methane/propane binary fuel and air mixtures. Unfortunately, autoignition did not occur for any mixture at the lowest test temperature (931 K). However, autoignition occurred at each of the other test temperatures for the tests at Φ of 0.5 and 1.0 at least for some of the binary compositions. Figure 4.11 presents the τ_{ig} measurements for methane/propane/air mixtures at Φ of 0.5 and 1.0 respectively as a function of propane mole fraction in the fuel. Figure 4.12 presents the same data as a function of reactor temperature.

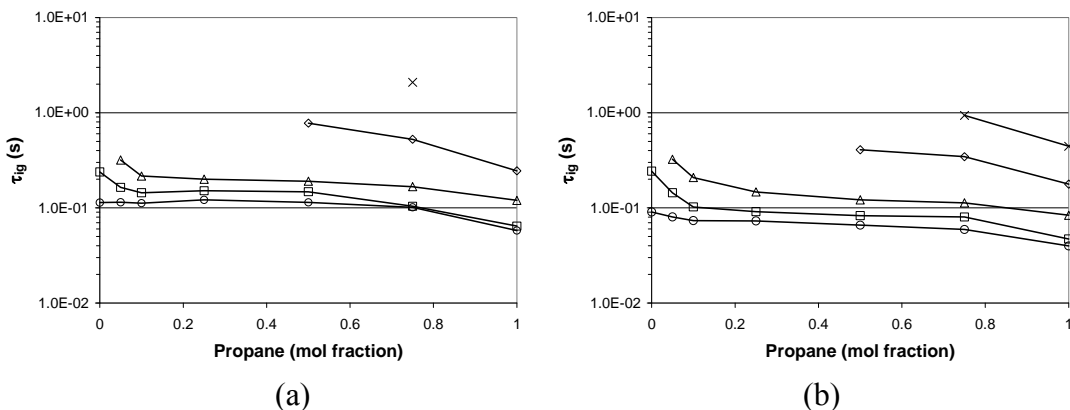


Figure 4.11. Binary methane/propane mixture autoignition delay time measurements as a function of propane mole fraction in the fuel mixture ($x=963$ K, $\diamond=989$ K, $\Delta=1037$ K, $\square=1085$ K, $\circ=1137$ K. (a) $\Phi = 0.5$, (b) $\Phi = 1.0$.

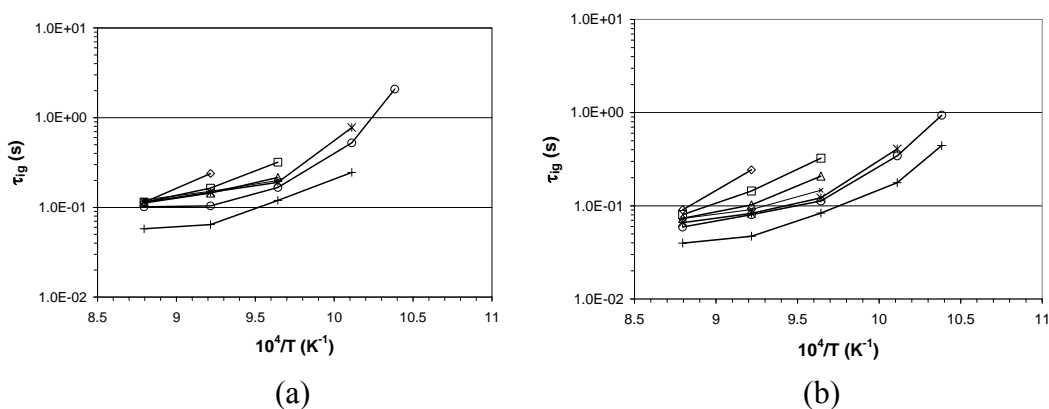


Figure 4.12. Binary methane/propane mixture autoignition delay time measurements as a function of temperature (propane mole %: $\diamond=0\%$, $\square=5\%$, $\Delta=10\%$, $x=25\%$, $*=50\%$, $\circ=75\%$, $+ =100\%$). (a) $\Phi = 0.5$, (b) $\Phi = 1.0$.

Very similar τ_{ig} trends were observed with the binary methane/propane mixtures as were seen with the binary methane/ethane mixtures. Again, as was observed with the pure fuel experiments, the results of the test involving ethane were slightly more reactive than those involving propane. Also, as was seen in the binary methane/ethane mixtures, Figure 4.11 shows that with the addition of small amounts (5-10 mole %) of propane to methane, τ_{ig} can be reduced significantly.

Unfortunately at the lower test temperatures, because autoignition of pure methane and mixtures containing little additive were not achievable in the experimental reactor, conclusions cannot be made regarding the effect of adding small amounts of propane to methane on methane τ_{ig} at lower temperatures. Similar to the binary methane/ethane results, reductions in methane τ_{ig} of up to 50% were observed in the mixtures composed of up to 10% propane by volume. It was also observed that the promotional effect of propane addition on methane autoignition greatly diminishes above fuel concentrations of about 25% by volume propane. Above this concentration, additional propane reduces the methane τ_{ig} only slightly.

A strong increase in ignition delay time between binary mixtures containing 25% methane and 75% propane and pure propane at many of the test temperatures and Φ indicates that small additions of methane to propane can significantly increase the τ_{ig} of propane. Increases in propane τ_{ig} of up to 50% were seen with the addition of 25% methane.

Figure 4.12 displays the τ_{ig} measurements as a function of temperature, so the trends of decreasing τ_{ig} with increasing temperature for each binary mixture are more evident. It can be seen for both stoichiometric mixtures and mixtures of $\Phi = 0.5$, at a given temperature, continued addition of propane will decrease the τ_{ig} of the binary fuel mixture. Also, as was seen for the measurements of τ_{ig} of the pure fuels, as well as binary methane/ethane mixtures, τ_{ig} of the binary methane/propane mixtures decreased near exponentially with increased temperature. However, at the higher

temperatures, τ_{ig} tended to decrease less severely; this trend, again, was more evident in the leaner mixtures.

Figure 4.13 presents the τ_{ig} data of stoichiometric binary methane/propane fuel mixtures along with predictions made using the GRI mechanism as well as relevant data from the literature. Many researchers have studied methane/propane fuel blend ignition in shock tubes in order to provide validation data for kinetics mechanisms. Petersen et al. collected τ_{ig} data [2] for a 80% methane/20% propane at 12 atm at temperatures between 1189 K and 1615 K and derived reaction parameters. Goy et al. studied a binary 85% methane/ 15% propane mixture between 952 K and 1112 K at 10 atm [15]. Huang et al. studied binary methane/propane mixtures having small (2-6% by volume) propane composition from 927 K to 1187 K and pressures ranging from 15 atm to 40 atm [33]. deVries et al. studied binary methane/ propane mixtures containing 25% propane at temperatures near 800 K and pressures averaging 20 atm [21]. The researchers found decreased τ_{ig} of methane with added propane as was found in the present study. The results from these experiments are compared with the results from the current study in Figure 4.13. The literature studies were all conducted at elevated pressures from 10 atm to 40 atm, resulting in τ_{ig} measurements orders of magnitudes faster than the ones measured in the current study.

Predictions of τ_{ig} of methane/propane mixtures were made using the GRI mechanism. The mixture used in the GRI mechanism predictions was a 90% methane/10% propane stoichiometric mixture at atmospheric conditions. The GRI mechanism predicts the measurements made for this mixture fairly well. However,

because measurements were not possible at many of the lower test temperatures, detailed analysis of the performance of the mechanism is not possible. Further, the GRI mechanism seems to maintain an exponential relationship between increasing τ_{ig} and decreasing temperature. The measurements again indicate that as temperature increases, τ_{ig} does not decrease exponentially at the higher test temperatures; the decrease tends to be less dramatic.

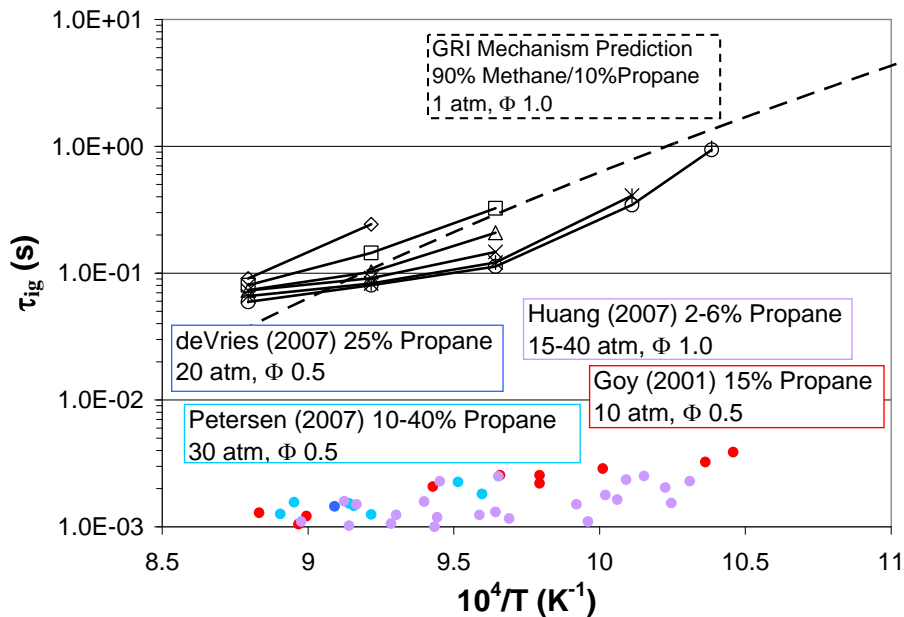


Figure 4.13. Stoichiometric methane/propane mixture autoignition delay time measurements (propane mole %: \diamond =0%, \square =5%, Δ =10%, \times =25%, $*$ =50%, \circ =75%, $+$ =100%) plotted alongside literature data and chemical kinetics predictions using GRI mechanism (--).

A regression analysis was performed to fit the methane/propane binary fuel mixture τ_{ig} measurements made to an Arrhenius correlation. Table 4.2 provides the empirically derived reaction parameters for the oxidation of binary methane/propane

mixtures. Figure 4.14 shows the fit of the correlation to the experimental data. As was seen with the fit of the respective Arrhenius expressions to the ethane, propane, and binary methane/ethane experimental data, the correlation approximates the values of τ_{ig} of methane/propane mixtures. However, it does not capture the asymptotic trend with higher temperatures seen in the experimental data.

The experiments conducted by Petersen et al. [2] resulted in the derivation of global E_{act} for the oxidation of the fuel blends studied. One mixture is relevant to the experiments conducted in the present study: 80% methane/20% propane. The empirically derived E_{act} found in this study was 41.9 kcal/mol for temperatures between 1189 K and 1615 K and a pressure of 12.2 atm. This E_{act} compares very closely with 41.83 kcal/mol derived from the data collected in the current study.

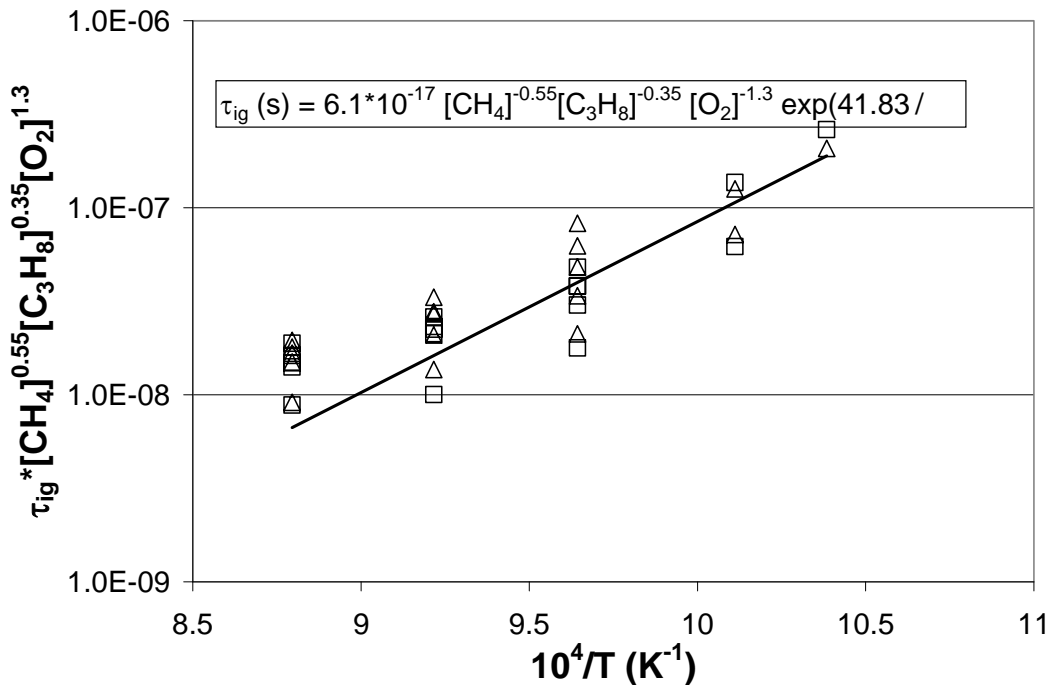


Figure 4.14. Methane/propane autoignition measurements ($\square \Phi = 0.5$, $\Delta \Phi = 1.0$) plotted with Arrhenius correlation (-).

4.2.3 Methane-Ethylene

Atmospheric pressure τ_{ig} were measured for methane/ethylene binary fuel and air mixtures. Successful autoignition events were achieved at all test temperatures.

Figure 4.15 presents the τ_{ig} measurements for methane/ethylene/air mixtures at Φ of 0.5 and 1.0 respectively as a function of ethylene mole fraction in the fuel. Figure 4.16 presents the same data as a function of reactor temperature.

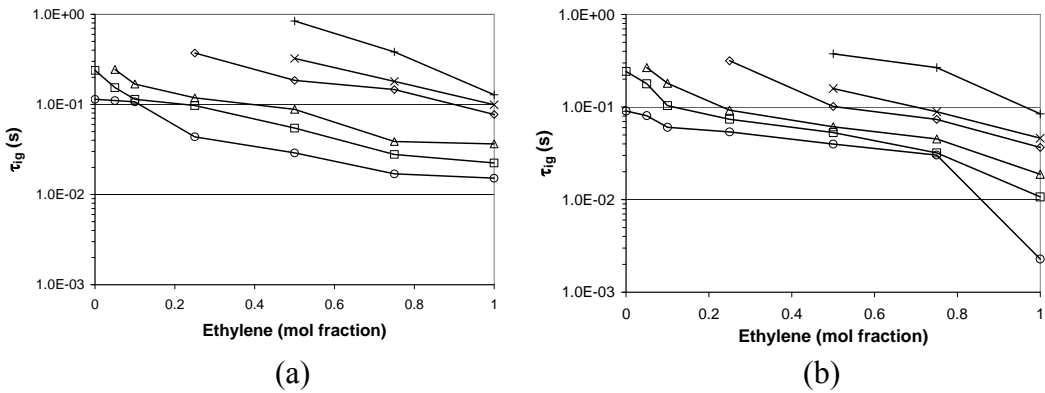


Figure 4.15. Binary methane/ethylene mixture autoignition delay time measurements as a function of ethylene mole fraction in the fuel mixture (+=931 K, x=963 K, \diamond =989 K, Δ =1037 K, \square =1085 K, \circ =1137 K. (a) $\Phi = 0.5$, (b) $\Phi = 1.0$.

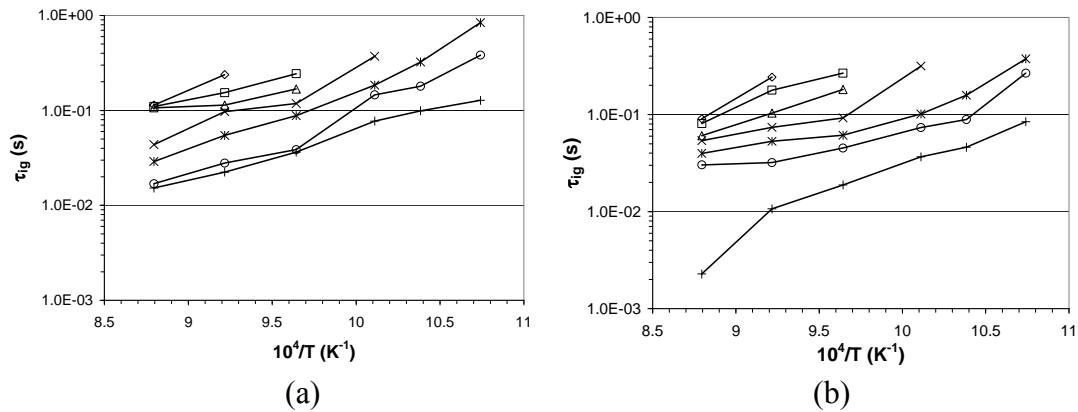


Figure 4.16. Binary methane/propane mixture autoignition delay time measurements as a function of temperature (propane mole %: \diamond =0%, \square =5%, Δ =10%, x=25%, *=50%, \circ =75%. +=100%). (a) $\Phi = 0.5$, (b) $\Phi = 1.0$.

Ethylene addition had a more significant effect on reducing methane τ_{ig} than did ethane or propane. As was seen in the measurements made for the other binary methane mixtures, and as seen in Figure 4.15, the addition of small amounts (5-10 mole %) of ethylene to methane significantly reduced the τ_{ig} of methane. Again, unfortunately at the lower test temperatures, because autoignition of pure methane and mixtures containing little additive were not achievable in the experimental reactor, broad conclusions cannot be made regarding the effect of adding small amounts of propane to methane on methane τ_{ig} at lower temperatures. Similar to the other binary methane mixture results, reductions in methane τ_{ig} of up to 50% were observed in the mixtures composed of up to 10% ethylene by volume. Further ethylene addition beyond 10% by volume continued to significantly reduce the τ_{ig} . This trend was not seen in the other binary methane mixtures. While the decrease is not as sharp as with the initial seeding of ethylene in methane, the decrease is nonetheless noteworthy. The decrease in τ_{ig} with continued addition of ethylene appears to be nearly exponential with composition. This trend seems to hold for the Φ studied between the composition space bounded by binary methane mixtures composed of 10% to pure ethylene.

Figure 4.16 displays the τ_{ig} measurements as a function of temperature. It can be seen for both stoichiometric mixtures and mixtures of $\Phi = 0.5$, at a given temperature, continued addition of ethylene will decrease the τ_{ig} of the binary fuel mixture. Also, as was seen for the measurements of τ_{ig} of the pure fuels, τ_{ig} of the binary

methane/propane mixtures decreased near exponentially with increased temperature. The trend of decreasing τ_{ig} reduction with increasing temperature seen at higher temperatures for the other mixtures and pure fuels, however, was not observed for binary methane/ethylene mixtures. τ_{ig} for binary methane/ethylene mixtures continued to decrease exponentially with increased temperature for all temperatures studied.

Figure 4.17 presents the τ_{ig} data of stoichiometric binary methane/ethylene fuel mixtures along with predictions made using the GRI mechanism. No known ignition data exists for binary methane/ethylene mixtures. Ethylene is typically not a component found in natural gas and has therefore not been included in many natural gas autoignition studies. Therefore, no data exists with which to compare the results of the current study. The results can, however, be compared to the predictions made by the GRI kinetics mechanism. The mixture used in the GRI mechanism predictions was a 90% methane/10% ethylene stoichiometric mixture at atmospheric conditions. The GRI mechanism underpredicted the measurements made in this study fairly significantly. This is not consistent with the performance of the GRI mechanism seen in the apparatus validation section, where the predictions made by the GRI mechanism were compared to the available pure ethylene τ_{ig} data found in the literature. The GRI mechanism consistently overpredicted the experimental results of the researchers' τ_{ig} experiments.

A regression analysis was performed to fit the methane/ethylene binary fuel mixture τ_{ig} measurements made to an Arrhenius correlation. Table 4.2 provides the

empirically derived reaction parameters for the oxidation of binary methane/ethylene mixtures. Figure 4.18 shows the fit of the correlation to the experimental data. As was seen with the fit of the respective Arrhenius expressions to the ethane, propane, and binary methane/ethane and binary methane/propane experimental data, the correlation approximates the values of τ_{ig} of methane/ethylene mixtures. Further, the exponential fit captures the trend of exponentially decreasing τ_{ig} with increasing temperature across all test temperatures seen in the experimental methane/ethylene mixture measurements.

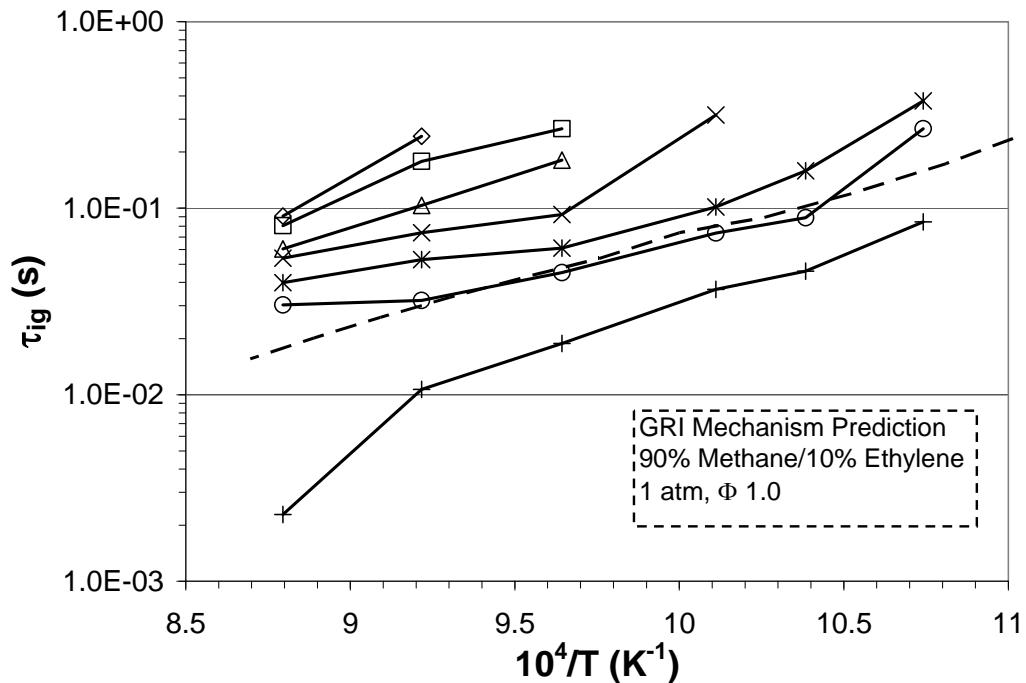


Figure 4.17. Stoichiometric methane/ethylene mixture autoignition delay time measurements (ethylene mole %: $\diamond=0\%$, $\square=5\%$, $\Delta=10\%$, $\times=25\%$, $\ast=50\%$, $\circ=75\%$, $\ +=100\%$) plotted alongside chemical kinetics predictions using GRI mechanism (--).

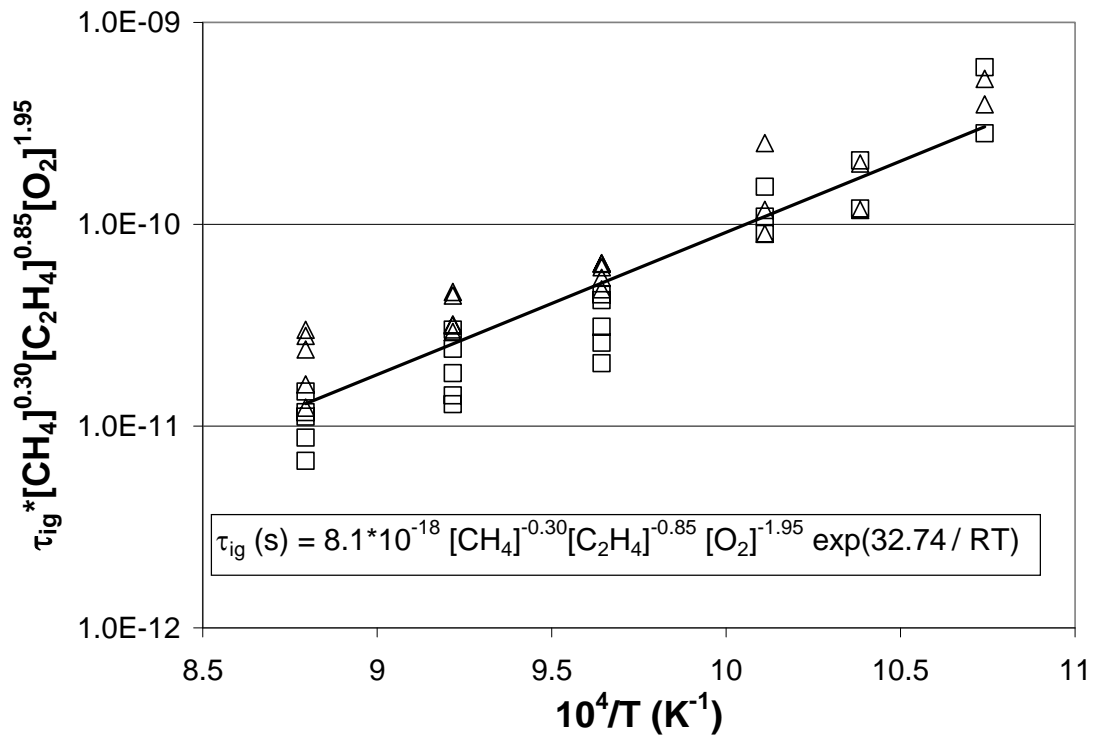


Figure 4.18. Methane/ethylene autoignition measurements ($\square \Phi = 0.5$, $\Delta \Phi = 1.0$) plotted with Arrhenius correlation (-).

4.3 Methane-Based Ternary Mixtures

Atmospheric pressure τ_{ig} were measured for methane/ethane/propane ternary fuel and air mixtures. Two ternary fuel mixtures were studied: mixture 1: 50% methane, 25% ethane, 25% propane; and mixture 2: 85% methane, 10% ethane, 5% propane. Each of these mixtures was studied at stoichiometric conditions as well as Φ of 0.5. Figure 4.19 presents the τ_{ig} measured for these mixtures as a function of mixture temperature.

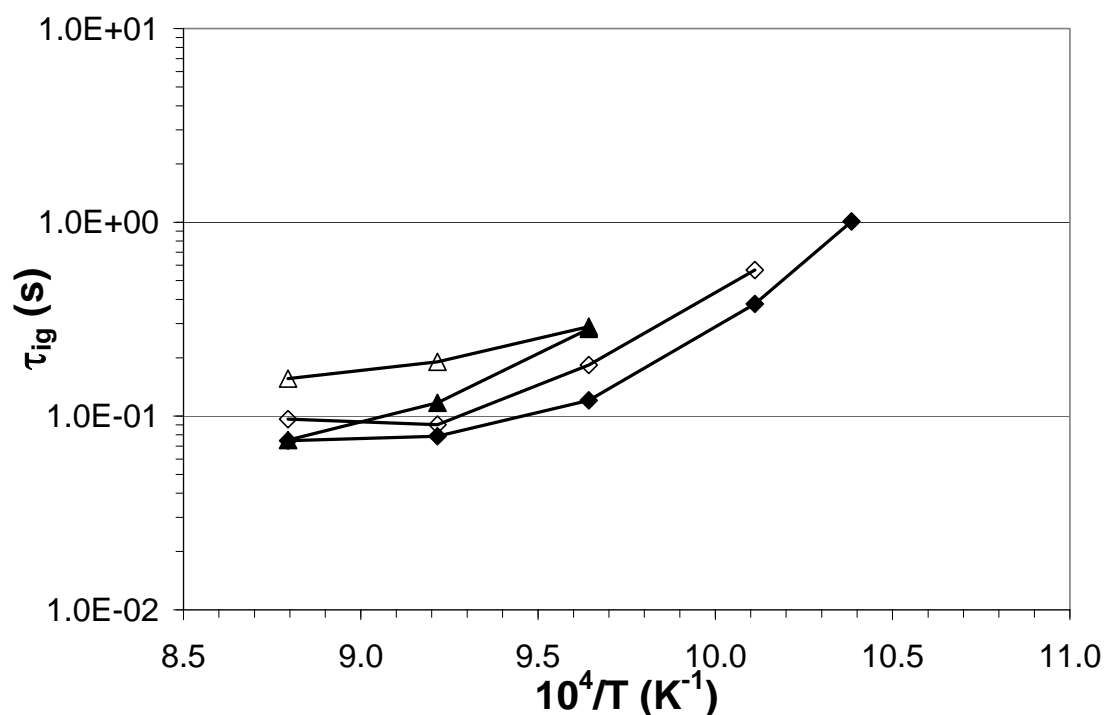


Figure 4.19. Ternary methane/ethane/propane mixture autoignition delay time measurements, $\Phi = 1.0$. Mixture 1 (\diamond): 50% methane, 25% ethane, 25% propane; Mixture 2 (Δ): 85% methane, 10% ethane, 5% propane. Open symbols, $\Phi = 0.5$; Closed symbols $\Phi = 1.0$.

Unfortunately autoignition events were not possible at some of the lower test temperatures, so the trends that can be inferred from the experimental data must be limited to the test temperatures that supported autoignition. Figure 4.19 shows that for both ternary mixtures, τ_{ig} decreased with increasing Φ , which had been observed for all pure fuels and mixtures as well. Further, the trend of decreasing τ_{ig} with increasing temperature was again observed. This trend was less evident at the higher test temperatures, which again was the case for the pure fuels and methane/ethane and methane/propane mixtures. Further, it was observed that the τ_{ig} of mixture 1 were significantly faster than τ_{ig} of mixture 2 at the same conditions. This was expected as

mixture 1 had significantly more ethane and propane added to the methane than did mixture 2 and increased addition of both ethane and propane had been observed to decrease τ_{ig} of methane.

Figure 4.20 presents the τ_{ig} data of the ternary methane/ethane/propane fuel mixtures along with predictions made using the GRI mechanism as well as relevant data from the literature. Other researchers have studied methane/ethane/propane fuel blend ignition in shock tubes in order to gain an understanding of the effect of compositional variations of higher order hydrocarbons on natural gas type fuels [9, 33]. Huang et al. measured τ_{ig} of a 95% methane/4% ethane/ 1% propane fuel mixture at temperatures ranging from 900 K to 1400 K and pressures averaging 40 atm [33]. Antonovski et al. studied several ternary fuel blends ranging from 70 to 90% methane, 7-20% ethane, and 3-15% propane at temperatures ranging from 1032 K to 1577 K and pressures ranging from 19 atm to 30 atm [9]. The researchers conclude that fuel composition is a very important factor, even more so than Φ , in affecting fuel τ_{ig} . The results from these experiments are compared with the results from the current study in Figure 4.20. The literature studies were all conducted at elevated pressures from 19 atm to 40 atm, resulting in τ_{ig} orders of magnitudes faster than the ones measured in the current study.

The GRI mechanism predictions of τ_{ig} for the ternary mixtures studied are significantly faster than the experimental results. This was also the case for the methane-ethane fuel mixtures but not for the methane-propane fuel mixtures. This indicates that the mechanism may overemphasize the promotional effects of ethane

on methane τ_{ig} . Further, the mechanism does not capture the trend of decreasing reduction in τ_{ig} with increasing temperature seen at the higher test temperatures. The GRI mechanism again follows the exponential relationship between temperature and τ_{ig} over the temperature range studied.

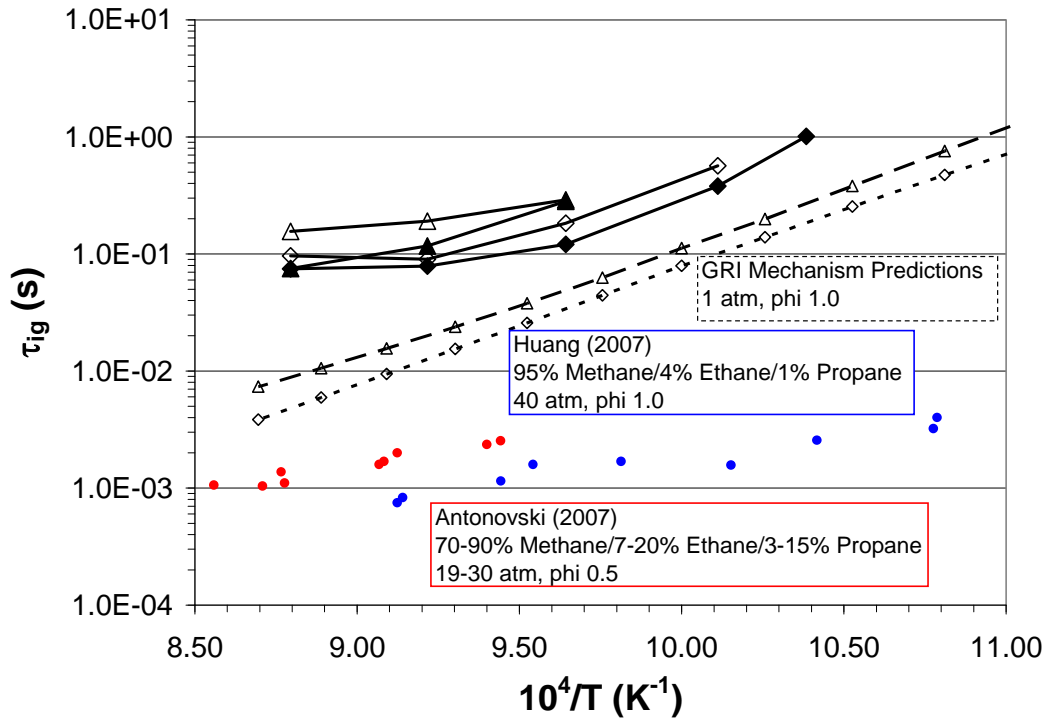


Figure 4.20. Ternary methane/ethane/propane mixture autoignition delay time measurements, $\Phi = 1.0$. Mixture 1 (\diamond): 50% methane, 25% ethane, 25% propane; Mixture 2 (Δ): 85% methane, 10% ethane, 5% propane. Plotted alongside literature data and chemical kinetics predictions using GRI mechanism (---). Open symbols, $\Phi = 0.5$; Closed symbols $\Phi = 1.0$.

4.4 CO_2 Addition

The effect of CO_2 addition on the ignition of natural gas type fuel blends was investigated. As shown in Table 1.1, CO_2 can make up a significant (up to 3% by volume) [49] portion of natural gas composition. Atmospheric pressure τ_{ig} were

measured for methane/ethane/CO₂ fuel and air mixtures. One binary methane/ethane fuel mixture was selected to serve as the basis for these tests: 75% methane/25% ethane. This mixture was then diluted with CO₂ such that mixtures containing 5% and 10% CO₂ by volume were created. τ_{ig} were measured for both stoichiometric mixtures and mixtures having Φ of 0.5. The τ_{ig} measured for the mixtures containing CO₂ are compared to the measurements made for the original mixtures in Figure 4.21.

The τ_{ig} for the mixtures containing CO₂ do not significantly deviate from the measurements of τ_{ig} for the mixture containing no CO₂. Only one data series offered insight into a possible effect of CO₂ on autoignition delay time. For the mixtures at a Φ of 0.5, it was observed that at the highest test temperature (1137 K), adding 5% CO₂ to the mixture lengthened the τ_{ig} by only 2%, but increasing the concentration to 10% CO₂ lengthened the τ_{ig} an additional 46%. This observation can be explained in part by third-body collision efficiencies of CO₂ being an order of magnitude greater than those of N₂ [19]. Therefore, the presence of CO₂ promotes recombination reactions and hence, reduces the fuel reactivity. However, because of the relatively small amount of data collected for this investigation, it is difficult to draw any further significant conclusions about the effect of CO₂ on τ_{ig} of fuel blends.

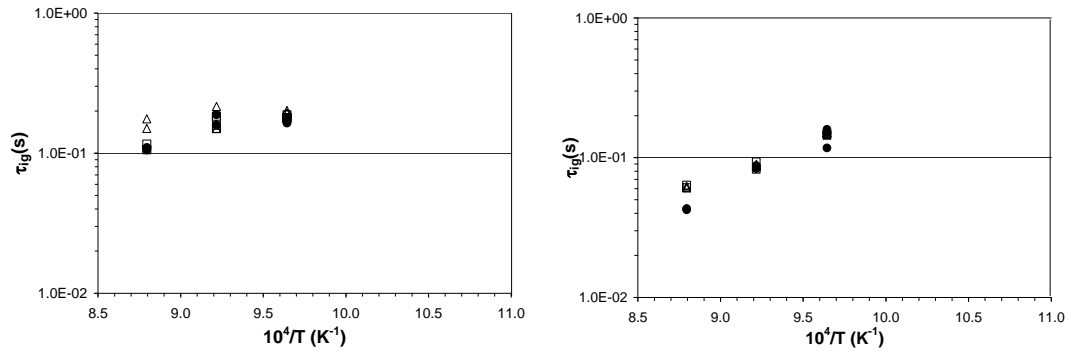


Figure 4.21. 75% Methane/25% ethane/CO₂ mixture autoignition delay time measurements as a function of reactor temperature (\bullet =0% CO₂, \square =5% CO₂, Δ =10% CO₂). (a) $\Phi = 0.5$, (b) $\Phi = 1.0$.

Chapter 5: Conclusions

The present study reports comprehensive autoignition delay time measurements for natural gas components made in an atmospheric pressure flow reactor over a broad range of temperatures and equivalence ratios. The effect of ethane, ethylene, propane, and CO₂ addition on methane τ_{ig} was investigated. The experimental apparatus capable of making these τ_{ig} measurements reliably and accurately was built, characterized, and validated. The measurements reported will both provide an understanding of the influence of temperature, equivalence ratio, and natural gas composition on fuel ignition behavior. Further, this data will extend the ignition database for natural gas fuels, promoting the development and validation of chemical kinetics models to improve predictions of ignition behavior of natural gas fuels.

5.1 Summary of Results

5.1.1 Autoignition Delay Time Trends

The expected reduction in τ_{ig} with increasing temperature and Φ were observed for all fuels across the temperature and pressure regimes studied. The data follows closely an Arrhenius expression fit with $\ln(\tau_{ig})$ being proportional to $1/T$ for most fuels. However, for pure alkane fuels and their mixtures, ignition delay times rise above correlations that fit the lower temperature data when T increases above 1000 K. Enough experimental data was not available to determine if this trend exists for

methane autoignition. This trend, however, was not observed with the τ_{ig} measurements made for ethylene, indicating the trend is not an artifact of the measurement technique.

Arrhenius rate expressions providing global E_{act} for the oxidation of the pure alkanes and methane fuel blends have been reported and summarized in Table 4.2. Reductions in E_{act} of methane oxidation were observed with the addition of ethane, propane, and ethylene. Further, the trends observed in this study indicate that addition of ethane, propane, and ethylene to methane has a very significant promotional effect on methane autoignition. The relative reactivity of methane, ethane, and propane was determined and global E_{act} of the oxidation of these pure fuels and mixtures of these fuels were derived. For the conditions studied, methane oxidation E_{act} was found to be 46.6 kcal/mol. It was found that both ethane and propane have very similar oxidation activation energies (40.0 and 38.5 kcal/mol, respectively).

As additives to methane, ethane, propane, and ethylene have the effect of reducing oxidation E_{act} . For temperatures between 963 K and 1137 K, binary methane/ethane fuels were found to have effective E_{act} of 35.2 kcal/mol, binary methane/propane fuels were found to have oxidation E_{act} of 41.8 kcal/mol, and binary methane/ethylene fuels were found to have oxidation E_{act} of 32.7 kcal/mol.

5.1.2 Accuracy of Predictive Tools

Comparisons of predictions made using the GRI 3.0 kinetics mechanism to the τ_{ig} measurements collected for each pure fuel and methane-based fuel blend in the

current study have been presented. The GRI mechanism predictions of methane τ_{ig} match very well with the measurements made in the current study. However, the predictions of τ_{ig} of ethane, propane, and methane-based mixtures containing ethane, propane, or ethylene do not match the experimental measurements well at all. The mechanism does not accurately capture the promotional effects of the additives on methane τ_{ig} , nor does it capture the asymptotic trend seen in τ_{ig} with higher temperature for these pure alkane fuels and mixtures. Because most data in the literature exists for higher pressure and temperature regimes, the predictive tools have not been validated at the conditions investigated in the current study.

5.1.3 Contribution to Combustion Community

The current study presents τ_{ig} measurements and analysis which benefit both the practical and analytical combustion communities. The measurements collected provide insight into the effects of composition, temperature and Φ on natural gas autoignition behavior which is beneficial to the practical combustion community. Further, the measurements contribute substantially to the natural gas autoignition database, which is beneficial to the analytical combustion community.

An important finding because of its application to practical natural gas fuels was that the most dramatic decrease (30-50%) in τ_{ig} of binary, methane-based fuels occurs with addition of 5-10% of ethane or propane. Further addition of ethane or propane continued to reduce τ_{ig} , but not as dramatically. This trend was found for all binary mixtures of methane/ethane and methane/propane. This information is important in

practical natural gas combustion applications where changes in fuel composition, and thus autoignition behavior, have the potential of affecting combustion stability.

The measurements made in this study extend the natural gas fuel component and mixture autoignition database. This data is useful in the development of chemical kinetics predictive tools designed to model the kinetics of combustion reactions. Validation data for these kinetics mechanisms is crucial for the improvement of their accuracy in predicting ignition, propagation, and extinction behavior.

5.2 *Future Work*

While the current study provides a great deal of autoignition data, it also suggests further natural gas fuel autoignition studies are needed. The results of the current experiment indicate that the influence of additives on methane autoignition can be very significant. Further research extending the parameter space of natural gas autoignition measurements is recommended to gain a deeper understanding of the promotional effects of other additives (higher-order hydrocarbons, H₂, and H₂S, for example) on methane autoignition at different pressure and temperature regimes. It is further recommended that current kinetics mechanisms be further optimized to capture the observations made in the current study.

The reported τ_{ig} measurements show that very significant reductions in methane τ_{ig} occur with the addition of just 5-10% higher hydrocarbon additive. More ignition research studying fuel compositions containing similar concentrations of additives are recommended to verify the results reported in the current study. The results of the CO₂ addition investigation indicate that CO₂ concentration has a potentially

significant effect on delaying fuel mixture autoignition. However, due to the limited amount of data collected, broad conclusions could not be made. Further investigation on the effect of CO₂ addition to natural gas on fuel autoignition is therefore recommended. Also, due to apparatus residence time constraints, many fuel τ_{ig} were unable to be measured, resulting in incomplete data sets for some of the less reactive fuel mixtures at lower temperatures and leaner Φ . It is recommended that these mixtures and conditions be investigated in other experimental apparatus having broader capabilities.

The current measurements made at low to intermediate temperature and atmospheric pressure fill some regions in the parameter space of the published autoignition delay time of natural gas fuels where previous data was sparse. It has been shown that the current chemical kinetics predictive tools do not adequately predict the experimental autoignition delay times measured herein, nor do they adequately capture the τ_{ig} trends observed with temperature. Because very little data exists in the literature for the fuel compositions and conditions studied this study, particularly atmospheric pressure, the models have not been rigorously validated within the parameter space of the measurements made here. Future work would include the optimization of current natural gas chemical kinetics mechanisms in predicting the τ_{ig} measurements reported in the current study.

References

1. Elliot, F.G., Kurz, R., Ethridge, C., and O'Connell, J.P., 2004, "Fuel Suitability Considerations for Industrial Gas Turbines," *J. Eng. Gas Turb. Power*, 126, pp. 119-126.
2. Petersen, E.L., Hall, J.M., Smith, S.D., deVries, J., Amadio, A.R., Crofton, M.W., 2005, "Ignition of Lean Methane-Based Fuel Blends at Gas Turbine Pressures," *ASME Turbo Expo 2005*, Reno, NV, GT2005-68517.
3. Spadaccini, L.J., Colket, M.B., 1994, "Ignition Delay Characteristics of Methane Fuels," *Prog. Energy Combust. Sci.*, 20, pp. 431-460.
4. Flores, R.M., Miyasato, M.M., McDonell, V.G., Samuelsen, G.S., 2001, "Response of a Model Gas Turbine Combustor to Variation in Gaseous Fuel Composition," *ASME International Gas Turbine and Aeroengine Congress and Expo*, Munich, Germany, 00-GT-141.
5. Petersen, E.L., Hall, J.M., Smith, S.D., deVries, J., Amadio, A.R., Crofton, M.W., 2007, "Ignition of Lean Methane-Based Fuel Blends at Gas Turbine Pressures," *J. Eng. Gas Turb. Power*, 129, pp. 937-944.
6. Liss, W.E., Thrasher, W.H., Steinmetz, G.F., Chowdiah, P., Attari, A., 1992, "Variability of Natural Gas Composition in Select Major Metropolitan Areas of the United States," GRI-92/0123
7. Westbrook, C.K., Pitz, W.J., Curran, H.C., Boercker, J., and Kunrath, E., 2001, "Chemical Kinetic Modeling Study of Shock Tube Ignition of Heptane Isomers," *Int. J. Chem. Kin.*, 33, pp. 868-877.
8. Petersen, E.L., Davidson, D.F., Hanson, R.K., 1999, "Ignition Delay Times of Ram Accelerator CH_4/O_2 /Diluent Mixtures," *J. Prop. Power*, 15, pp. 82-91.
9. Antonovski, V., Zinner, C., Barrett, A., Kalitan, D., Petersen, E., 2007, "Ignition of Methane/Ethane/Propane Mixtures at Engine Pressures," 5th US Combust. Meeting, Western States Section of the Combust. Inst., Univ. Cal. San Diego, Paper #E13.
10. Petersen, E.L., Hall, J.M., Kalitan, D.M., Rickard, M.J.A., 2004, "Ignition Delay Time Measurements of C_2H_x Fuels and Comparison to Several Detailed Kinetics Mechanisms," *ASME Turbo Expo 2004*, Vienna, Austria, GT2004-53926.
11. Bretecher, B., 2000, "An Experimental Investigation into Chemical Additive Effects on Ignition Delay of Methane Injected into Air," MS Thesis, University of Toronto.
12. Richards, G.A., McMillian, M.M., Gemmen, R.S., Rogers, W.A., and Cully, S.R., 2001, "Issues for Low-Emission, Fuel-Flexible Power Systems," *Prog. Energy Combust. Sci.*, 27, pp. 141-169.
13. Leiuwen, T., McDonell, V., Petersen, E., Santavicca, D., 2006, "Fuel Flexibility Influences on Premixed Combustor Blowout, Flashback, Autoignition, and Stability," *ASME Turbo Expo 2006*, Barcelona, Spain, GT2006-90770.
14. Leiuwen, T., McDonell, V., Petersen, E., Santavicca, D., 2008, "Fuel Flexibility Influences on Premixed Combustor Blowout, Flashback, Autoignition, and Stability," *J. Eng. Gas Turb. Power*, 130.
15. Goy, C.J., Moran, A.J., Thomas, G.O., 2001, "Autoignition Characteristics of Gaseous Fuels at Representative Gas Turbine Conditions," *ASME Turbo Expo 2001*, New Orleans, LA, 2001-GT-0051.
16. Kalitan, D.M., Rickard, M.J.A., Hall, J.M., Petersen, E.L., 2004, "Ignition Measurements of Ethylene-Oxygen-Diluent Mixtures with and without Silane Addition," 42nd AIAA Aerospace Sci. Meeting and Exhibit, Reno, NV, AIAA 2004-1323.
17. Petersen, E.L., Rohrig, M., Davidson, D.F., Hanson, R.K., Bowman, C.T., 1996, "High-Pressure Methane Oxidation behind Reflected Shock Waves," *Twenty-Sixth Symp. (Int.) Combust./Combust. Inst.*, pp. 799-806.
18. Petersen, E.L., Davidson, D.F., and Hanson, R.K., 1999, "Ignition Delay Time of Ram Accelerator CH_4/O_2 /Diluent Mixtures," *J. Prop. Power*, 15, pp. 82-91.

19. Frenklach, M., Bowman, T., Smith, G., Gardiner, B., GRI 3.0 Mechanism. http://www.me.berkeley.edu/gri_mech.
20. Huang, J., Hill, P.G., Bushe, W.K., Munshi, S.R., 2004, "Shock-Tube Study of Methane Ignition under Engine-Relevant Conditions: Experiment and Modeling," *Combust. Flame*, 136, pp. 25-42.
21. de Vries, J., Petersen, E.L., 2007, "Autoignition of Methane-Based Fuels under Gas Turbine Conditions," *Proc. Combust. Inst.*, 31, pp. 3163-3171.
22. de Vries, J., Hall, J.M., Simmons, S.L., Rickard, M.J.A., Kalitan, D.M., Petersen, E.L., 2007, "Ethane Ignition and Oxidation behind Reflected Shock Waves," *Combust. Flame*, 150, pp. 137-150.
23. Lefebvre, A., Freeman, W., Cowell, L., 1986, "Spontaneous Ignition Delay Characteristics of Hydrocarbon Fuel/Air Mixtures," NASA Contractor Report 175064.
24. Brown, C.J., Thomas, G.O., 1999, "Experimental Studies of Shock-Induced Ignition and Transition to Detonation in Ethylene and Propane Mixtures," *Combust. Flame*, 117, pp. 861-870.
25. Cadman, P., Thomas, G.O., Butler, P., 2000, "The Autoignition of Propane at Intermediate Temperatures and High Pressures," *Phys. Chem. Chem. Phys.*, 2, 5411-5419.
26. Herzler, J., Jerig, L., Roth, P., 2004, "Shock-Tube Study of the Ignition of Propane at Intermediate Temperatures and High Pressures," *Combust. Sci. Tech.*, 176, pp. 1627-1637.
27. Varatharajan, B., Williams, F.A., 2002, "Ethylene Ignition and Detonation Chemistry, Part 2: Ignition Histories and Reduced Mechanisms," *J. Prop. Power*, 18, No. 2, pp. 352-362.
28. Baker, J.A., and Skinner, G.B., 1972, "Shock Tube Studies on the Ignition of Ethylene-Oxygen-Argon Mixtures," *Combust. Flame*, 19, pp. 347-350.
29. Colket, M.B., Spadaccini, L.J., 2001, "Scramjet Fuels Autoignition Study," *J. Prop. Power*, 17, No. 2., pp. 315-323.
30. Cadman, P., Bambrey, R.J., Box, S.K., and Thomas, G.O., 2002, "Ethylene Combustion Studied over a Wide Temperature Range in High-Temperature Shock Waves," *Comb. Sci. Tech.*, 174, pp. 111-127.
31. Sims, G., Clague, A.R., Coppelstone, R.W., Menzies, K.R., MacQuisten, M.A., 2005, "The Measurement and Prediction of Gaseous Hydrocarbon Fuel Auto-Ignition Delay Time at Realistic Gas Turbine Operating Conditions," ASME Turbo Expo 2005, Reno-Tahoe, NV, GT2005-68736.
32. Kumar, K., Mittal, G., Sung, C., Law, C.K., 2008, "An Experimental Investigation of Ethylene/O₂/Diluent Mixtures: Laminar Flame Speeds with Preheat and Ignition delays at High Pressures," *Combust. Flame*, 153, pp. 343-354.
33. Huang, J., Bushe, W.K., 2006, "Experimental and Kinetic Study of Autoignition in Methane/Ethane/Air and Methane/Propane/Air Mixtures under Engine-Relevant Conditions," *Combust. Flame*, 144, pp.74-88.
34. Gokulakrishnan, P., Gaines, G., Currano, J., Klassen, M.S., Roby, R.J., 2007, "Experimental and Kinetic Modeling of Kerosene-Type Fuels at Gas Turbine Operating Conditions," *J. Eng. Gas Turb. Power*, 129, pp. 655-663.
35. Gokulakrishnan, P., Gaines, G., Klassen, M.S., Roby, R.J., 2007, "Autoignition of Aviation Fuels: Experimental and Modeling Study," 43rd AIAA/ASME/SAE/ASEE Joint Prop. Conf. and Exhibit, Cincinnati, OH, AIAA 2007-5701.
36. Serban, M., Lewis, M.A., Marshall, C.L., and Doctor, R.D., 2003, "Hydrogen Production by Direct Contact Pyrolysis of Natural Gas," *Energy Fuels*, 17, pp. 105-713.
37. Samuelsen, S., McDonell, V., Greene, M., and Beerer, D., 2006, "Correlation of Ignition Delay with Natural Gas and IGCC Type Fuels," DOE Award DE-FC26-02NT41431.
38. Mesarch, S.E., 2005, "A Computer Modeling Study of Methane Oxidation," MS Thesis, University of Akron.
39. Simmie, J.M., 2003, "Detailed Chemical Kinetic Models for the Combustion of Hydrocarbon Fuels," *Prog. Energy Comb. Sci.*, 29, pp. 599-634.

40. Hunter, T.B., Litzinger, T.A., Wang, H., and Frenklach, M., 1996, "Ethane Oxidation at Elevated Pressures in the Intermediate Temperature Regime: Experiments and Modeling," *Comb. Flame*, 104, pp. 505-523.
41. Wantanabe, M., Adschiri, T., and Arai, K., 2001, "Overall Rate Constant of Pyrolysis of n-Alkanes at low Conversion Level," *Ind. Eng. Chem. Res.*, 40, pp. 2027-2036.
42. Koch, A., Naumann, C., Meier, W., Aigner, M., 2005, "Experimental Study and Modeling of Autoignition of Natural Gas/Air-Mixtures Under Gas Turbine Relevant Conditions," ASME Turbo Expo 2005, Reno, NV, GT2005-68405.
43. Petersen, E.L., Kalitan, D.M., Barrett, A.B., Reehal, S.C., Mertens, J.D., Beerer, D.J., Hack, R.L., and McDonell, V.G., 2007, "New Syngas/Air Ignition Data at Lower Temperature and Elevated Pressure and Comparison to Current Kinetics Models," *Comb. Flame*, 149, pp. 244-247.
44. Petersen, E.L., Kalitan, D.M., Simmons, S., Bourque, G., Curran, H.J., and Simmie, J.M., 2007, "Methane/Propane Oxidation at High Pressures: Experimental and Detailed Kinetic Modeling," *Proc. Combust. Inst.*, 31, pp. 447-454.
45. Schultz, E., Shepherd, J., 2000, "Validation of Detailed Reaction Mechanisms for Detonation Simulation," Explosion Dynamics Laboratory Report FM99-5.
46. Wang, H., 2001, "A New Mechanism for Initiation of Free-Radical Chain Reactions During High-Temperature, Homogenous Oxidation of Unsaturated Hydrocarbons: Ethylene, Propyne, and Allene," *Int. J. Chem. Kin.*, 33, pp. 698-706.
47. Chen, J., McDonnell, V., and Samuelsen, S., 2004, "Effects of Ethane and Propane Additives on the Autoignition Behavior of Natural Gas Fuels," Proceedings of Spring Meeting of Western States Section, The Combustion Institute, UC Davis, CA.
48. Turbiez, A., El Bakali, A., Pauwels, J.F., Meunier, P., 2003, "Experimental Study of a Low Pressure Stoichiometric Premixed Methane, Methane/Ethane, Methane/Ethane/Propane and Synthetic Natural Gas Flames," *Fuel*, 83, pp. 933-941.
49. Flores, R.M., McDonnell, V.G., Samuelsen, G.S., 2003, "Impact of Ethane and Propane Variation in Natural Gas on the Performance of a Model Gas Turbine Combustor," *J. Eng. Gas Turb. Power*, 125, pp. 701-708.
50. Marinov, N.M., Malte, P.C., 1995, "Ethylene Oxidation in a Well-Stirred Reactor," *Int. J. Chem. Kinetics*, 27, pp. 957-986.
51. Thorton, M.M., 1989, PhD Thesis, University of Washington.
52. Wang, H., You, X., Joshi, A.V., Davis, S.G., Laskin, A., Egolfopoulos, F., Law, C.K., 2007, "USC Mech Version II. High-Temperature Combustion Reaction Model of H₂/CO/C₁-C₄ Compounds," http://ignis.usc.edu/USC_Mech_II.htm.
53. Konnov, A.A., 2000, "Development and Validation of a Detailed Reaction Mechanism for the Combustion of Small Hydrocarbons," 28th Symp. (Int.) Combust./Combust. Inst., Abstr. Symp. Paper, p. 317.
54. Li, S.C., Williams, F.A., 2000, "Reaction Mechanisms for Methane Ignition," ASME Turbo Expo 2000, Munich, Germany, 2000-GT-145.
55. Cowell, L.H., Lefebvre, A.H., 1986, "Influence of Pressure on Autoignition Characteristics of Gaseous Hydrocarbon-Air Mixtures," SAE paper 860068.